Physical Performance of Clayey Soil-Geocomposite Drainage Layer Interfaces subjected to Environmental Loadings

by

Zhiming Chao

A thesis submitted in partial fulfilment of the requirements for the degree of

Doctor of Philosophy in Engineering

University of Warwick, School of Engineering

January 2021

Table of Contents

Table of Figures

Table of Tables

Acknowledgements

First of all, I wish to express my greatest appreciation to my supervisor Dr Gary Fowmes. It is really lucky for me to be supervised by Dr Gary. During the last three and a half years, Dr Gary gave me consistently valuable guidance, inspiration and encouragement in my research. When I struggled to determine a suitable research direction, Dr Gary discussed with me many times and gave many useful suggestions to help me find an appropriate research topic. When I conducted the laboratory experiments, Dr Gary worked with me to establish the experimental apparatus and discuss the experimental scheme. When I wrote the academic papers and the thesis, Dr Gary modified them many times and provided me with countless helpful guidance. These things just account for a small proportion of numerous Dr Gary's help to me. Moreover, Dr Gary provided me with sufficient resources to conduct research, including experimental materials, experimental apparatus, experimental spaces, etc. Without Dr Gary's huge help and valuable guidance, I definitely cannot complete my PhD project successfully, especially in this special time due to the pandemic. Also, Dr Gary focuses on cultivating my comprehensive capability. For example, Dr Gary helped me to strengthen my teaching and demonstration ability, which is really helpful for my future career development. Only words cannot express my sincere gratitude to Dr Gary. I cannot imagine a better supervisor than Dr Gary. After three years of working together, Dr Gary is not only a kind mentor for me but also a good friend of mine. After I graduate, I will absolutely continue to work with Dr Gary.

I also would like to acknowledge ABG Ltd. that provided me with the experimental materials and the database for establishing the predictive models, in particular to the Chief Engineer in ABG Ltd: David Shercliff. It is not possible for me to complete my physical experiments and numerical modelling without their help.

I am indebted to China Scholarship Council that provides me with the funding to support my PhD study. I also wish to pay my special regards to the staff in the School of Engineering of our university that provides crucial study and technical support for me, including the head of the school: Professor David Tower, design manager: Mr Martin Millson, electrical electronics technician: Meadows, Jonathan, and all the technicians in the civil engineering laboratory: Mr Saif Aldin Alshalmani, Mr Fahim Atify, etc.

I would like to recognize my panel members: Dr Mohammad Rezania and Dr Reyes Garcia. Thanks very much for their efforts and assistance for helping me to complete my PhD project successfully.

I wish to show my deepest gratitude to my examiners: Dr Alireza Tatari and Dr Mohammad Rezania. Sincere appreciation for their commitment on reviewing and modifying my thesis to improve its quality and help me to make a nice ending of my PhD project.

I would like to thank all my friends during my PhD study.

Last but not least, I wish to acknowledge the support and eternal love of all my family members, in particular to my beautiful girlfriend Nora and my parents. Thanks to Nora's careful care, I can pay all my attention to my research and succeed to complete my PhD project. The company and help from Nora also promote me to advance rapidly. More importantly, I would like to express my sincere appreciation to my parents, because of their consistent and pure love, I can grow up and obtain opportunities to acquire education to realize my own value. The support and love from my parents are the source with endless power to encourage me to continuously progress.

Declaration

This thesis is submitted to the University of Warwick in support of my application for the degree of Doctor of Philosophy in Engineering. I declare that the thesis is my own work except where I have otherwise stated. No part of this thesis has been submitted for a research degree at any other institution.

The work presented in this thesis has been published in the following peer-reviewed paper:

Zhiming Chao, Gary Fowmes. Modified stress and temperature-controlled direct shear apparatus on soil-geosynthetics interfaces. *Geotextiles and Geomembranes*. (Published)

Abstract

Geocomposite Drainage Layers (GDL) are applied in a broad range of geotechnical and geo-environmental applications, including mining facilities, embankments, landfills, etc., which can substitute traditional methods of placing layers of gravel and graded sand to drain excess water effectively and decrease pore water pressure, improving the stability of engineering projects. For the applications with GDLs installed, their stability is mainly controlled by the mechanical characteristics of GDL-cover soil interfaces. Therefore, the correct evaluation of the mechanical behaviour for GDL-cover soil interfaces is crucial. Additionally, during the service life, the GDL cover systems can experience climatic variations, such as the increase in ambient temperature, consecutive rainfall and drought, etc. to result in obviously elevated temperature, drying-wetting cycles, and thermal cycles on cover soil-GDL interfaces to affect their mechanical properties, which may impact the stability of GDL cover systems.

This thesis quantifies the mechanical behaviour of cover soil-GDL interfaces subjected to environmental factors. In this thesis, a stress and temperature-controlled large direct shear apparatus was established. With use of the apparatus, the impacts of environmental factors, including drying-wetting cycles, thermal cycles, and elevated temperature, on the short-term and creep mechanical characteristics of cover clayey soil-GDL interfaces were quantified.

Key Words: Clayey soil-GDL interfaces; Landfill cover systems; Stress and temperature-controlled large direct shear apparatus; Rapid loading shear tests; Creep shear tests.

Full List of Publications

Parts of the research described in this thesis have been published in the following papers:

Journal papers:

1. **Zhiming Chao**, Gary Fowmes. Modified stress and temperature-controlled direct shear apparatus on soil-geosynthetics interfaces. *Geotextiles and Geomembranes*. (Published)

2. **Zhiming Chao**, Gary Fowmes. The short-term and creep mechanical behaviour of clayey soil-Geocomposite Drainage Layer interfaces subjected to environmental loadings. *Geotextiles and Geomembranes*. (In proofreading)

Conference paper:

1. **Zhiming Chao**, Gary Fowmes. Creep testing of clay-geocomposite interfaces during drying-wetting cycles. *EuroGeo 7 – 7th European Geosynthetics Congress*, Warsaw, Poland, May 2021. (Accepted) Awarded the best paper prize in IGS UK Chapter Student Contest 2020.

List of Symbols and Abbreviations

CM	Medium plasticity clay
CL	Low plasticity clay
DSA	Direct shear apparatus
GCL	Geosynthetic Clay Liner
GDL	Geocomposite Drainage Layer
GDSTAS	GDS Triaxial Automated System
HDPE	High-density polyethene
IGS	International Geosynthetics Society
LLDPE	Linear low-density polyethene
MDPE	Linear medium-density polyethene
PE	Polyethene
PP	Polypropylene
PET	Polyester
PVC	Polyvinyl Chloride
PLA	Polylactic acid fibre
RSA	Ring shear device
SIM	Stepped Isothermal Method
TTS	Time-Temperature Superposition

Chapter 1

Introduction

1.1 Background Research

Geosynthetics widely exist in civil, environmental, geotechnical, and hydraulic engineering applications (Benson et al., 2010; Chinkulkijniwat et al., 2017; McCartney and Berends, 2010). Use of such can provide both single or multiple functions such as drainage, filtration, protection, reinforcement, separation and watertight (Datta, 2010; Ferreira et al., 2015; Lackner et al., 2013).

Geosynthetics can be categorised based on their properties, material and functions, such as geotextiles, geomembranes, geogrids, geocomposite, etc. Amongst them, geocomposite is an important category of geosynthetics. There is a combination of, for example, geotextiles, geogrids, geonets, and geomembranes. Geocomposite drainage layers (GDL) are an example of a type of multi-function geocomposite that is being rapidly applied within a broad range of geotechnical and geo-environmental applications, including embankments, landfills and mining facilities. This material can substitute the traditional methods of adopting layers of gravel and graded sand to drain excess water effectively and decrease pore water pressure, improving the stability of engineering projects (Bahador et al., 2013; Chinkulkijniwat et al., 2017; Jang et al., 2015; Stormont et al., 2009). When GDL are placed underneath cover soil above landfills, it can also provide separation and reinforcement functions as well as acting as a capillary break to prevent the migration of contaminated water and gas produced from the waste (Bahador et al., 2013; Chinkulkijniwat et al., 2017; Jang et al., 2015; Khire and Haydar, 2007; Othman et al., 2018; Stormont et al., 2009). In practical engineering, GDL are commonly installed underneath cover soil above engineering containment facilities. The stability of engineering projects installed with

GDL is mainly controlled by the mechanical characteristics of the GDL-cover soil interfaces (Othman, 2016). Therefore, the correct evaluation of the mechanical behaviour for GDL-cover soil interfaces is crucial. This is essential to the integrity and stability of engineering applications.

Although some experimental research on mechanical properties of soil-GDL interfaces has been conducted, the existing studies did not involve the impacts of environmental factors, such as elevated temperature, drying-wetting cycles, and thermal cycles, on the short -term and creep mechanical behaviour of soil-GDL interfaces (Bilodeau et al., 2015; Edil et al., 2007; McCartney et al., 2005; Müller et al., 2009; Othman et al., 2014). In general, the usage of GDL in engineering projects usually requires a minimum guaranteed service life of many tens of years. In the service life, the soil-GDL interfaces can experience climatic variations, such as an increase in ambient temperature, consecutive rainfall and drought. Due to the thin thickness of cover soil, environmental variations can result in elevated temperatures, drying-wetting cycles and thermal cycles on soil-GDL interfaces. This can affect both short-term and creep mechanical properties of the interfaces caused by constant or increasing shear stresses, which may lead in the failure of the soil-GDL interfaces and impact the stability of GDL cover systems (Benson et al., 2012).

Temperature is one of crucial environmental factors believed to impact the stableness of GDL cover systems. The temperature of GDL cover systems is susceptible to the ambient environment. GDL cover systems that are specifically in waste containment facilities, such as in landfills, etc., are also exposed to elevated temperatures due to the exothermal reaction from waste degradation (Abuel-Naga and Bouazza, 2013; Ishimori and Katsumi, 2012; Singh and Bouazza, 2013). Some researchers have indicated that the temperature inside landfills is usually higher than that of the external environment, with temperatures inside landfills often in the range of 30 ℃ to 60 ℃ (Abuel-Naga and Bouazza, 2013; Hanson et al., 2015; Jafari et al., 2014). This results in the measured temperature of GDL cover systems being

higher than the ambient temperature due to the elevated temperature of the underlying wastes, with the prevailing direction of heat flow in the cover systems being upward. Due to the presence of thermos-softening plastics in geosynthetics, exposure to elevated temperatures can reduce the mechanical properties of cover soil-GDL interfaces, such as shear strength, reducing the stability of landfill cover systems (Bouazza et al., 2011).

Apart from elevated temperature, climatic change, including rainfall and drought, also has effects on the mechanical properties of cover soil and cover soil-GDL interfaces during the long-term operation of engineering projects (Hosney and Rowe, 2013). In general, the thickness of cover soil is relatively small (about 0.5 m to 2 m), thus susceptible to rain water and ambient air temperature cycles through its full thickness to form drying-wetting cycles or thermal cycles on cover soil-GDL interfaces (McCartney and Zornberg, 2010). For cover soil-GDL interfaces in the cover systems of landfills, the high temperature inside landfills further accelerates the evaporation of water in cover soil-GDL interfaces during the drying cycles. This leads to the formation of apparent drying-wetting cycles or thermal cycles on the GDL cover systems during climatic change and causes potential safety hazards on the long-term operation of landfills (Li et al., 2016).

In existing studies, the impacts of environmental loadings, such as elevated temperature, drying-wetting cycles and thermal cycles on the mechanical characteristics of soil and polymer geosynthetics under stress states have been investigated (Fleureau et al., 2002; Guan et al., 2010; Zhang et al., 2015). The research results have shown that environmental factors can significantly influence the mechanical behaviour of soil and geosynthetics, affecting their mechanical behaviour, respectively (Guney et al., 2007; Md et al., 2016; Rezania, 2008; Wang et al., 2016a). For instance, due to the presence of thermos-softening materials, a fall in tensile strength and modulus of polymer geosynthetics occurs at elevated temperature, and a decrease in shear strength of soil was observed due to the development of cracks and structural damage

of soil when subjected to drying-wetting cycles (Guney et al., 2007; Md et al., 2016; Wang et al., 2016a; Zhang et al., 2015). However, the influence of environmental factors on the short-term and creep mechanical behaviour of soil-geosynthetics interfaces under environmental loadings has not been widely researched, let alone the impacts on soil-GDL interfaces.

Displacement-controlled direct tests are the most commonly adopted approach to research the mechanical behaviour of soil-geosynthetics interfaces (Abu-Farsakh et al., 2007; Ferreira et al., 2015; Lee and Manjunath, 2000; Liu et al., 2009). However, displacement-controlled direct shear tests are not representative of real situations within engineering applications, since shear deformation of soil-geosynthetics interfaces is controlled by stress in real project sites, rather than displacement. Furthermore, the conventional displacement-controlled direct shear apparatus cannot hold constant stresses whilst varying other parameters, such as temperature, drying and wetting conditions, etc (Müller et al., 2008). Additionally, displacement-controlled direct shear testing does not simulate the long-term field situation under which elevated temperature, thermal cycles, and drying-wetting cycles can significantly impact the mechanical behaviour of soil-geosynthetics interfaces (Ghazizadeh and Bareither, 2018a; Zanzinger and Saathoff, 2012). More importantly, it is impossible for displacement-controlled direct shear apparatus to conduct creep tests on soil-geosynthetics interfaces (Fox and Stark, 2015). Therefore, it is necessary to use a temperature and stress-controlled direct shear apparatus that can conduct creep tests/rapid loading shear tests on soil-geosynthetics interfaces during/after elevated temperature, thermal and drying-wetting cycles. To compensate for the aforementioned research gap, this thesis quantifies the mechanical behaviour of cover soil-GDL interfaces subjected to environmental factors. In this thesis, a stress and temperature-controlled large direct shear apparatus was established. With use of the apparatus, the impacts of environmental factors, including drying-wetting cycles, thermal cycles, and elevated temperature, on the short-term and creep mechanical characteristics of cover clayey soil-GDL interfaces were quantified.

1.2 Aim and objectives

1.2.1 Aim

The aim of the research is to quantify the mechanical behaviour of cover soil-GDL interfaces subjected to environmental loadings.

1.2.2 Objectives

The aforementioned aim is achieved by accomplishing the following objectives:

(1) To measure the impacts of elevated temperature, drying-wetting cycles and thermal cycles on the short-term mechanical behaviour of cover clayey soil-GDL interfaces;

(2) To measure the impacts of drying-wetting cycles and thermal cycles on the creep mechanical behaviour of cover clayey soil-GDL interfaces.

1.3 Original contributions to knowledge

By achieving the above aim and objectives of the study, the original contributions of this research to knowledge are presented in the following, a majority of which have been included in completed journal articles:

(1) A bespoke stress and temperature-controlled direct shear apparatus to test soil-geosynthetics interfaces has been designed and built. The modified apparatus allows for the short-term and creep shear deformation behaviour of soil-geosynthetics interfaces subjected to environmental factors, including elevated temperature, drying-wetting cycles, and thermal cycles, etc. to be investigated. The

functionality of the modified apparatus has been validated by conducting a series of validation tests.

(2) The impacts of environmental loadings, including elevated temperature, drying-wetting cycles, and thermal cycles on the short-term mechanical characteristics of clayey soil-GDL interfaces have been measured according to the results of rapid loading shear tests using the self-designed temperature and stress-controlled large direct shear apparatus.

(3) The impacts of environmental loadings, including drying-wetting cycles and thermal cycles, on the creep mechanical characteristics of clayey soil-GDL interfaces have been measured according to the results of creep shear tests using the self-designed temperature and stress-controlled large direct shear apparatus.

1.4 Thesis structure

To present the study, the thesis has been divided into ten chapters:

Chapter 1 presents the introduction, justification**, aim and objectives** of the study, and highlights the original contributions of the study to knowledge.

Chapter 2 **Literature review**. This chapter covers geosynthetic materials, especially GDL, the application of these materials and quantification of interface performance criteria.

Chapter 3 **Methodology**. This chapter introduces and justifies the methodology that is adopted to achieve the aim and objectives of the study.

Chapter 4 **Shear box design and construction.** This chapter introduces a bespoke stress and temperature-controlled large shear apparatus on soil-geosynthetics interfaces. Such an apparatus allows for the shear deformation behaviour of soil-geosynthetics interfaces under environmental loadings, including elevated temperature, drying-wetting cycles, and thermal cycles to be investigated. The results of validation tests for the functionality of the modified apparatus are presented.

Chapter 5 details the results of **rapid loading direct shear tests** on clayey soil-GDL interfaces subjected to drying-wetting cycles, thermal cycles as well as elevated temperature using the self-designed large direct shear apparatus. Quantification about the impacts of environmental factors on the short-term mechanical characteristics of clayey soil-GDL interfaces has been detailed.

Chapter 6 details the results **of creep shear tests** on clayey soil-GDL interfaces subjected to drying-wetting cycles and thermal cycles using the self-designed large direct shear apparatus. Quantification about the impacts of environmental factors on the creep mechanical characteristics of clayey soil-GDL interfaces has been conducted.

Chapter 7 **Discussion**. A discussion of the research results presented in Chapter 5 and Chapter 6, presenting an in-depth mechanism analysis of the research results.

Chapter 8 **Conclusions and recommendations.** This chapter reviews the completed research work in relation to the aim and objectives of the study. Moreover, the main findings in correspondence to the aim and objectives are listed, respectively. Finally, the limitations of the research and recommendations for future work are highlighted.

Chapter 2

Literature Review

2.1 Geosynthetics

2.1.1 Overview of geosynthetics

According to the definition presented by the International Geosynthetics Society (IGS), geosynthetics refers to "planar products manufactured by polymeric materials adopted with soil, rock, earth, or other geotechnical engineering related materials as an integral component of human-man projects, structures or systems" (Shukla and Shukla, 2002). Geosynthetics have been widely applied in almost all areas of civil, coastal, environmental, geotechnical, hydraulic and transportation engineering to achieve the functions of enhancing drainage, durability, flexibility, strength, waterproofing, as well as controlling degradation. The wide span application of geosynthetics can be attributed to the following reasons (Sarsby, 2006):

• Simple installation and low cost

• Partially or completely replacing natural materials, including clay, gravel, sand, etc.

• High resistance to biological, chemical and physical degradation

• Long service life span

• Straightforward transportation and storage

• High flexibility and light weight

• Being environmentally friendly

To satisfy the different demands of engineering projects in today's society, a large number of different kinds of geosynthetics are available. These geosynthetics can broadly be categorised to various types according to their manufacturing method, basic properties and particular functions such as geotextiles, geogrids, geonets, geomembranes, geosynthetics clay liners, geopipes, geofoams and geocomposite, etc. In this research, the focus is GDL. Thus, GDL and geotextile (a component of GDL) are described in detail in the following sections.

2.1.2 Geosynthetic Drainage Layers (GDL)

GDL are a combination of at least one kind of geosynthetic products, including geotextiles, geogrids, geonets and geomembranes, etc. in order to achieve multi-functions and reduce costs. In general, GDL consists of a polymeric drainage core laminated to filter or separate materials to transmit in-plane flow, which can substitute traditional methods of adopting layers of gravel and graded sand, with significantly smaller thickness and higher flow capacity (Pilarczyk, 2000).

GDL can be broadly classified into three types: wick drains (prefabricated vertical drain) (Figure 2.1) , sheet drains (Figure 2.2) and highway edge drains (Figure 2.3) (Shukla and Shukla, 2002). Wick drains are typically composed of plastic nubbed or fluted drainage cores that are wrapped by geotextile filters. Compared to conventional vertical sand drains, the advantages of applying wick drains as a rapid method to consolidate fine-grained saturated soil include that, wick drains can provide tensile reinforcement for structures and have marginal resistance against water flow, with simple installation, smaller volume and low cost.

Figure 0.1 Geocomposite wick drain

The second category is sheet drains. Sheet drains are panel-like, rigid polymer drainage cores that can be nubbed, columned, or dimpled to constitute a three-dimensional net. Geotextile is bonded on one or two sides of the polymer drainage core as filter and separator. The sheet geocomposite drain is often applied in large planar areas, such as behind retaining walls, against soil or rock slopes, beneath athletic fields, etc. According to its structure, the sheet drains can be classified as biplanar geonets, triplanar geonets or cuspate core, as shown in Figure 2.1. After testing by researchers, the cuspate core sheet drain has the highest transmission capability amongst the different types of sheet drains (Koerner, 2012). The GDL adopted in this research belongs to the cuspate core sheet drain. A cuspate core sheet drain is typically composed of a single cuspate drainage core with geotextile filter laminated on both sides. The geotextile on the studded dimple side of the drainage core functions as a drainage filter, whilst the geotextile on the flat side is to enhance interface shear strength. Usually, fluid entry is only possible from one side of the GDL. Typical applications of the GDL include capping, cut-off trenches, embankments, gas vents, landfills, mining containments, retaining walls, roadworks and tunnels, etc. They are suitable for such purposes as they avoid the water from penetrating and drain the overlying water to improve the stability of structures.

The biplanar geonet sheet drain is typically composed of two extruded, identically dimensional, parallel, HDPE ribs that overlap with different angles to the machine direction. The biplanar geonet geocomposite can achieve better resistance to compression, but its transmission capability of fluid flow is the smallest compared to other types of geocomposite drains.

The triplanar geonet sheet drain is generally comprised of three sets of ribs: one set of major ribs and two sets of minor ribs. The major ribs run in parallel to the direction of fluid flow and are sandwiched between the two sets of minor ribs that are bonded to the top and bottom of the major ribs. The triplanar geonet geocomposite drain has high compressive resistance, which makes them useful for use in airports, dams, embankments, landfills and roads.

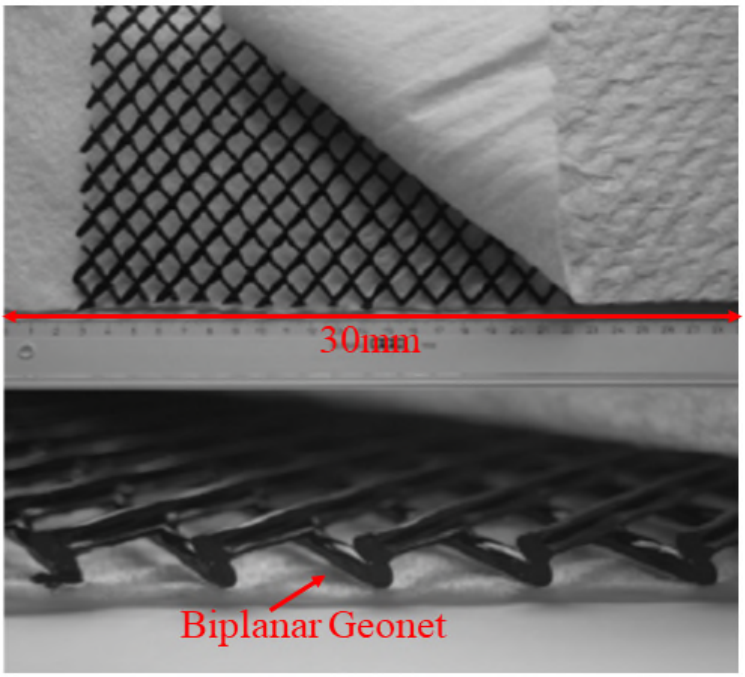

(a) Biplanar geonets

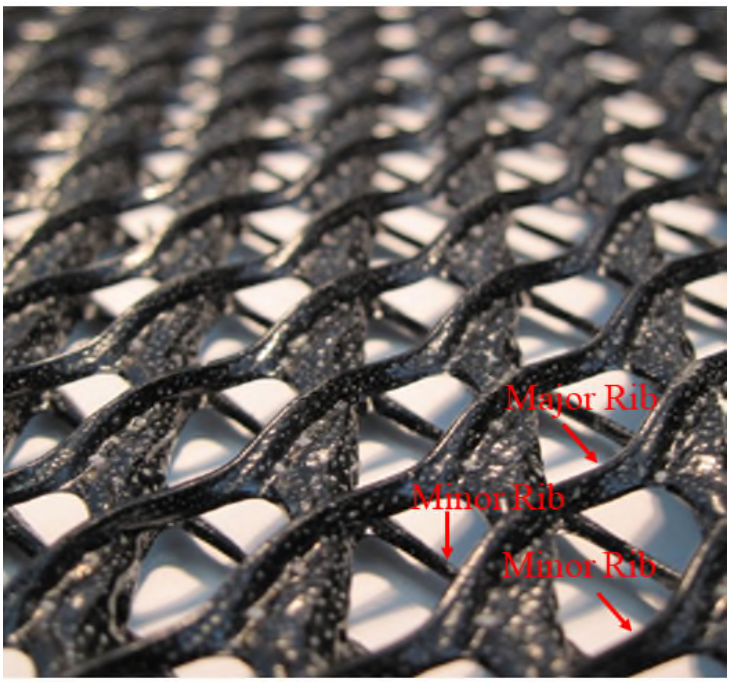

(b) Triplanar geonets

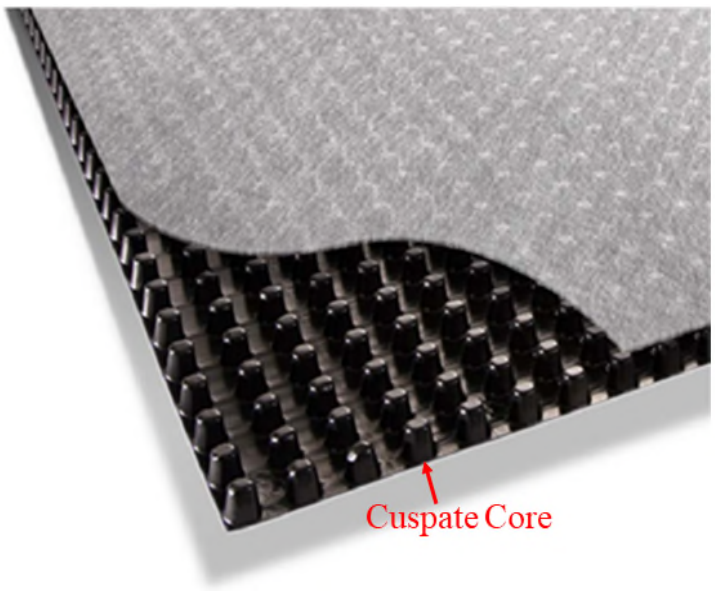

(c) Cuspate core

Figure 2.2 Sheet drain geocomposite layer (Othman, 2016)

The third type is prefabricated geocomposite edge drains, which is a perforated geocomposite drain serving as a complete edge drain system consisting of a perforated pipe bonded by geotextiles, as shown in Figure 2.3. This type of geocomposite drain is often placed underneath the stone base of

highway and airfield pavements to improve the performance and lifetime of highways.

Figure 0.3 Geocomposite edge drain

2.1.3 Geotextiles

As above mentioned, geotextile is often adopted to encapsulate the drain core of GDL to provide filtration and separation functions. According to its name, geotextiles are textiles, but they are composed of polymers, such as polypropylene (92%), polyester (5%), polyethene (2%), and polyamide (1%), instead of natural textiles like cotton, wool, silk, etc. Thus, they have a long lifetime and strong resistance to biodegradation (Koerner, 2012). Based on the style of fabrics, geotextiles are broadly categorised as woven, non-woven and knitted geotextiles, as shown in Figure 2.4.

The woven geotextile is cloth-like fabrics produced by traditional weaving loom, composed of interlacing multiple sets of parallel threads or yarns. The threads or yarns run along the length direction called the warp and those run perpendicularly are called the weft, as shown in Figure 2.5.

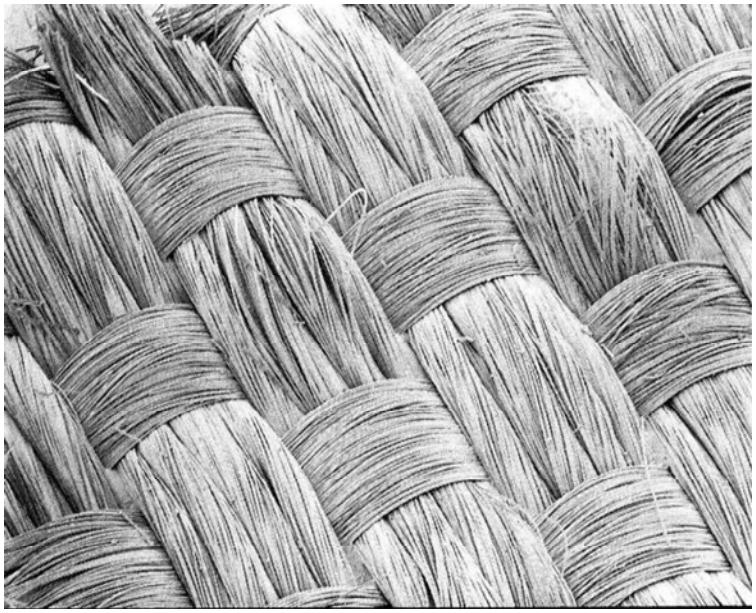

(a) Woven

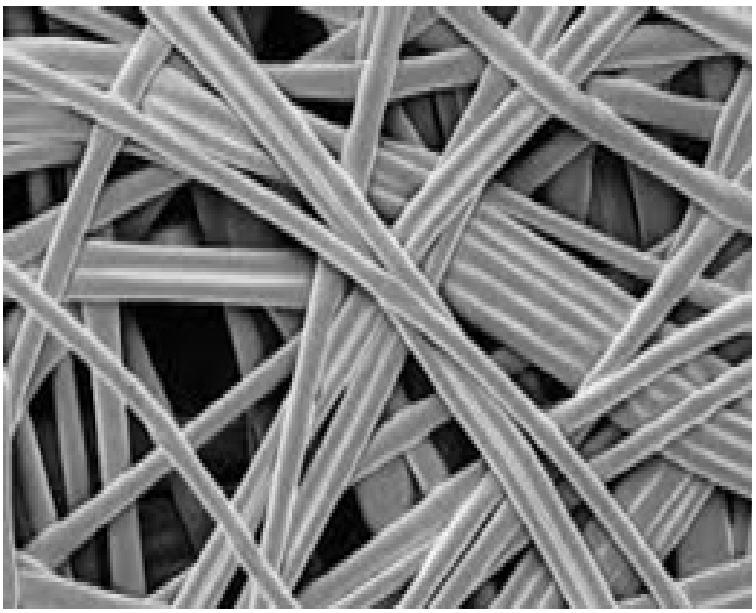

(b) Nonwoven

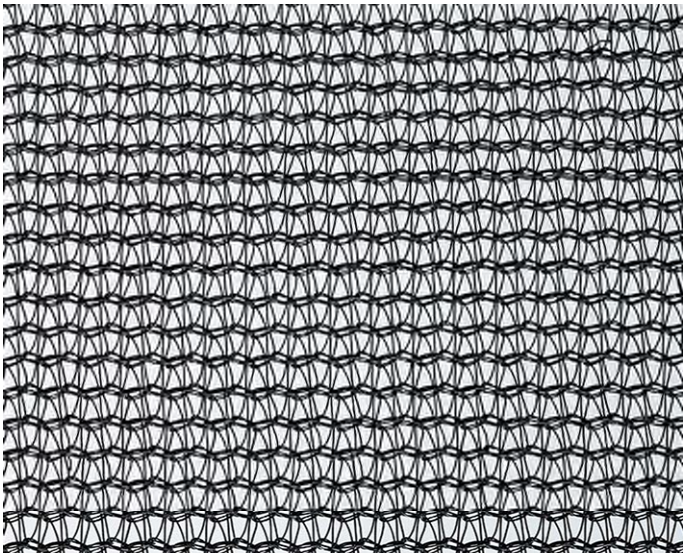

(c) Knitted

Figure 2.4 Geotextiles (Koerner, 2012)

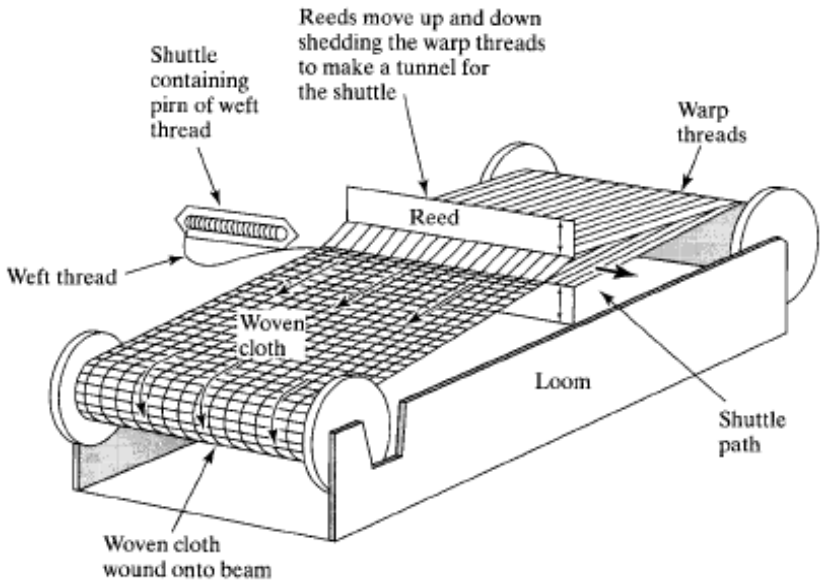

Figure 2.5 Weaving of woven geotextiles (Shukla and Yin, 2006)

The non-woven geotextile is felt-like fabrics, made by stochastically placing fibres on a running conveyor strap with random orientation to form a continuously loose web and bonding them together. The bonding process can be categorised into three types: mechanical bonding (needle punching),

thermal bonding, and chemical bonding, depending on the applied bonding technique. Needle punching is conducted by adopting many barbed needles to pass through the loose fibre web to bond them together, improving fabrics strength and integrity, as shown in Figure 2.6, which is the most common non-woven geotextile bonding approach. It can produce geotextiles with high mass per unit area and yet retain considerable volume (Shukla and Yin, 2006). During the thermal bonding, the fibre web is melted together at filament or fibre crossover points to impose extra strength on the fabrics by heat rollers to form stiff and thin geotextiles. During the chemical bonding process, acrylic resin is impregnated or sprayed on or into the fibre web. After curing or calendering, bonds are generated between the filaments or fibres. Usually, an air-drying operation is applied to reconstitute the open structure of fabrics before the hardening or curing of the resin.

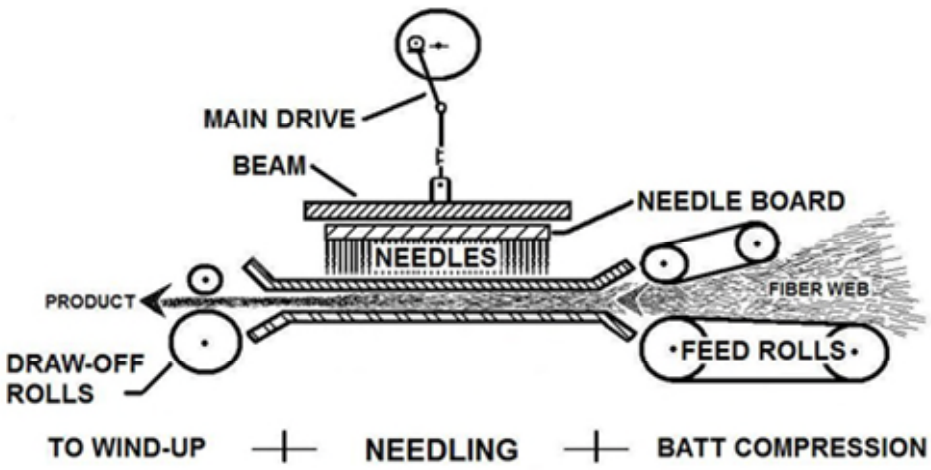

Figure 2.6 Needle punching process (Shukla, 2017)

2.1.4 Discussion

The above analysis provides a brief description of the used GDL in this thesis. It allows the general understanding of the basic properties, functions, components of the used GDL, which is helpful for understanding the research of quantifying the mechanical behaviour of cover soil-GDL interfaces subjected to environmental loadings. The above analysis also demonstrates

the wide application of GDL in engineering projects, which further indicates the importance of the research.

2.2 Landfill cover systems

2.2.1 Overview of landfills

Along with human activities, multiple waste sources, including domestic, hazardous, industrial and municipal solid waste are generated around the world. In the UK, there are approximately 300 million tonnes of waste created every year (Crawford and Smith, 2016). Despite the increasing reuse and recycling of these wastes, there is still a large amount of waste that needs to be disposed of in the environment. Landfills are the main method to dispose of wastes in many countries due to their economical and environmental acceptability.

Landfills are constructed into or on top of the ground. The waste is isolated in it from the surrounding environment, including groundwater, air, rain, etc. with a bottom liner and top cover system. To prevent the escape of pollutants in landfills that may contaminate the environment, a high degree of tightness is an essential requirement for the safe operation of the landfill site. Thus, landfills are composed of a multi-barrier system, including bottom and side lining systems and cover systems (Fowmes et al., 2008). The bottom and side lining systems are generally composed of a geomembrane/ geosynthetic clay liner (GCL) and are installed underneath waste to raise the efficiency of leachate collection and reduce potential contamination to the soil beneath and groundwater. A typical landfill is presented in Figure 2.7. This research mainly focuses on landfill cover systems; thus, the landfill cover system is introduced in detail in the following section.

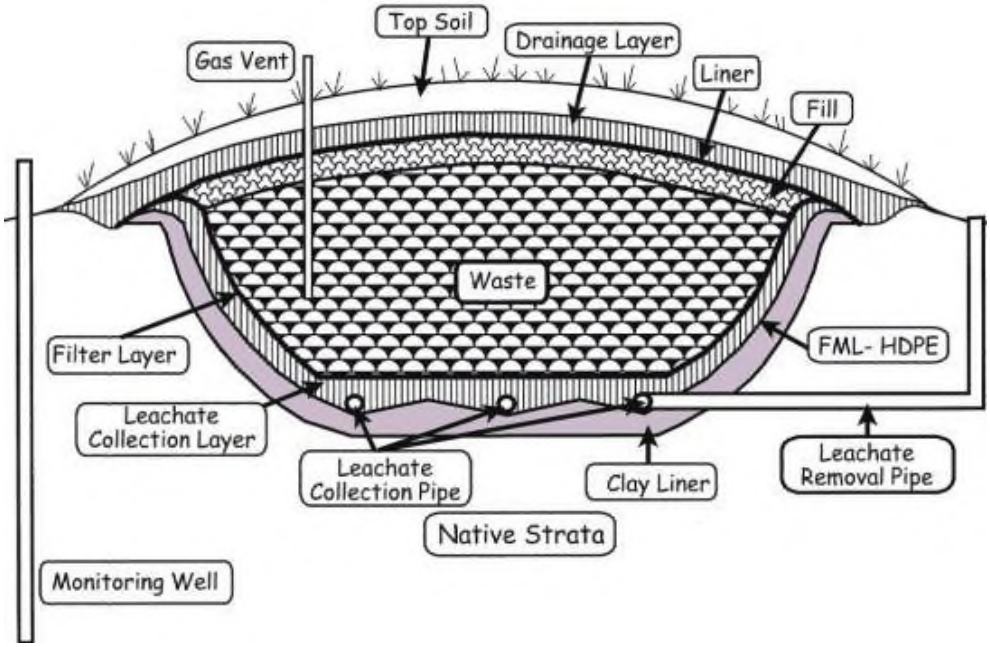

Figure 2.7 Typical cross-section of landfills (Fred Lee and Jones-Lee, 2005)

Different types of geosynthetics have been applied in landfills to minimize the pollutions migration into the surrounding environment (Othman, 2016). In general, geosynthetics are often adopted as drainage materials (GDL), filter materials (geotextiles), hydraulic and gas barriers (geomembranes) as well as protection and reinforcement materials (geotextiles). The application of geosynthetics can provide more economical and technical benefits than traditional materials. For example, geomembrane infiltration barriers and GDL with a thickness of a few millimetres can produce similar performance to soil infiltration and a drainage barrier composed of gravel and granular soil with a thickness of up to several metres.

2.2.2 Overview of landfill cover systems

The landfill cover system is an impermeable cap installed on top of landfills once the construction of landfills is complete. The main functions of the cover system are as follows (Crawford and Smith, 2016):

• To separate the waste from the environment in order to protect public health

• To prevent precipitation, including rainwater and melted snow, from penetrating underlying waste and limit the contamination of groundwater by leachate

• To control the release of generated gases, odour, etc., into the atmosphere

• To save on maintenance costs

• To reduce erosion

• To form a proper surface for revegetation and reclamation of the place

• To avoid animals and insects from coming into contact with waste

The design of landfill cover systems depends on the specific conditions of the sites and the expected functions of cover systems. Thus, the constitution of landfill cover systems ranges from a single layer of soil with vegetation to a complicated multi-component system of soil and geosynthetics. However, in general, all landfill cover systems should include a barrier layer with low permeability, a surface water drainage layer, and cover soil. The soil that is often adopted in landfill cover systems is sand and clay, usually used as drainage material and cover soil, respectively.

2.2.3 Individual constitute of landfill cover systems

A typical landfill cover system is illustrated in Figure 2.8.

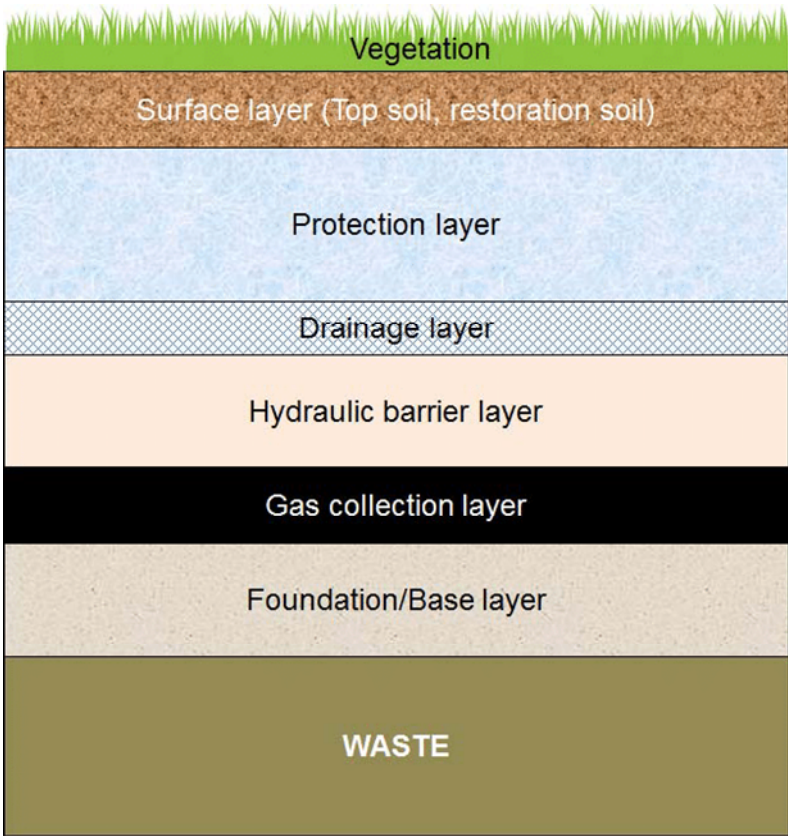

Figure 2.8 Typical landfill cover system (Othman, 2016)

Based on Figure 2.8, the common landfill cover system is composed of (from bottom to top) a foundation layer, gas collection layer, hydraulic/ barrier layer, drainage layer, and a protection cover soil layer. A description of each component is detailed below.

Foundation layer

This layer serves as a base for the capping construction, which is composed of sand or gravel soil. As the initial waste separator, the foundation layer also can contour the existing surface of the landfill.

Gas collection layer

The main functions of gas collection layers are to collect and remove gases that may be generated due to the anaerobic decomposition of waste. The gas collection layer can be constructed by coarse-grained soil with high permeability, such as sand, gravel, etc. (up to 300 mm thickness), along with geosynthetics with high in-plane transmissivity, such as geotextiles, geonets, geocomposite, etc.

Hydraulic barrier layer

The hydraulic barrier layer can directly avoid water from percolating through the cover system into the underlying waste and facilitate drainage in the overlying layer. Furthermore, the hydraulic barrier layer can also prevent generated gases from escaping into the atmosphere. The hydraulic barrier layer can be constructed by a single material of naturally compacted clayey soils, geomembranes, geosynthetics clay liners, etc. Normally, when compacted clay is used as the hydraulic barrier layer, it requires at least 1 m thickness and a hydraulic conductivity less than 1×10^{-9} m^2. Due to the small thickness, straightforward instalment and low hydraulic conductivity, GCL is often adopted as the hydraulic barrier layer. The GCL installed in cover systems must be resistant to cracking caused by a change of moisture content (Guyonnet et al., 2009). The aforementioned single materials can also be combined to form a hydraulic barrier layer with better performance, such as the combination of clayey soil and a geomembrane.

Drainage layer

The drainage layer is a vital component of landfill cover systems in the aspect of preventing the infiltration of precipitation into underlying waste, which is very important for the overall stability of cover systems (Khire and Haydar, 2005). The drainage layer can decrease the water head of the hydraulic barrier layer, and contribute to both controlling and reducing the pore water pressure of cover soil. Moreover, the drainage layer can drain water in the overlying protection soil layer and diminish the moisture content of the surface soil

layer timely following rainfall or snowfall. If a drainage layer is not installed, the percolation of water can apply hydrostatic head to the barrier layers and ultimately infiltrate into the underlying waste. This can result in the generation of excessive leachate and excessive water head in both the basal protection layer and surface soil layer, decreasing the stability of landfill cover systems.

Materials for constructing the drainage layer should have sufficient filtration to operate without clogging during its lifespan. It is an essential requirement for water to freely discharge from the drainage layer of landfill cover systems into the outlets. With the wide application of geosynthetics in engineering projects, geosynthetics such as GDL and geonets are increasingly applied as the drainage layer. Such materials have a smaller thickness than that of granular soil, whilst maintaining a sufficient flowability (Chinkulkijniwat et al., 2017).

Cover soil layer

Cover soil is adopted to protect the underlying layers of landfill cover systems from frost damage and loads and to withstand the erosion of wind and water. The cover soil can also reduce the influence of temperature and moisture content variations on the underlying layers. Most cover soil layers allow for the growth of grasses and plants. In general, 0.5 - 1 m is the minimum thickness of cover soil layers, which is thick enough to avoid the penetration of roots. The cover soil is often derived from sites or adjacent areas to reduce construction cost. In general, the process of building cover soil layers is very straightforward. Cover soil is typically placed loosely then spread by excavators, without a specific compaction plan being deployed (Othman, 2016).

2.2.4 Geosynthetics used in landfill cover systems

Geosynthetics have almost become the standard material used in the cover and liner systems of landfills. Nearly every type of geosynthetics has been adopted in landfill cover and liner systems to serve one or several functions, replacing traditional material, such as clay, sand, gravel, etc. (Guyonnet et al., 2009).

In cover systems, geomembranes are often used to replace clay as the hydraulic/gas barriers. Geotextiles are frequently installed in combination with geomembrane, sand, and clay as protection layers, separation layers or filtration layers. Geogrids can be installed to reinforce slopes underneath the waste and cover soil above geomembranes. Geogrids and geotextiles also provide support functions for geomembranes installed above them to resist differential settlement of the below wastes. GDL, which are often placed on the downslope in the direction of roll in combination with textured geomembranes, sand or cover soil layers, are mainly employed to collect/remove surface water and vent gas. The placement of GDL at slope corners and in confined spaces does not need to follow the same pattern. The geomembrane infiltration barrier layer and GDL, with a thickness of a few millimetres, can achieve equivalent performance to the clay infiltration layer and gravel/sand drainage and collection layer, with a thickness of up to several metres. This is more economical, straightforward to install and environmentally friendly since less filling of materials means lower carbon dioxide emissions.

2.2.5 GDL in landfill cover systems

For landfill cover systems, rain often results in the build-up of water head in the cover soil layer and the generation of pore water pressure at the cover soil-geosynthetics interfaces. This reduces the stability of cover systems. Thus, the drainage system is a vital component in landfill cover systems to decrease the moisture content of waste and cover soil. Traditional solutions involve the

use of coarse sand and gravel as the drainage layer. Considering the benefits of high hydraulic transmission, low costs and simple installation, GDL has more recently been utilised as the hydraulic cover layer in landfill cover systems in order to diminish the water head in cover soil layers, with low-cost (Khire and Haydar, 2007).

The GDL utilised in landfill cover systems should meet the following basic requirements: high hydraulic transmission (higher than 3×10^{-5} m/s), with a non-woven geotextile filter bonded on the upside of the drainage core to avoid the penetration and clogging of the upper cover soil, and with a geotextile bonded on the downside of the drainage core to raise friction and minimise sliding between the drainage core and underlying hydraulic barrier layer. As aforementioned, the primary purpose of non-woven geotextiles bonded on the upper side of the drainage core is filtration. To satisfy the filtration function, the non-woven geotextiles should allow for the passage of water into the drainage core to reduce pore water pressure, whilst preventing soil particles from migrating as this can clog the drainage core during the lifetime of the cover systems. Thus, the design of non-woven geotextiles should guarantee high hydraulic transmission whilst retaining a tight fabric structure to keep soil retention.

2.2.6 Stability analysis of landfill cover systems

In general, failure of landfill cover systems is owed to the sliding of the cover soil layer on the hydraulic barrier layer, which is controlled by soil-geosynthetics interface shear strength. Consequently, knowledge regarding the shear strength of cover soil-geosynthetic interfaces is vital for the design of landfill cover systems.

The stability of landfill cover systems is mainly controlled by the smallest value amongst the interface shear strength between different geosynthetics

and soil-geosynthetics. With a rise in inclination angle and length of slopes, the shear force induced by gravity also rises. If the shear resistance of soil-geosynthetics or geosynthetics-geosynthetics interfaces is lower than the shear stress caused by the overlying materials, sliding of the cover soil occurs and results in the failure of cover systems. Usually, the weakest shear resistance is the soil-geosynthetics interfaces. Thus, the peak shear strength of soil-geosynthetics interfaces is important variables in the design of landfill cover systems.

2.2.7 Influence of environmental factors on the stability of landfill cover systems

During operation, it is inevitable that landfill cover systems will be subject to different environmental conditions, including rainfall, drought, temperature variations, etc. The environmental factors have non-negligible influences on the stability of landfill cover systems because the environmental factors can result in drying-wetting cycles, thermal cycles, elevated temperature, etc. on cover soil-GDL interfaces, respectively (Bouazza et al., 2011; Fleureau et al., 2002; Koerner and Koerner, 2006a). Environmental factors have large influences on the interaction mechanism between installed GDL and cover soil, significantly changing the mechanical properties of cover soil-GDL interfaces (Othman, 2016). For example, cover soil-GDL interfaces in landfills are usually exposed to elevated temperature due to exothermal reaction from waste biodegradation and hydration, with temperatures ranging from 30 ℃ to 60 ℃ within the landfills (Abuel-Naga and Bouazza, 2013; Hanson et al., 2015; Jafari et al., 2014). Additionally, climatic effects, such as drying-wetting cycles and thermal cycles, generated by rainfall and ambient temperature variation, also have non-negligible impacts on the mechanical properties of cover soil-GDL interfaces over the lifespan of landfills, respectively (Hosney and Rowe, 2013). This is due to the thickness of cover soil for landfills being relatively small (about 0.5 m to 2 m), making them susceptible to the presence of rainwater and ambient air temperature cycles (McCartney and Zornberg, 2010). Moreover, the high temperature

inside landfills further accelerates the evaporation of water in cover soil-GDL interfaces during the drying cycles, promoting the formation of drying-wetting cycles on the cover soil-GDL interfaces during climatic changes (Li et al., 2016). Particularly in the summer, the high ambient temperature further accelerates the evaporation of water in cover soil-GDL interfaces, forming apparent drying-wetting cycles. The influence of varying the moisture content of soil has been pointed out by researchers (Kong et al., 2018; Liu et al., 2020). The drying-wetting cycles can cause shrinkage and expansion in the volume of soil to generate cracks and reduce the shear resistance of soil. Considering the detrimental impacts of drying-wetting cycles on soil, the shear resistance of cover soil-GDL interfaces would also be influenced, which may cause potential safety hazards on the long-term operation of landfills. However, a detailed study related to the variation of mechanical properties for soil-GDL interfaces during drying-wetting cycles and thermal cycles has not been reported to date.

Another vital factor that leads to the failure of landfill cover systems is percolation water from rainfall and melted snow. The softening effect of cover soil-GDL interfaces due to the saturation of cover soil caused by extreme rainfall significantly reduces the interface shear strength. This affects the stableness of cover systems. The softening behaviour also can be attributed to the capillary break, which refers to water that cannot flow from soil to GDL until a certain moisture saturation within the soil is reached. The existence of water not only increases the lubrication between soil particles and resolves the cement between them but also results in the generation of pore water pressure on the interfaces. A large number of reported landfill cover system failures can be attributed to the influence of water (Othman et al., 2018). Corresponding research has also been conducted by scholars to assess the impact of soil moisture content on the mechanical properties of soil-GDL interfaces (Othman et al., 2015).

Temperature is also a crucial factor affecting the stability of landfill cover

systems. Over the last decades, extreme high and low temperature as a result of global warming has led to the generation of thermal cycles on landfill cover systems. Additionally, due to the exothermal reaction from waste biodegradation and hydration, temperature rises within landfills and fluctuates over the operational term. This also leads to the elevated temperatures in landfill cover systems. Investigation into the cover systems of municipal solid waste landfills reveals that the temperature of cover systems changes seasonally along with the change of ambient temperature, and the elevated temperature in the underneath waste leads to a higher temperature in the cover systems compared to that of the external environment. Overall, the main direction of heat flow in landfill cover systems is upwards (Yeşiller et al., 2005). A summary of temperature in different landfills is presented in Table 2.1. Moreover, the mechanical properties, including modulus, strength and stiffness, etc. of polymeric materials change with the variation of temperature to influence the mechanical properties of cover soil-GDL interfaces. Thus, it is necessary to investigate the influence of temperature-related environmental factors, including drying-wetting cycles, thermal cycles and elevated temperatures on the stability of GDL cover systems.

2.2.8 Influence of other factors on the stability of landfill cover systems

For municipal solid waste landfills, landfill gas is produced due to the decomposition of waste. Even in the presence of a gas collection system, the produced gas cannot be extracted entirely in a short amount of time. For the landfill cover systems installed with geomembrane, the gas pressure just likes an excess pore pressure to reduce the effective normal pressure on the geomembrane layer. Hence, attention should be paid on the impact of produced gas on the stability of landfill cover systems when conducting design.

The shear strength of waste is also crucial for the stability of landfill cover

systems because the differential settlement of waste can impact the integrity of landfill liner and gas/leachate collection systems. Thus, proper shear strength of waste should be adopted in designing landfills.

Table 2.1 Summary of temperature in landfills

	Temperature measured (°C)	Measurement location	Landfill sites	Notes
Oweis et al. (1990)	As high as 55	At the bottom of waste in the base	Northern New Jersey, USA	Municipal Solid Waste Landfill
Collins (1993)	Between 30 to 40	In waste from top to the base	Germany	
Bleiker et al. (1995)	Highest at 59	Above the base of refuse	Toronto, Canada	Measurements at the bottom of boreholes drilled to the base
Yoshida and Rowe (2003)	As high as 50	In landfill base	Tokyo, Japan	
Barone et al. (2000)	Between 10 to 37	In bottom liner	Toronto, Canada	Municipal Solid Waste Landfill
Koerner and Koerner (2006b)	From 18 to 40	In final cover	Eastern Pennsylvania, USA	
Montgomery and Parsons (1990)	Between 7 and 27	In final cover	Southern Wisconsin, USA	
Corser and Cranston (1991)	As high as 43	In final cover	Southern California, USA	Measurements in a test section simulating a final cover
Khire et al. (1997)	From 1 to 30	In final cover	Central Washington State, USA	
Koerner and Koerner (2006b)	Between 0 and 30	In final cover	Philadelphia, Pennsylvania, USA	

During the construction process, the method of cover soil placement is important for the stability of landfill cover systems. It is recommended that cover soil is placed on slopes by a light bulldozer moving upslope. The method can compact the past placed soil by the gravity of newly placed cover soil and the equipment, as well as avoid the slippage of cover soil caused by the excessive loading of oversized equipment.

Vegetation is also a vital part of landfill cover systems. The root of vegetation can prevent erosion and decrease the rate of water flow by retaining water in cover soil to rise transpiration. Detrimental effects of vegetation include penetration of roots to the underlying waste can cause transportation of contamination to the surface and a rise in the hydraulic conductivity of soil, resulting in more water infiltrating underlying waste. Additionally, the roots may cause clogging on the geotextile of GDL, as shown in Figure 2.9. Thus, the unfavourable effects of roots cannot be negligible in the design process, and the root depth of vegetation is necessary to be assessed to guide the specification of the cover soil layer thickness.

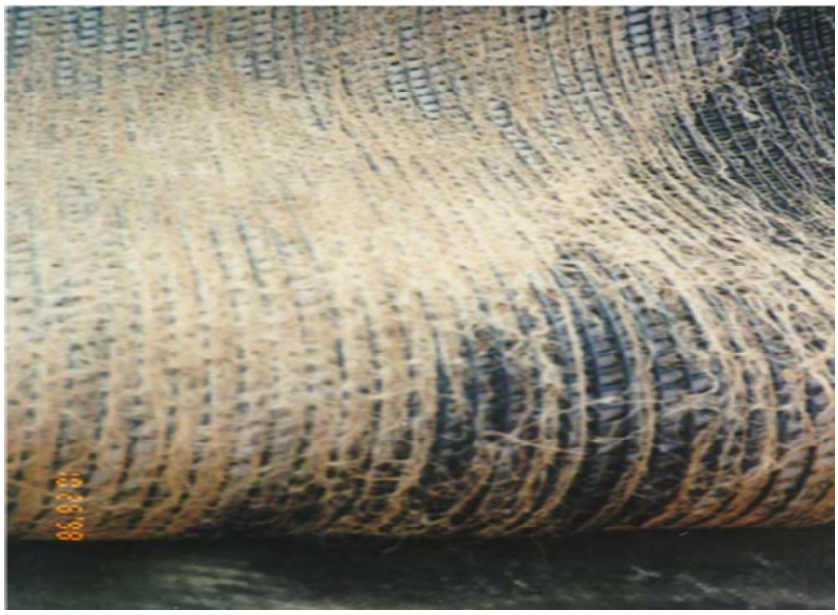

Figure 2.9 Root penetration in GDL (Othman, 2016)

2.2.9 Discussion

This section demonstrates that landfills are the main method to dispose of wastes in the world. Besides, the basic functions and components of landfill cover systems are introduced. Through introducing the widespread application of GDL in landfill cover systems and the advantages of using GDL to replace natural materials in landfill cover systems, the wide applicability of the research is emphasised. By conducting the stability analysis of landfill cover systems, it is manifested that the mechanical properties of cover soil-GDL interfaces govern the stability of cover systems. Additionally, the analysis of influence factors on the stability of landfill cover systems indicates the important effects of environmental factors, including temperature, drying-wetting cycles, thermal cycles, on the mechanical properties of cover soil-GDL interfaces and the stability of landfill cover systems. Overall, this section demonstrates the necessity and significance of conducing the research about quantifying the mechanical behaviour of cover soil-GDL interfaces subjected to environmental loadings.

2.3 Mechanical responses of geosynthetics subjected to environmental loadings

2.3.1 Geosynthetics subjected to temperature variation

Temperature has large effects on the mechanical characteristics of geosynthetics. The majority of geosynthetics are composed of HDPE, Polyvinyl Chloride (PVC), PP, etc., which have specific glass transition temperatures and melting temperatures. Below the glass temperature, the polymeric materials are in the glassy state. In this state, the thermal energy is not sufficient to allow polymer chains to move and the polymeric materials are only able to be deformed in a small amount before brittle rupturing. The melting temperature is higher than the glass transition temperature. When the temperature is higher than glass transition temperature but lower than melting temperature, the polymer materials are in the rubber state and become more flexible. This is due to the rising polymer chain mobility and rising free

volume resulting from the expansion of materials compared to that in the glassy state. Increasing chain mobility leads to a reduction in the tensile strength of polymeric materials and raises their capability to deform without breaking, as shown in Figure 2.10. The phenomenon becomes evident with a rise in temperature because molecules have more freedom of movement.

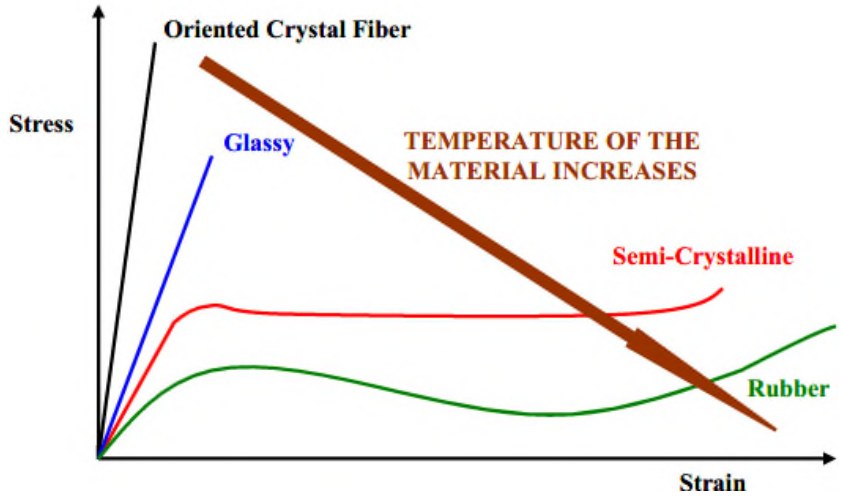

Figure 2.10 Stress-strain relationship curves of polymers under different temperatures (Karademir, 2011)

The relationship between the modulus of polymer materials and the temperature is shown in Figure 2.11. When the temperature is less than the glassy transition temperature, the modulus is steady. When the temperature is above the melting temperature, the modulus reduces considerably. Therefore, when the temperature is between that of the glassy transition temperature and melting temperature, an increase in temperature leads to higher malleability and surface pliability of the polymeric materials. The elevated temperature also can lead to higher softness and a reduction in the degree of roughness in geosynthetics. Subsequently, temperature is vital to the mechanical properties of polymeric materials, such as their modulus, strength and stiffness, etc.

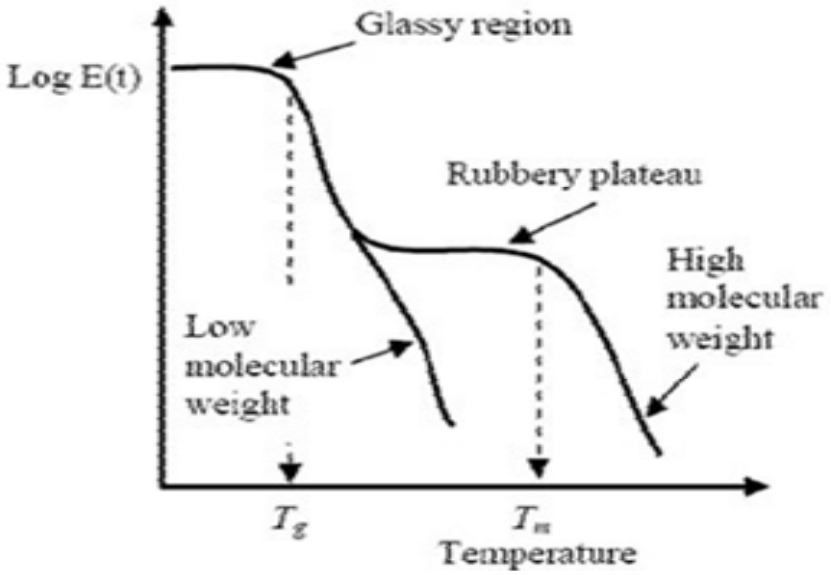

Figure 2.11 Relationship curve between modulus and temperature (Karademir, 2011)

Some scholars have carried out research into the temperature-dependent mechanical characteristics of geosynthetics. The impacts of temperature on the mechanical performance of a new sensor-enabled geosynthetics material named sensor-enabled geobelts were investigated by Cui et al. (2019). The study outcomes implied that, when temperature ranges from 10 ℃ to 20 ℃, the tensile strength of the geobelts rises rapidly, whilst within the range of 10 ℃ to 40 ℃, the tensile strength does not change much; Jafari et al. (2014) assessed the service life of HDPE geomembrane as the composite liner system in landfills. When the temperature of landfills rises from the range of 35 ℃- 45 ℃ to the range of 60℃-80℃, the service life of HDPE geomembrane reduces from around 300 years to approximately 90 years; Rowe et al. (2009) examined the service life of HDPE geomembrane with a 2 mm thickness submerged in air, water and replicated municipal solid waste landfill leachate under different temperatures. It was reported that the antioxidant depletion rate is the highest for the sample exposed to leachate and the slowest for the sample exposed to air. The predictive service life of the tested samples submerged in leachate is over 700 years at a temperature of 20 ℃, which is higher than 150 years at 35 ℃ and between 50-90 years at 50 ℃; Stępień and Szymański (2015) implemented tensile tests on woven

geotextile at different temperatures. The research indicated that the tensile strength reduces around 20 %, and the strain at the tensile strength increases from 10 % to 25 % as the temperature is increased from 20 ℃ to 100 ℃.

2.3.2 Geosynthetics subjected to other environmental factors

Other environmental factors, including erosion by saline solutions and exposure to ultraviolet, etc., also have relatively large effects on the mechanical characteristics of geosynthetics. Suits and Hsuan (2003) evaluated the degradation degree of geosynthetics exposed to Xenon Arc and ultraviolet-fluorescent at different temperatures by photo-degradation tests. The research indicates that elevated temperature can significantly accelerate the degradation of geosynthetics; The evaluation of mechanical and hydraulic characteristics of geomembrane, geotextile and GDL immersed in synthetic acidic mine drainage, acidic water, and de-ionized water for 22 months, with minimal exposure to oxygen and ultraviolet radiation, respectively, was performed by Gulec et al. (2005). The results of wide-strip, puncture and trapezoidal tear strength tests on the samples suggested that no noticeable change of the mechanical and hydraulic characteristics of the materials was observed; The impacts of ultraviolet exposure on the mechanical characteristics of woven and unwoven geotextiles were explored by Benjamim et al. (2008). The study indicated that after nonwoven geotextile samples were exposed to ultraviolet for around 200 days, the ultimate tensile load decreased to 44 % in the machine direction and 38 % in the cross-machine direction. Similarly, when woven geotextile samples were exposed to ultraviolet for approximately 1000 days, the ultimate tensile load decreased by 33 % and 84 % in the machine and cross-machine direction, respectively; Sumi et al. (2018) investigated the durability of coir geotextiles in a range of environments including acidic, alkaline, neutral and saline environments, as well as during wetting-drying cycles, freeze-thaw cycles, and biological degradation. It was found that the tensile strength of coir geotextiles decreased by 40 %, 45 % and 38 % after submersion in acidic (pH 5), alkaline (pH 9) and neutral (pH 7) conditions, respectively. In comparison, the saline

environment and wetting-drying cycles led to a minor decrease in the tensile strength (7 %). After freeze-thaw cycles, the tensile strength decreased by 12 %. In terms of biological degradation, the tensile strength of geotextiles buried in soil with a depth of 25 cm was too low to measure. Whilst the decreasing percentage in tensile strength of those buried in soil with a depth of 50 cm and 75 cm were less than 20 %.

2.3.3 Discussion

In this section, the mechanical responses of polymer geosynthetics subjected to environmental loadings are analysed. Particular attention is paid on the influence of temperature on the mechanical properties of polymer geosynthetics, including the mechanism analysis and the summarisation of relevant existing research about the change in mechanical properties of polymer geosynthetics due to temperature variation. Based on the analysis in this section, temperature has large effects on the mechanical characteristics of geosynthetics. More specifically, the mechanical properties of polymer geosynthetics, such as modulus, strength and stiffness, deteriorate with a rise in temperature. Due to the deteriorated mechanical properties of polymer GDL at elevated temperature, the detrimental impacts of temperature-related environmental loadings on the mechanical properties of soil-GDL interfaces cannot been ignored.

2.4 Shear strength of soil-geosynthetics interfaces

2.4.1 Shear mechanism of soil-geosynthetics interfaces

The interaction mechanism between soil and geomembrane/geotextile can be attributed to two major parts: the interlocking between soil and filaments/ roughness of geosynthetics and the friction between soil and geosynthetics (Jones and Dixon, 1998). The interlocking mechanism has a close relationship with the roughness of the geosynthetics surface and the height of asperity. Rough surface and high asperity can allow for a high peak shear strength of the interfaces (Koutsourais et al., 1991). Under low normal stress, the

asperities are modestly inserted into the soil. Sliding is the dominating mechanism between soil and geomembrane/geotextile, in which shear resistance is developed from the friction between soil and asperities. Under high normal stress, the asperities are totally inserted into the soil. Ploughing is the dominating mechanism between soil and geomembrane/geotextile, in which shear resistance is developed by two aspects: the internal shear strength of soil and the friction force between the geosynthetics and soil. The critical normal stress for the conversion between sliding and ploughing relies on the kind of soil and the properties of geomembrane/geotextile. For soil-geotextile interfaces, the fibres type of geotextile also impacts the shear mechanism. More loose filaments and larger gaps can produce higher interlocking, resulting in larger friction strength compared to thermally bonded geotextiles (Dove and Frost, 1999).

The interaction mechanism between soil-GDL interfaces has some differences to that of soil-geomembrane/geotextile interfaces. Under low normal stress, the interaction mechanism of soil-GDL interfaces is similar to the above-mentioned soil-geotextile interfaces since non-woven geotextile is considered as the shear surface of GDL. However, under high normal stress, the bonded non-woven geotextile is compressed around the cuspate elements on the drainage core, with soil being embedded into the drainage core. The interlocking between soil and the cuspate elements on the drain core provides extra shear resistance for the interfaces, which improves the peak shear strength of the interfaces (Othman, 2016). A detailed analysis of such is presented in Chapter 7.

2.4.2 Influence of geosynthetics properties

The properties of geosynthetics have significant influence on the shear strength of soil-geosynthetics interfaces. A large number of scholars have carried out corresponding studies (Giroud et al., 1993; Mosallanezhad et al., 2016; Palmeira et al., 2002).

To research the influence of geosynthetic tensile strength on the shear strength of soil-geosynthetics interfaces, large direct shear tests on soil/PET-yarn geotextile interfaces were conducted by Liu et al. (2009). The experimental results indicated that the shear strength of interfaces was significantly smaller than that of soil. The shear strength was also found to increase with the increase in the transverse tensile strength of the PET-yarn geogrids and decrease with the rise in the aperture length and open area per cent of PET-yarn geogrids; A similar conclusion was presented by Mahmood et al. (2000), who suggested that the shear strength of clayey soil-nonwoven geotextile interfaces rises in correspondence to the increase in geotextile tensile strength.

To investigate the mechanical responses of interfaces between soil and different geosynthetic, Athanasopoulos (1996) explored the mechanical behaviour of the interfaces between wet cohesive soil and woven / nonwoven geotextiles. The research revealed that, although the woven geotextile has high tensile strength, it could not provide substantial strength to the wet cohesive soil-geotextile interface. In comparison, the nonwoven geotextile could lead to a rise in shear resistance of the interface since the openings in the geotextile could be filled with soil to form interlocking between soil and geotextile.

Regarding the geometry of geosynthetics, Basudhar (2010) performed experimental research on interfaces between sand and two multifilament woven geotextiles, one with a fine and one with a coarse texture. The peak shear strength of the interfaces between soil and coarse-textured geotextile with openings was evidently larger than that of the interfaces between soil and fine-textured geotextile with visible openings; Fowmes et al. (2017) introduced rapid prototyping techniques to produce geomembranes with different spacings between the ribs and heights of asperities. The

experimental study on the interfaces between the produced geomembrane and clay revealed that the spacing of ribs and height of asperities have relatively large effects on the shear strength of the interfaces. It was found that an optimum spacing between ribs ranged from 7 mm to 9 mm and a height of 0.4 mm for asperities was found to be sufficient in transferring stress to the soil in unsubmerged states.

2.4.3 Influence of soil properties

The moisture content of soil has a vital influence over the mechanical performance of soil-geosynthetics interfaces. Choudhary and Krishna (2014) carried out direct shear tests on the interfaces between sandy soil with varying moisture content ranging from 5.5 % to 66 % and smooth/ textured HDPE geomembranes. The experimental results revealed that increasing moisture content had marginal influence on the friction angle of the interfaces; The impacts of water content and the dry density of soil on shear properties for interfaces between four types of cohesive soils (one sand and three clay with different plasticity) and four types of geosynthetics (three different geogrids and one woven geotextile) were researched by Abu-Farsakh et al. (2007). The study revealed that a rise in water content and/or the decline in the dry density of soil could result in a significant decrease in shear strength of the interfaces; An experimental study regarding the shear behaviour of interfaces between clayey soil with different moisture contents and geotextiles was performed by Chai and Saito (2016). An increase in shear strength of the interfaces was seen with a rise in soil moisture content since a higher soil moisture content was able to promote soil particles to enter the openings of geotextiles.

Considering the size of soil particles, a range of direct shear tests on interfaces between poorly graded soil and woven geotextiles / uniaxial geogrids were carried out by Hsieh et al. (2011). The study suggested that when soil particles were smaller than the openings of geotextiles, soil particles were able to interlock with geosynthetics, causing shear resistance of the interfaces to be

close to the soil. If not, the soil particles were considered to turn around and slide along the geosynthetics surface and the shear resistance was markedly smaller than that of soil particles; Wang et al. (2016b) carried out direct shear tests on interfaces between coarse silica soil with different soil particle sizes and geogrids. The experimental results indicated that the peak shear strength and residual shear strength of the interfaces increase with an increase in soil particle size; Direct shear tests on interfaces between four types of diverse soils (fine, medium, coarse sand and fine gravel) and planar / 3D geogrids were carried out by Makkar et al. (2019) to investigate the impacts of particle size on the shear behaviour of the interfaces. The research pointed out that, the interface shear strength coefficient, which refers to the ratio of shear strength between soil and the soil - geosynthetics interface, of soil-geogrid interfaces reduces with an increase in soil particle size. Overall, the interface shear strength coefficient (1.25) of the medium sand-planar geogrid interface is the highest amongst those of the interfaces studied; Choudhary and Krishna (2014) explored the shear deformation of interfaces between four kinds of cohesionless soil and two different geosynthetics (woven and nonwoven geotextiles). It was found that the mean particle size of the soil had significant impacts on the shear strength of soil-geosynthetics interfaces and the kind of geosynthetics determines whether the impacts are promotional or detrimental. The soil gradation can also alter the shear resistance of interfaces, where soil that has a flatter gradation curve results in higher shear resistance.

A systematic investigation about the influence of silt content of soil on the shear behaviour of silty sand-geogrid interfaces was performed by Naeini et al. (2013). The research outcomes showed that with an increase in silt content of the soil, the interfaces reach peak shear strength under greater shear strain. The shear strength declines as silt content increases from 0 to 35 %. After 35 %, the impacts of variation in the silt content of soil on the shear strength is not measurable.

Regarding the relative density of soil, Tuna and Altun (2012) carried out the

tests on interfaces between sand with 65 % and 25 % relative densities and woven/nonwoven geotextiles. It was found that the denser sand had higher interface shear strength and dilation deformation than those of loose sand during the shearing process.

The impacts of sand particle shape on the shear behaviour of sand-woven geotextile interfaces were studied by Anubhav and Basudhar (2013). The study revealed that both the peak and large displacement friction coefficients of rounded sand-geotextile interfaces were measurably smaller than those of angular sand-geotextile interfaces.

Bacas et al. (2015) suggested that there was a positive correlation between the shear strength of soil and the shear strength of soil-geomembrane interfaces. The higher the soil shear strength, the higher the shear strength of soil-geomembrane interfaces.

2.4.4 Experimental conditions

Normal stress plays a crucial role in the shear strength of soil-geosynthetics interfaces. As reported by Mofiz et al. (2004) who conducted direct shear tests on cohesive soil-nonwoven geotextiles, the shear strength rises around 160 % when normal pressure is increased from 50 kPa to 400 kPa; Based on the direct shear tests on soil-geomembrane interfaces, the conclusion that the shear strength of the interfaces doubled when pressure was increased from 50 kPa to 200 kPa was obtained by Feng and Cheng (2014).

The impacts of consolidation on the shear strength of clay-textured HDPE geomembrane interfaces by direct shear tests were investigated by Ellithy and Gabr (2000). The research pointed out that the rise in shear strength of the interfaces was due to the consolidation process. This process allowed for the interlocking between the clay particles and the texturing of geomembranes;

Direct shear tests on silty clay-geocomposite and geogrid interfaces under drained, undrained and partially drained conditions were conducted by Ling and Tatsuoka (1994). The higher shear strength of interfaces under drained conditions relative to undrained conditions could be attributed to the build-up of pore water pressure under undrained conditions since this build-up decreases the effective normal pressure on the interfaces.

The duration of water submersion also influences the mechanical behaviour of soil-geosynthetics interfaces. Suzuki et al. (2017) pointed out that the shear strength of bentonite clay-woven/nonwoven geotextiles reduces over prolonged water submersion due to the swelling of bentonite clay.

In terms of experimental scale, Roodi et al. (2018) evaluated the shear behaviour of soil-geosynthetics interfaces by pullout tests with different scales, including small, standard and large scales. The shear stress-displacement relationship curves for the standard and large-scale tests are similar, whilst those of the small-scale tests are different.

.

Frost and Karademir (2016) performed direct shear tests on sand-geomembrane interfaces in temperatures ranging from 21 ℃ to 50 ℃. The research showed that, under higher temperature, the peak shear strength is higher than that under low temperature because the sand particles can penetrate deeper into the geomembrane surface at higher temperatures.

Regarding the shear rate, Fishman and Pal (1994) conducted consolidated drained / undrained direct shear tests on smooth/textured HDPE geomembrane-clay interfaces, with different shear displacement rates varying from 0.005 mm/min to 12.7 mm/min. The research revealed that within this range, the rate of shear displacement had a marginal influence on the shear strength of smooth HDPE geomembrane-clay interfaces. In comparison, the

shear behaviour of clay-textured HDPE geomembrane interfaces was correlated to the shear displacement rate. In drained conditions, under a low shear displacement rate, the shear strength of the interfaces was less than or equal to that of the clay. Whilst under a high shear displacement rate, the shear strength of the interfaces was larger than that of the clay under the same shear displacement rate.

2.4.5 Discussion

According to the above analysis, the mechanical performance of soil-geosynthetics interfaces, with differing properties of soil and geosynthetics, have been extensively investigated under various experimental conditions. However, research into the influence of environmental factors, including drying-wetting cycles, thermals cycles, and elevated temperature, etc. on the mechanical behaviour of soil-geosynthetics interfaces is rarely reported, let alone, the investigation into soil-GDL interfaces. The environmental factors have a noteworthy influence on the mechanical properties of soil-GDL interfaces. For example, in regard to the existence of thermos-softening plastics in GDL, exposure to elevated temperature can alter the mechanical properties of GDL. This includes, but is not limited to, a decrease in modulus, stiffness and tensile strength, all of which can cause detrimental effects on the mechanical properties of soil-geosynthetics interfaces. For example, it has been reported that when soil is subjected to drying-wetting cycles, a decline in the shear strength of soil occurs due to the development of cracks and structural damage of the soil (Guney et al., 2007; Md et al., 2016; Wang et al., 2016a; Zhang et al., 2015). A decrease in strength of both the soil and GDL unavoidably impacts the mechanical properties of soil-GDL interfaces. Hence, there is a need to explore environmental factors such as drying-wetting cycles, thermal cycles and elevated temperature on the mechanical performance of soil-GDL interfaces.

2.5 Creep deformation of soil-geosynthetics interfaces

2.5.1 Creep mechanism of individual materials

Creep behaviour refers to the time-dependent deformation of materials under constant tensile or compressive stress, less than the strength of materials (Bagheri et al., 2019; Rezania et al., 2020). Geosynthetics and many soils are visco-elastic-plastic materials, where if the constant loading exceeds a specific value, creep deformation can occur (Bagheri et al., 2020; Sawicki and Kazimierowicz-Frankowska, 1998). In general, the load imposed on soil and geosynthetics is tensile stress.

The typical tensile creep behaviour is drawn in Figure 2.12, where creep strain and creep strain rate are represented by a solid line and a dashed line, respectively. The creep behaviour can be classified into three stages: primary stage, secondary stage, and tertiary stage. In the primary stage, strain gradually rises with a decrease in strain rate after the immediate elastic deformation caused by imposed stress. In the secondary stage, the rise in strain is linear in elapsed time because of the constant strain rate. In the tertiary stage, creep behaviour is illustrated by a sharply rising strain and strain rate before reaching creep failure (Karademir, 2011). The creep strain of polymeric materials under high temperature or constant load over a long period is mainly attributed to the movement of molecules. Such movement includes distortion of lengths and angles of chemical bonds between atoms, and the rearrangement of atoms. Atomistic variations result in changes to the molecular chains in semi-crystalline polymers, including uncoiling, straightening and breaking in amorphous regimes as well as slipping between chains in crystalline regimes.

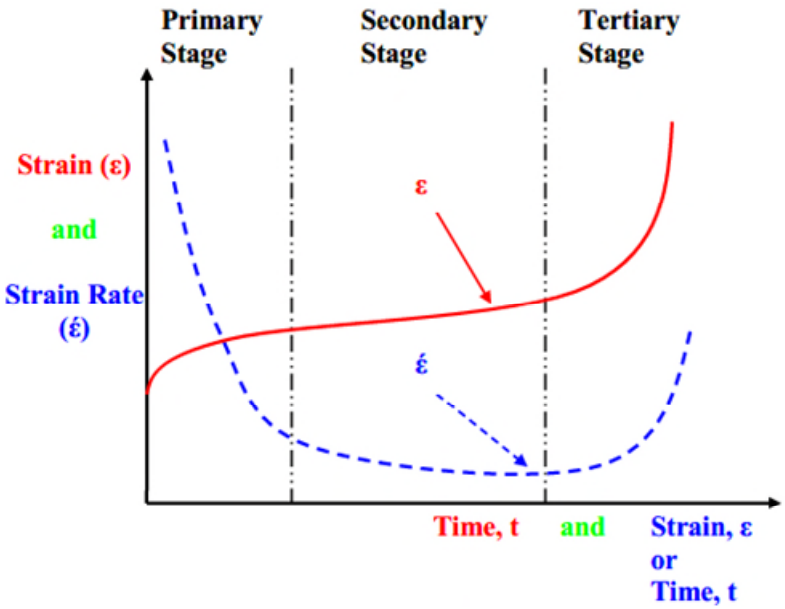

Figure 2.12 Typical tensile creep behaviour (Yeo, 2007)

Many variables, such as shear stress and temperature, can influence the creep strain of geosynthetics and soil. In landfills, temperature and shear stress change in elapsed time. Therefore, the effects of temperature and shear stress on the creep behaviour of geosynthetics and soil is crucial. At high temperature, molecules can have a larger free volume and more freedom of motion, as shown in Figure 2.13. Thus, a rise in temperature can lead to an increment in immediate strain when imposing stress and a rise in the strain rate of the secondary creep stage. This can result in a corresponding decline in the time of failure, which has the same effect as that of higher loads on the creep strain. The relationship between temperature and creep strain rate, as well as the detrimental influence of high temperature on the mechanical and durability characteristics of polymeric materials, can be applied to accelerate the creep process and diminish testing time. Such relationships include Time Temperature Superposition Method (TTS), etc. (Van Gurp and Palmen, 1998).

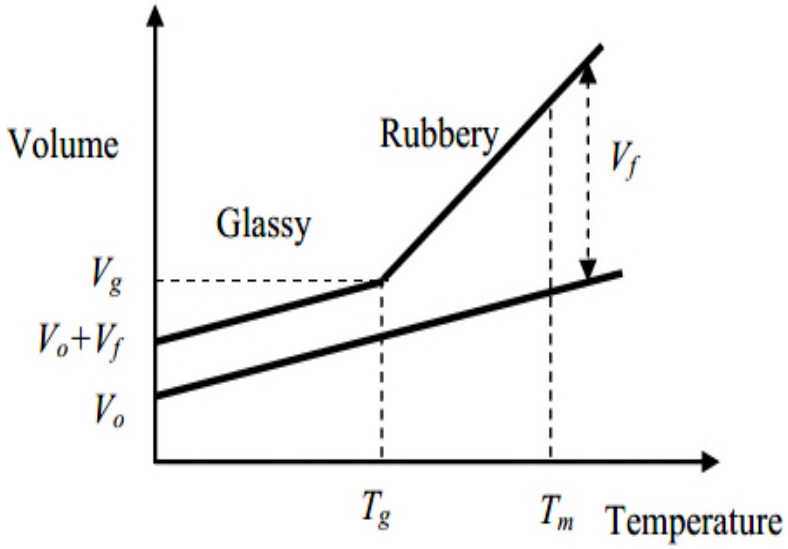

Figure 2.13 Relationship between the free volume of polymer and temperature (Yeo, 2007)

2.5.2 Creep behaviour of geosynthetics

Evaluation of creep behaviour on geosynthetics at room temperature often requires a long time, typically over one year. This is referred to as the conventional creep test method. According to the experimental results obtained, the long-term behaviour of geosynthetics is attained via the extrapolated method. The conventional creep test method is the most reliable, and some investigators have adopted this method to evaluate the creep behaviour of geosynthetics. For example, Zanzinger and Alexiew (2000) assessed the creep deformation of a stitch-bonded GCL under 75 % shear stress of the peak strength and 20 kPa normal stress. They conducted 11 different individual tests, with a duration over 1000 hours. However, long measurement durations may cause some inconveniences for researchers when adopting the conventional creep test method.

To save experimental time and labour, the TTS principle was adopted by some scholars to accelerate the creep deformation of geosynthetics (Alwis and Burgoyne, 2006; Li, 2000; Tajvidi et al., 2005). In TTS, creep curves attained at elevated temperatures are moved along the log-time scale to

produce a creep master curve at a smaller reference temperature. This is shown in Figure 2.14. Some scholars have used this method to evaluate the creep deformation of geosynthetics. For example, Jeon et al. (2002) investigated the creep behaviour of multiple geogrids under creep shear loading with 40 %, 50 % and 60 % of the design strength by TTS procedure, respectively. Based on the experimental results, the creep strain of the geogrid over 10000 hours was predicted. When using the TTS method, each temperature stage requires the use of a new sample. Thus, multiple tests on different specimens are required to be conducted simultaneously in order to produce a single master creep curve. This allows the experimental results to be easily influenced by variability in specimens.

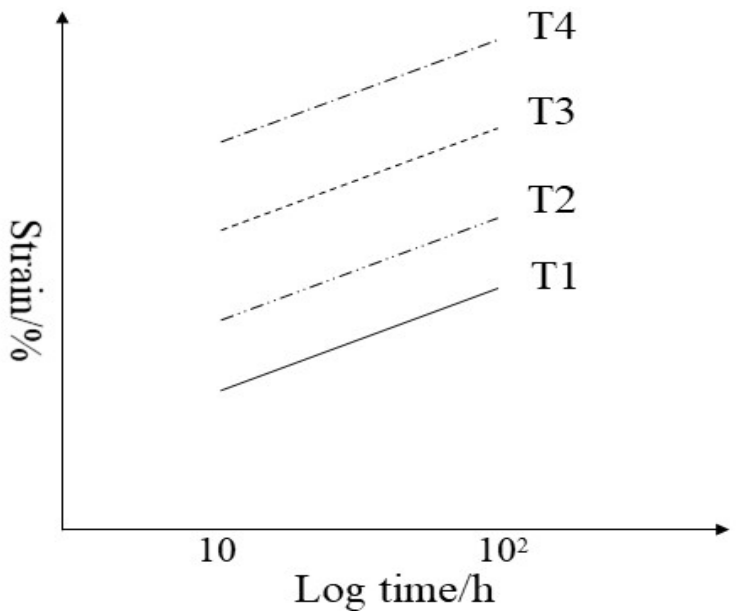

(a) Raw data

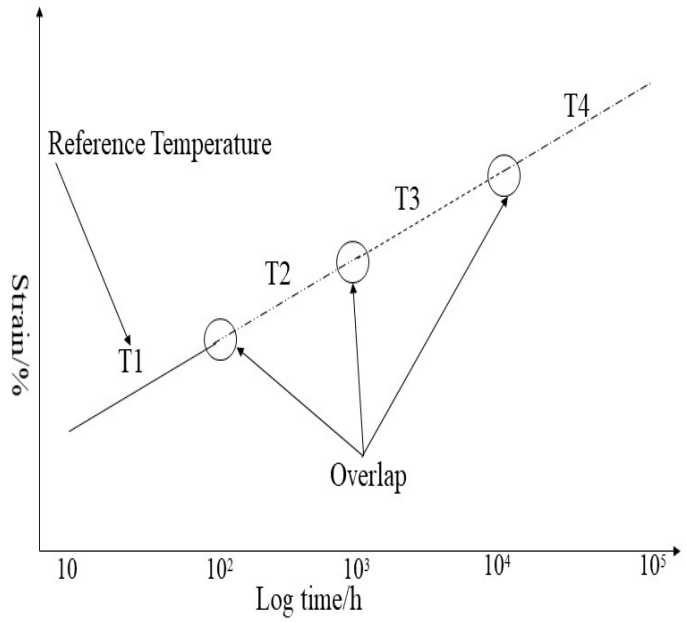

(b) Prediction of creep deformation by shifting

Figure 2.14 Procedure of TTS (Karademir, 2011)

To solve the shortcomings of TTS, the Stepped Isothermal Method (SIM) is used to assess the long-term creep deformation of geosynthetics based on short-term creep experiments by combining the principles of TTS and Boltzmann superposition (Achereiner et al., 2013; Grebneva et al., 2015; Hsiehl et al., 2008; Hsuan et al., 2005). In SIM, a single test specimen is loaded with shear stress continually, whilst being exposed to a number of elevated temperature steps. The creep deformation at different elevated temperatures is moved along the log-time scale to a lower reference temperature to establish a creep master curve, as shown in Figure 2.15. The main improvement of SIM, compared to TTS, is the reduction in specimen variability along with the avoidance of using multiple experimental devices by conducting tests on a single specimen.

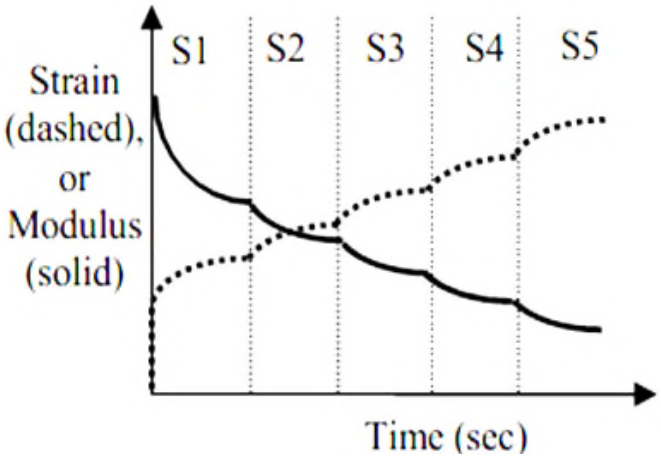

(a) Raw data

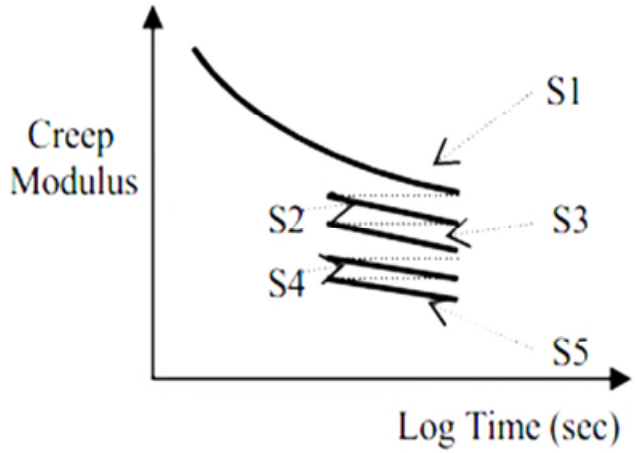

(b) Before shifting

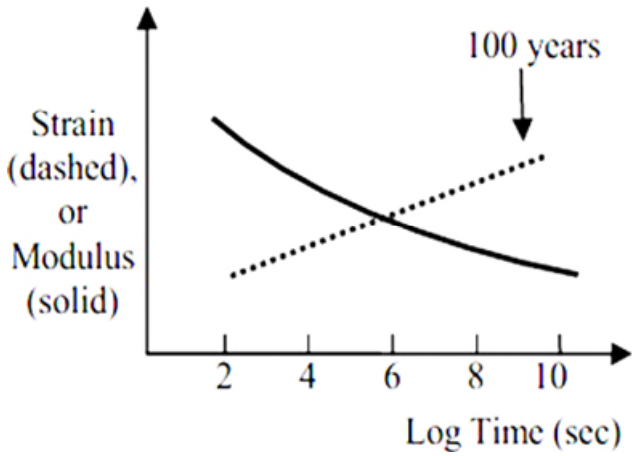

(c) Master curve after shifting

Figure 2.15 Procedure of SIM (Karademir, 2011)

SIM has been widely adopted by scholars to investigate the creep behaviour of polymers. Comparisons between experimental results obtained by conventional creep tests, TTS and SIM have been conducted. The longitudinal and lateral creep behaviour of nonwoven needle-punched geotextiles was studied by Bueno et al. (2005), who adopted both conventional and SIM procedures. The results obtained by conventional and SIM methods were in satisfactory agreement, where longitudinal creep deformation of the nonwoven geotextiles was found to be higher than that in the lateral direction; Jones and Clarke (2007) assessed the creep behaviour of geogrid with the duration of 120 years under a consistent shear stress of 40 % tensile strength using SIM. Based on the test results, rupture of the specimen was estimated to occur after 302 years; Yeo and Hsuan (2010) performed SIM, TTS, and conventional creep tests on PET and HDPE geogrids. The research implied that the different creep test methods gave similar results. Before the occurrence of failure, the PET geogrid had smaller creep deformation than that of the HDPE geogrid. The HDPE geogrid experienced primary, secondary and tertiary creep stages before rupture, whilst the PET geogrid merely experienced primary and tertiary creep stages before failure; Hsuan and Yeo (2005) compared the predictive creep behaviour of HDPE geomembrane by TTS and SIM procedures, respectively. The study concluded that the master creep curves attained from both TTS and SIM were similar; The applicability of SIM in evaluating the creep behaviour of geosynthetics was also validated by Zornberg et al. (2004) who performed creep tests on woven geotextiles by conventional and SIM procedures, respectively. The residual tensile strength, which refers to the tensile strength of geosynthetics after creep deformation, of the woven geotextiles was over 90 % of the peak tensile strength and independent of the creep loading level and time.

To simulate a real situation, some researchers have evaluated the creep behaviour of geosynthetics confined by soil. França and Bueno (2011) conducted both in-isolation and confined creep tests on three different geosynthetics (biaxial geogrid, woven geotextile and nonwoven geotextile) at

elevated temperature. For both of the geogrid and nonwoven geotextile, soil confinement reduced the creep deformation of the geosynthetics, whilst for the woven geotextile, creep deformation was not impacted by the soil confinement.

Ghazizadeh and Bareither (2018b) established a stress-controlled direct shear apparatus that can assess the creep behaviour of GCL exposed to elevated temperature and hydration in saline solutions. The research revealed that the time to fail decreased with a rise in shear stress and that the shear stress at failure is linearly correlated to the logarithm of the time to fail. Additionally, the decline in internal shear strength of GCL subjected to elevated temperature was observed. In terms of the influence of saline solutions, hydration by the calcium-rich mining solution could increase the internal shear strength of GCL. Meanwhile, a decrease in internal strength was found after hydration in a highly alkaline mining solution.

2.5.3 Creep behaviour of soil

A majority of research regarding the creep deformation of soil was conducted under triaxial shear conditions. The creep deformation of artificially frozen soil in triaxial unloading conditions was investigated by Li et al. (2017). The study revealed that the creep rate reduces with an increase in consolidation confining pressure. Under low deviatoric stress, only the first and second stages of the creep deformation occur. The third creep stage only occurs when the stress level surpasses a specific value; Triaxial creep tests, with suction-controlled on unsaturated clay, were carried out by Li et al. (2017). The experimental outcomes implied that the axial strain had a positive linear relationship with respect to time, whilst the axial strain rate had a negative linear relationship with time. Stress and suction also have effects on the axial strain and strain rate, whereby axial strain and strain rate increase with an increase in deviator stress and fall in matrix suction, respectively; Tang et al. (2020) studied the creep behaviour of Loess with varying water content under

different triaxial stress conditions. An increase in creep deformation was observed during a rise in water content and a decline in confining pressure, respectively; Triaxial shear creep tests on coral sand and silica sand with different relative densities under varying deviatoric stresses and confining pressures were conducted by Lv et al. (2017). The findings illustrated that the volumetric, axial and shear creep strain of the coral sand were approximately 5, 20, and 10 times higher those of silica sand, respectively; Lechowicz et al. (2019) carried out triaxial shear creep tests and torsional shear creep tests on organic soil. The experimental results implied that the strain rate of the soil is not only related to time but also related to volumetric and deviatoric stress.

Duttine et al. (2015) assessed the creep behaviour of three different kinds of sand and gravel with different particle shapes in drained direct shear conditions. It was found that the shear displacement of soil was enhanced as the soil particles became rounder, the grading became more uniform, and the specimens became looser, respectively.

2.5.4 Creep behaviour of soil-geosynthetics interfaces

There is a lack of information relating to the creep behaviour of soil-geosynthetics interfaces. Amongst the limited studies available, Liu and Martinez (2014) investigated the creep behaviour of sand-smooth/textured geomembrane interfaces with a duration of 240 minutes at room temperature. The results of tests demonstrated that the shear creep deformation of the interfaces was similar to the creep deformation of many other materials. The interfaces exhibited primary creep deformation at first, followed by the secondary creep deformation. The creep deformation was found to rise with an increase in the creep shear stress level. However, the study did not involve the impacts of environmental factors on the creep behaviour of soil-geosynthetics interfaces. Additionally, the creep period was short and therefore does not sufficiently reflect the creep behaviour of soil-geosynthetics interfaces during extended durations. Rhodes (2019)

researched the long-term creep behaviour of the interfaces between needle punched geotextile and embossed geomembrane with different asperity heights and temperatures based on SIM for around 12 hours at creep stress levels between 45% to 70% of the peak interface shear strength in order to predict the creep deformation of the interfaces over 114 years. The investigation showed that both higher asperity and temperature resulted in an increase in the creep strain rate and the interface failed faster under higher temperature. However, this research did not involve the creep behaviour of soil-geosynthetics interfaces.

2.5.5 Discussion

Based on the details mentioned above, most existing research focuses on the creep behaviour of individual materials, rather than the interfaces between them. Referring to analysis in Section 2.5.1, the interaction mechanism between soil and geosynthetics can be divided into two major parts: the interlocking between soil and filaments/roughness of geosynthetics and the friction between soil and geosynthetics. This is different from the creep mechanism of individual materials. A similar interaction mechanism between soil and adjacent structures during creep deformation was reported by Yang et al. (2020). In this research, Yang investigated the creep deformation of clayey soil-rough concrete interfaces. It was found that, during creep deformation, the interaction mechanism between soil and concrete includes the bonding force between soil and concrete surface and the sliding friction force between soil and concrete structure. Thus, based on the above analysis, creep behaviour of individual soil and geosynthetics cannot characterise the creep behaviour of soil-geosynthetics interfaces, especially for soil-GDL interfaces. It is, therefore, necessary to conduct an investigation about the creep behaviour of soil-GDL interfaces, particularly for soil-GDL interfaces subjected to such environmental loadings.

2.6 Shear test devices for soil-geosynthetics interfaces

2.6.1 Direct shear test device

Currently, two main types of experimental apparatus are adopted to estimate the shear strength of interfaces between soil and geosynthetics. These include Direct Shear Apparatus (DSA) and inclined plane device. Additionally, for specialist testing, the ring shear device (RSA) has occasionally been adopted. Amongst these apparatus, the utilisation of DSA is the commonest because of its relatively easy operational procedure and accurate results (Zaharescu, 2018). According to the dimension of the shear box, DSA can be divided into two different types: small DSA with a dimension of 60×60 mm^2 and 100×100 mm^2, and large DSA with a dimension of 300×300 mm^2 and 300×400 mm^2. Based on the design of the top box, DSA can be classified as a fixed top box and floating top box. The floating top box is fixed at one point and can rotate around that point. Interface shear tests using the apparatus require a large test area. Figure 2.16 presents a typical DSA that consists of a fixed upper shear box and a movable bottom shear box. In the tests, the geosynthetics is clamped on the bottom shear box, and soil is filled in the upper shear box. The normal pressure is imposed vertically on the upper shear box, and the shear stress is imposed horizontally on the bottom shear box.

For the DSA with a fixed top shear box, since the upper box is restricted from rotation and displacement, the load plate may be subjected to a small rotating moment during the shearing process. The rotation of the load plate may impact the applied normal stress and result in the interface behaviour without strain-softening (Sia, 2007).

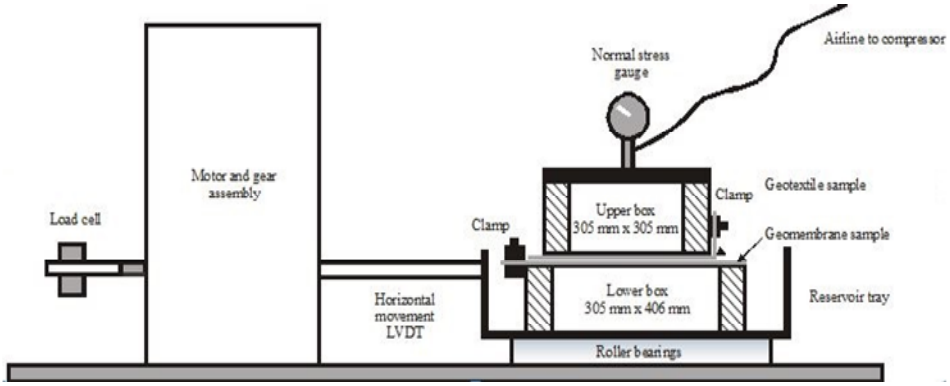

Figure 2.16 Typical DSA (Dixon et al., 2006)

Some researchers have conducted some modifications on DSA. Arulrajah et al. (2014) used a geosynthetics-clamping steel frame to be fixed on the upside of the bottom shear box. This can result in the height of the shear plane being over the geosynthetics placement level to increase the interlocking between geosynthetics and soil. The modified apparatus was adopted to conduct direct shear tests on the interfaces between biaxial/triaxial geogrids and aggregates. The experimental results were found to be closer to the real value than those obtained by conventional apparatus; Vieira et al. (2013) designed a large-scale DSA that can perform cyclic tests on soil-geosynthetics interfaces by adding a hydraulic actuation with closed-loop command computer controller. Using the apparatus, monotonic and cyclic direct shear tests on sand-geotextile interfaces were conducted. The research revealed that cyclic loading on the interface did not result in the fall of the monotonic peak shear strength; Fleming et al. (2006) modified a DSA by adding a miniature pore pressure transducer to measure pore water pressure variation of soil-geomembrane interfaces during shearing. Using such an apparatus allowed for the effective stress of the interfaces between soil and non-textured geomembrane during direct shear tests to be analysed.

RSA, which allows specimens to be continually sheared, is occasionally used to assess the mechanical behaviour of soil-geosynthetics interfaces. The main advantage of this device is that it is able to obtain a more accurate estimation

of the residual strength by applying unlimited displacement. Initially, RSA was designed to measure the mechanical properties of clay. After the modification by Stark and Poeppel (1994), the RSA was able to measure the shear strength of soil-geosynthetics and geosynthetics-geosynthetics interfaces. A typical RSA is presented in Figure 2.17, where the sample has a thickness of 5 mm and inner and outer diameters of 70 mm and 100 mm, respectively.

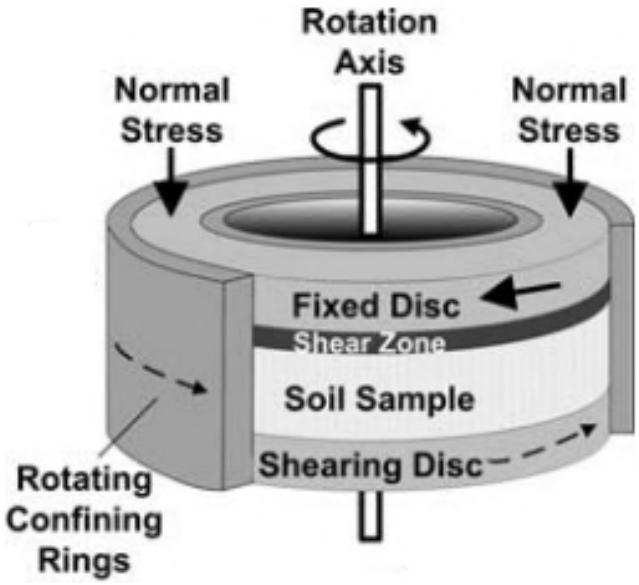

(a) Shear zone at the underneath of the sample

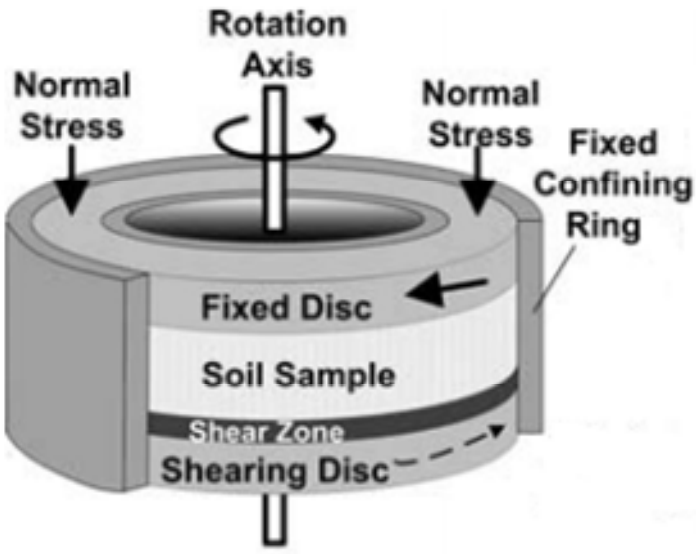

(b) Shear zone at the upside of the sample

Figure 2.17 Typical RSA (Sadrekarimi and Olson, 2009)

Ring shear tests on medium sand-geotextile interfaces were conducted by Tan et al. (1998). The experimental results were compared to those of direct shear tests. The study indicated that the shear rate of ring shear tests had marginal impacts on the shear strength of interfaces and the measured shear strength in the direct shear tests is higher than that obtained from the ring shear tests; Stark and Santoyo (2017) implemented torsional ring shear tests on interfaces between 10 different geomembranes (7 smooth and 3 textured) and 2 different soils (a clayey glacial till and Ottawa fine sand). The experimental results showed that when the geomembrane changes from smooth to textured, the increasing amplitude in interface shear strength for the glacial till is higher than that of Ottawa sand. This is due to the textures of geomembrane being able to embed into glacial till tightly during the shearing process, generating ploughing effects on the soil to provide more shear resistance.

The inclined plane apparatus can simulate better real field conditions, such as embankments, slopes of containment facilities, etc. because the shear deformation of interfaces using the inclined plane apparatus is controlled by stress rather than displacement. However, tests conducted by the apparatus is only under low normal stress (less than 10 kPa). Other disadvantages of the device are that the relative displacement between soil and geosynthetics is restrained by the length of the inclined plane and the displacement rate is difficult to control. A common inclined plane apparatus is presented in Figure 2.18.

As shown in Figure 2.18, the inclined plane apparatus is composed of an upper box for filling soil and a plane that can adjust the inclination angle for the soil-geosynthetic interface. In inclined plane tests, the gravity of soil can impose shear stress and normal stress on the specimen. In general, there is a normal stress loading system to impose excessive normal stress on the specimens. By adjusting the inclination angle of the plane, the normal stress and shear stress on the specimen can change.

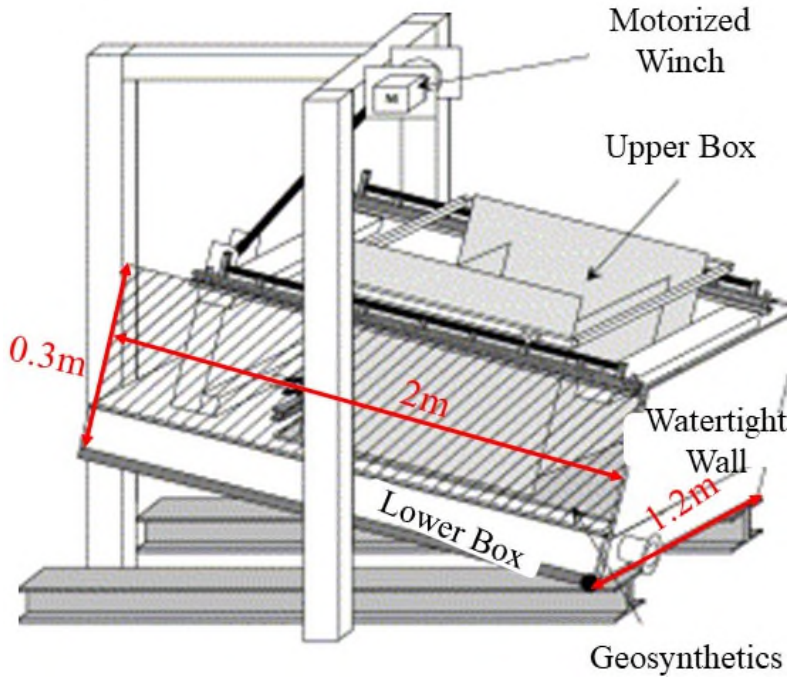

Figure 2.18 Typical inclined plane apparatus (Briançon et al., 2002)

Palmeira et al. (2002) carried out inclined plane tests on interfaces between two different soils (granular and cohesive) and 6 different geosynthetics (nonwoven geotextile, woven geotextile, geogrid, geonet, PVC geomembrane and HDPE geomembrane). The research indicated that the frictional conditions of the inclined plane surface could considerably influence the relative displacement between soil and geosynthetics; Lopes et al. (2014) researched the effects of soil water content and geosynthetics type on the interaction behaviour of residual soil and three different geosynthetics (geocomposite and geotextile) interfaces through inclined plane shear tests. The study revealed that the decrease in interface shear resistance is higher than 10 % when the soil water content is varied from dry to the optimum value; Monteiro et al. (2013) compared the experimental outcomes of direct shear tests and inclined plane shear tests on the interfaces between soil and three different geomembranes (PVC, smooth HDPE and textured HDPE). The study implied that the experimental outcomes from the direct shear tests and inclined plane shear tests were similar based on the interface friction angle.

2.6.2 Creep test device

Although there are many different types of existing creep test devices on geosynthetics and soil, respectively, the experimental apparatus on assessing the creep behaviour of soil-geosynthetics interfaces is rarely reported (Kongkitkul and Tatsuoka, 2007; Sawicki, 1999; Sawicki and Kazimierowicz-Frankowska, 1998). In the existing literature, Liu and Martinez (2014) presented a direct shear apparatus that can automatically control shear stress to keep a steady value during tests, which is able to conduct creep tests on soil-geosynthetics interfaces. However, the apparatus cannot adjust the temperature of soil-geosynthetics interfaces to explore the creep behaviour of soil-geosynthetics interfaces subjected to environmental loadings.

2.6.3 Discussion

According to the aforementioned analysis, a majority of currently adopted experimental devices, including DSA and RSA, for conducting shear tests on soil-geosynthetics interfaces are displacement-controlled, which is not representative of the real situation in engineering applications because, at real project sites, shear deformation of soil-geosynthetics interfaces is controlled by stress rather than displacement. Inclined plane apparatus can conduct stress-controlled direct shear tests, but the selectable range of normal stress is low (less than 10 kPa normal stress). Additionally, for all of the above-mentioned experimental devices, there is an inability to adjust the temperature of soil-geosynthetics interfaces to investigate the impacts of environmental factors, such as drying-wetting cycles, thermal cycles, elevated temperature, etc. on the short-term and creep mechanical behaviour of interfaces. Furthermore, conventional displacement-controlled direct shear apparatus cannot hold constant stresses whilst varying other parameters, such as temperature, drying and wetting conditions, etc. More importantly, it is impossible for the displacement-controlled apparatuses to conduct creep tests on soil-geosynthetics interfaces to explore their creep mechanical behaviour.

2.7 Summary

To provide the context of the study, this chapter conducts a description of geosynthetics and GDL and a depiction of landfills and landfill cover systems as well as the utilisation of geosynthetics and GDL in landfill cover systems. The literature illustrates that the mechanical properties of cover soil-GDL interfaces are vital to the stability of landfill cover systems, and environmental factors, such as drying-wetting cycles, elevated temperature and thermal cycles, have crucial impacts on the stability of landfill cover systems.

The summarisation of the existing literature found that the research about the influence of environmental loadings, such as drying-wetting cycles, thermal cycles, and elevated temperature, etc. on the short-term mechanical behaviour of soil-geosynthetics interfaces is seldomly reported, let alone, the investigation about soil-GDL interfaces. Thus, it is urgent to have a deeper understanding in this research area.

The review indicates that the creep shear mechanism of soil-geosynthetics interfaces is significantly different from that of individual geosynthetics and soil. Corresponding investigation into the creep shear behaviour of soil-geosynthetic interfaces subject to environmental factors is rare, let alone on the creep behaviour of soil-GDL interfaces. Thus, the influence of environmental factors on the creep deformation of soil-GDL interfaces requires more investigation.

The summary implies that the majority of currently adopted experimental devices are displacement-controlled, which is not representative of the real situation of stress-controlled shear deformation in engineering applications. Inclined plane apparatus can conduct stress-controlled direct shear tests, but the selectable normal stress range is low (less than 10 kPa normal stress). In terms of the devices for measuring creep shear deformation, although there

are many different types of existing creep test devices on geosynthetics and soil individually, the experimental apparatus on assessing the creep behaviour of soil-geosynthetics interfaces is rarely reported. Additionally, for all of the above-mentioned experimental devices, varying temperature of soil-geosynthetics interfaces to investigate the impacts of environmental loadings, including drying-wetting cycles, thermal cycles, elevated temperature, etc. on the short-term and creep mechanical behaviour of interfaces is not viable.

Chapter 3

Methodology

3.1 Research overview

This aim of this research focuses on quantifying the mechanical behaviour of cover soil-GDL interfaces subjected to environmental loadings. The following content briefly introduces the adopted methodology for achieving this aim.

To achieve the aim, a bespoke stress and temperature-controlled large shear apparatus on soil-geosynthetics interfaces was developed to allow the short-term and creep shear deformation behaviour of soil-geosynthetics interfaces subjected to drying-wetting cycles, thermal cycles and elevated temperature to be investigated; A series of rapid loading shear tests were conducted on clayey soil-GDL interfaces subjected to drying-wetting cycles, thermal cycles, drying-wetting cycle without heating, and elevated temperature, using the self-designed large direct shear apparatus to research the impacts of the environmental factors on the short-term mechanical behaviour of clayey soil-GDL interfaces (Objective 1); A series of creep shear tests were conducted on clayey soil-GDL interfaces subjected to drying-wetting cycles, thermal cycles and drying-wetting cycle without heating, using the self-designed large direct shear apparatus to research the impacts of the environmental factors on the creep mechanical behaviour of clayey soil-GDL interfaces (Objective 2).

3.2 Research tasks

Table 3.1 presents the research tasks for achieving the research aim and objectives in this study. The related journal papers have been identified in Table 3.2.

Table 3.1 Research tasks

Research task	Research methodology	Objective	Chapter
Literature review, state of the art for the research	Literature review	1-2	2
Designing and building the bespoke large direct shear apparatus		1-2	Chapter 4
Validating the functionality of the bespoke large direct shear apparatus			
Designing the rapid loading shear tests scheme		1	Chapter 5 and Section 7.2
Preparing soil-GDL interfaces specimens for rapid loading shear tests			
Conducting rapid loading shear tests			
Analysis of the experimental results of the rapid loading shear tests			
Designing the creep shear tests scheme		2	Chapter 6 and Section 7.3
Preparing soil-GDL interfaces specimens for creep shear tests			
Conducting creep shear tests			
Analysis of the experimental results of the creep shear tests			

Table 3.2 Publications associated with this thesis

Publication	Associated Chapters in this thesis
Zhiming Chao, Gary Fowmes. Modified stress and temperature-controlled direct shear apparatus on soil-geosynthetics interfaces. *Geotextiles and Geomembranes*. (Published)	Chapter 4
Zhiming Chao, Gary Fowmes. The short-term and creep mechanical behaviour of clayey soil-Geocomposite Drainage Layer interfaces subjected to environmental loadings. *Geotextiles and Geomembranes*. (Under review)	Chapter 5, Chapter 6, Section 7.2 and Section 7.3
Zhiming Chao, Gary Fowmes. Creep testing of clay-geocomposite interfaces during drying-wetting cycles. *EuroGeo 7 – 7th European Geosynthetics Congress*, Warsaw, Poland, May 2021. (Accepted)	Chapter 6

3.3 Development of a bespoke stress and temperature-controlled large direct shear apparatus on soil-geosynthetics interfaces

To achieve the aim of the thesis, a bespoke stress and temperature-controlled large direct shear apparatus on soil-geosynthetics interfaces was designed and built. This is because, in real project sites, the shear deformation of soil-geosynthetics interfaces is controlled by stress rather than displacement, thus the stress-controlled equipment can better represent real situations in engineering applications. Furthermore, the bespoke stress and temperature-controlled large direct shear apparatus can hold constant stresses whilst varying other parameters, such as drying and wetting conditions as well as temperature, similar to reality, whereas conventional displacement-controlled direct shear apparatus cannot.

More importantly, the soil-geosynthetics interfaces often experience creep shear deformation due to constant shear stress. However, it is impossible for the displacement-controlled direct shear apparatus to conduct creep tests on soil-geosynthetics interfaces to investigate their creep mechanical properties. Additionally, throughout the service life, soil-geosynthetics interfaces usually are exposed to environmental loadings, but existing direct shear apparatus on soil-geosynthetics interfaces cannot simulate the variations of environmental factors in field conditions. This renders such apparatus ineffective in their ability to research the impacts of drying-wetting cycles, thermal cycles and elevated temperature on the short-term and creep mechanical behaviour of soil-geosynthetic interfaces within field conditions.

The bespoke apparatus allows for the short-term and creep mechanical behaviour of soil-geosynthetics interfaces under environmental loadings, such as drying-wetting cycles, thermal cycles and elevated temperature to be investigated. By conducting preliminary tests on Kaolin Clay/Mercia Mudstone Clay-GDL interfaces, the functionality of the bespoke apparatus was validated. The replicability and reliability of the bespoke apparatus on measuring the mechanical properties of soil-geosynthetics interfaces was validated by repetitive tests on soil-GDL interfaces under different normal stresses. The detailed experimental scheme is tabulated in Table 3.3. The experimental results obtained from the bespoke apparatus were also compared with the results obtained from conventional displacement-controlled equipment to further support the reliability of the established apparatus. Detailed contents are presented in Chapter 4.

Table 3.3 Experimental scheme for validation tests

Sample	Shearing rate (10 kg in X minutes)	Normal pressure (kPa)	Experimental condition	Total Experimental number
Mercia Mudstone Clay- GDL interfaces	5	15, 20, 25, 40, 50	Consolidated undrained rapid loading shear tests	21
	2, 5, 7, 10, 15	25		
Kaolin Clay - GDL interfaces	5	15,25,50		

3.4 Quantifying the impacts of environmental loadings on the short-term mechanical behaviour of cover clayey soil-GDL interfaces

To achieve Objective 1, the bespoke large direct shear apparatus was used to conduct a series of rapid loading shear tests on Kaolin Clay and Mercia Mudstone Clay-GDL interfaces under different normal stresses subjected to drying-wetting cycles, thermal cycles, drying-wetting cycle without heating and elevated temperature. There are two reasons as to why Kaolin Clay and Mercia Mudstone Clay are used as the research samples. The first reason is that both Kaolin Clay and Mercia Mudstone Clay are distributed widely in the world. Kaolin Clay is distributed extensively in China, UK, USA, Australia, etc, and Mercia Mudstone Clay widely occurs in the UK, especially in Midland. Hence, the research outcomes of the two types of clayey soils - GDL interfaces are representative. The second reason is that Kaolin Clay and Mercia Mudstone Clay are classified as medium plasticity clay (CM) and low plasticity clay (CL), respectively, according to BS5930 (Dumbleton, 1981). Therefore, their research results can indicate the influence of environmental loadings on the mechanical properties of interfaces between GDL and clayey soils with different plasticity. The results of soil classification tests for Kaolin Clay and Mercia Mudstone Clay are presented in Figure 3.1 and Table 3.4.

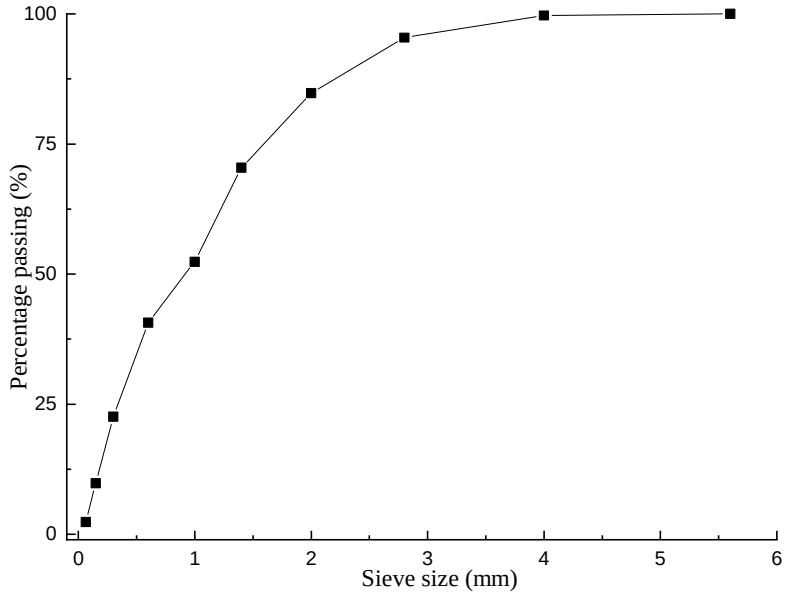

(a) Mercia Mudstone Clay

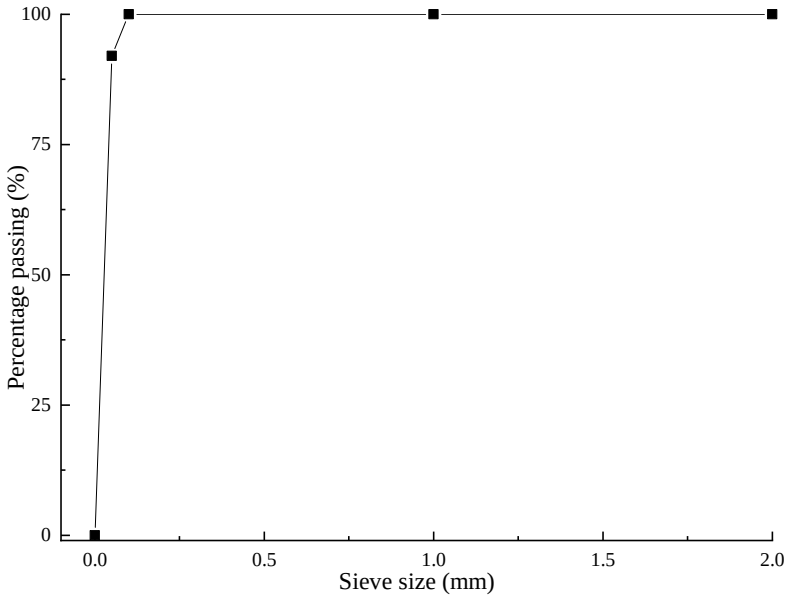

(b) Kaolin Clay

Figure 3.1 Soil gradation curves

Table 3.4 The basic characteristics of soil specimens

Properties			Kaolin Clay	Mercia Mudstone Clay
Liquid limit (%)			47	33.63
Plastic limit (%)			26.58	17.42
Plasticity index (%)			20.42	16.23
Maximum dry density (g/cm^3)			2.0	1.93
Optimum water content (%)			20	11.76
Saturated water content (%)			56.36	68.43
Triaxially consolidated undrained shear strength (kPa)	Cell Pressure (kPa)	20	18.59	24.12
		35	27.29	39.72
		50	35.99	55.32
Percentage passing (%)	Sieve size (mm)	5.6	100	100
		4	100	99.68
		2	100	84.79
		1	100	52.36
		0.1	100	6.26
		0.05	92	2.39

The rapid loading shear tests replicate the short-term mechanical responses of clayey soil-GDL interfaces after experiencing environmental loadings, with rapidly rising shear stress under consolidated undrained conditions. Drying-wetting cycles can simulate the consecutive alternation of rainfall and drought on soil-GDL interfaces. Thermal cycles and elevated temperature can replicate the alternative temperature variation and constant temperature elevation of soil-GDL interfaces whilst submerging into water, respectively. The drying-wetting cycle without heating can reproduce the sole effect of drying on soil-GDL interfaces with a constant temperature. Different normal stress (0-50 kPa) can resemble the soil-GDL interfaces underneath cover soil with different thicknesses (0-2.5m). The selection of temperature in drying cycles, heating cycles and elevated temperature stages as 40 ℃, and fully submerging the interfaces into water during wetting cycles and shearing

processes, can simulate the extreme climatic conditions in reality. The detailed experimental scheme is tabulated in Table 3.5.

Table 3.5 Experimental scheme for rapid loading shear tests

Sample	Environmental loadings	Cycle number/ Temperature /creep stress level	Normal pressure (kPa)	Experimental condition	Total experimental number
Mercia Mudstone Clay/ Kaolin Clay-GDL interfaces	Normal condition	None	15, 20, 25, 40, 50	Consolidated undrained rapid loading shear tests	42
	Creep deformation	50 %, 60 %, 70 %	25		
	Drying cycle without heating	1			
	Elevated temperature	40 ℃	15，25, 50		
	Drying-wetting cycle	1, 3			
	Thermal cycle	1			

The detrimental influences of environmental factors on the mechanical characteristics of soil and polymer geosynthetics have been reported, respectively, (Fleureau et al., 2002; Guan et al., 2010; Guney et al., 2007; Md et al., 2016; Wang et al., 2016a; Zhang et al., 2015)but their impacts on the interfaces between soil and geosynthetics have not been documented due to the limitation of experimental apparatus. Thus, according to the experimental results, the impacts of drying-wetting cycles, thermal cycles, drying-wetting cycle without heating, elevated temperature, and normal stress on the short-term mechanical characteristics of clayey soil-GDL interfaces were investigated. A corresponding mechanism analysis was also conducted. This is detailed in Chapter 5 and Section 7.2.

3.5 Quantifying the impacts of environmental loadings on the long-term mechanical behaviour of cover clayey soil-GDL interfaces

To achieve Objective 2, the bespoke large direct shear apparatus was used to conduct a series of creep shear tests on Kaolin Clay and Mercia Mudstone Clay-GDL interfaces under different creep shear stress levels subjected to drying-wetting cycles, thermal cycles and drying-wetting cycle without heating, respectively. In engineering projects, soil-GDL interfaces can experience creep shear deformation due to constant shear stresses whilst involving the variation in environmental factors. However, due to the limitation of typical experimental apparatus, research on creep shear deformation of soil-geosynthetics interfaces is rare, let alone the creep shear deformation of soil-GDL interfaces subjected to environmental loadings. Thus, the tests resemble the creep mechanical response of soil-GDL interfaces subjected to constant shear stress whilst experiencing environmental loadings. Drying-wetting cycles and thermal cycles can simulate the consecutive alternation of rainfall and drought, as well as the alternative temperature variation on soil-GDL interfaces when submerged in water, whilst bearing constant shear stress, respectively. The drying-wetting cycle without heating can reproduce the sole effect of drying on soil-GDL interfaces whilst bearing constant shear stress. The selection of normal stress as 25 kPa can resemble the common thickness (1.25m) of cover soil on GDL. The selection of drying temperature in drying cycles and heating cycles as 40 ℃, and fully submerging the interfaces in water during wetting cycles can simulate extreme climatic conditions in reality. The selection of different creep shear stress levels can reproduce the creep mechanical response of soil-GDL interfaces under different slope gradients. The detailed experimental scheme is tabulated in Table 3.6.

Table 3.6 Experimental scheme for creep shear tests

Sample	Environmental loadings	Cycle number	Normal pressure (kPa)	Creep stress level (%)	Experimental condition	Total Test number
Mercia Mudstone Clay - GDL interfaces	Normal condition	None	25	95	Consolidated undrained creep shear tests	18
	Drying-wetting cycle	3		90, 80, 70, 60, 50		
	Thermal cycle	3		90, 80, 70		
	Drying cycle without heating	1		70		
Kaolin Clay – GDL interfaces	Normal condition	None		80		
	Drying-wetting cycle	3		70, 60, 50, 40		
	Thermal cycle	3		70, 60		
	Drying cycle without heating	1		60		

According to the experimental results, the impacts of drying-wetting cycles, creep shear stress level, thermal cycles and drying-wetting cycle without heating, on the creep mechanical characteristics of clayey soil-GDL interfaces were investigated. A corresponding mechanism analysis was also conducted. Details of such are presented in Chapter 6 and Section 7.3.

3.6 Summary

This chapter introduces and justifies the methodology adopted to achieve the research aim and objectives stated in Chapter 1. The detailed research tasks are also presented in this chapter.

To quantify the mechanical behaviour of cover soil-GDL interfaces subjected to environmental loadings (Aim), a bespoke stress and temperature-controlled large direct shear apparatus on soil-geosynthetics interfaces was developed to allow the short-term and creep mechanical characteristics of soil-geosynthetics interfaces subjected to drying-wetting cycles, thermal cycles and elevated temperature to be investigated; A series of rapid loading shear tests and shear creep tests were conducted on clayey soil-GDL interfaces subjected to drying-wetting cycles, thermal cycles, elevated temperature and drying-wetting cycles without heating, using the self-designed large direct shear apparatus, to measure the impacts of the environmental factors on the short-term and creep mechanical behaviour of clayey soil-GDL interfaces, respectively.

Chapter 4

Development of stress and temperature-controlled large direct shear apparatus on soil-geosynthetics interfaces

4.1 Introduction

To obtain a better understanding about the short-term and creep mechanical behaviour of soil-geosynthetics interfaces under environmental loadings, such as elevated temperature, thermal cycles and drying-wetting cycles, in this chapter, a stress-controlled direct shear apparatus with heating function on soil-geosynthetics interfaces was developed. The bespoke apparatus allows the short-term and creep mechanical characteristics of soil-geosynthetics interfaces under environmental loadings to be investigated. The performance of the bespoke apparatus was validated by conducting a series of tests, which indicates the reliable functionality of the apparatus. Additionally, the experimental results from the bespoke apparatus were compared with the results from the conventional displacement-controlled equipment to further support the reliability of the apparatus.

4.2 Development of the temperature and stress-controlled direct shear apparatus

4.2.1 Overview of the developed apparatus

The schematic diagram of the temperature and stress-controlled direct shear apparatus established in this study is presented in Figure 4.1. The photos of the real developed apparatus are shown in Figure 4.2. The direct shear apparatus consists of four primary systems: normal stress system, shear stress system, heating system, and data recording and control system. The normal stress system is to impose and keep an even normal pressure on soil-geosynthetics interfaces during testing. The normal stress system comprises

an air-pressure bladder which applies normal stress on the soil in the upper box via a loading plate. The description of other components is detailed below.

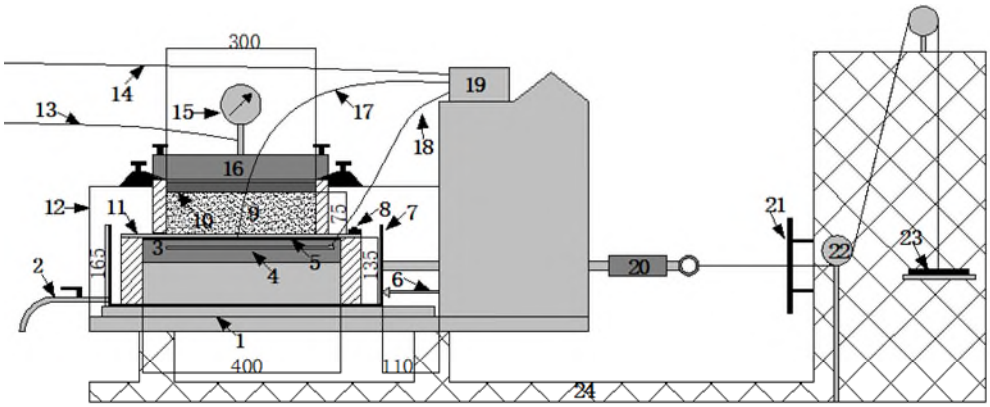

1. Bearing rail 2. Drainpipe 3. Aluminium heating plate 4. Heater mat 5. Pyramid teeth gripping plate 6. Horizontal movement sensor 7. Water bath 8. Clamping bar 9. Soil 10. Loading plate 11. Geosynthetics 12. Sidewalls 13. Pressurised air inlet tube 14. Main power wire 15. Normal stress gauge 16. Air pressure bladder 17. Thermocouple 18. Power wire to heater mat 19. PID temperature controller 20. Load cell 21. Protection plate 22. Pulley 23. Dead weight 24. Reaction frame

Figure 4.1 The schematic diagram of the developed stress-controlled direct shear apparatus (mm) (Chao and Fowmes, 2021)

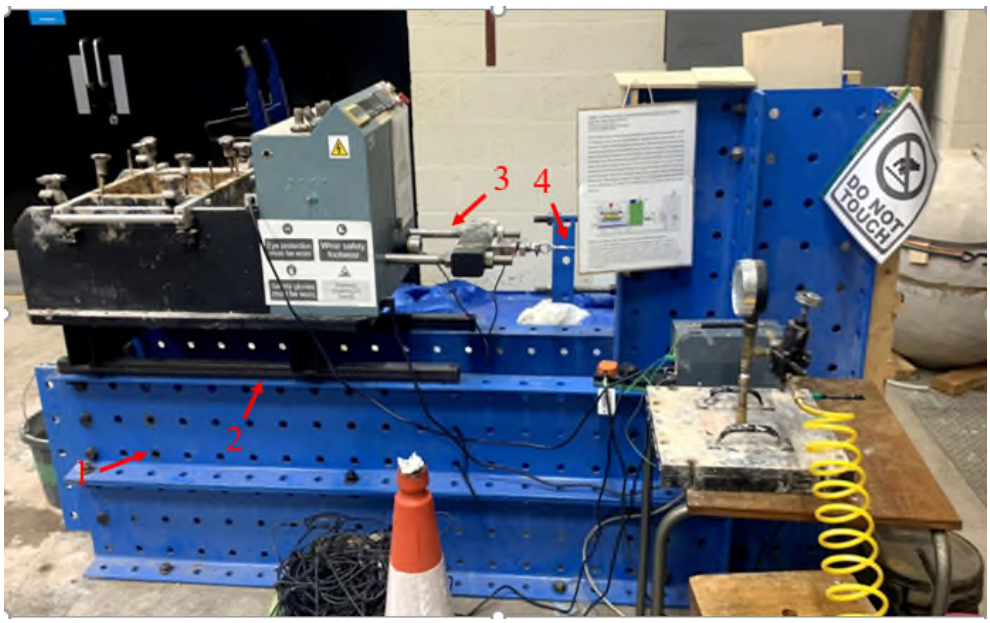

1. Reaction frame 2. Bearing rail 3. Shear rod 4. Steel wire

(a) Side view

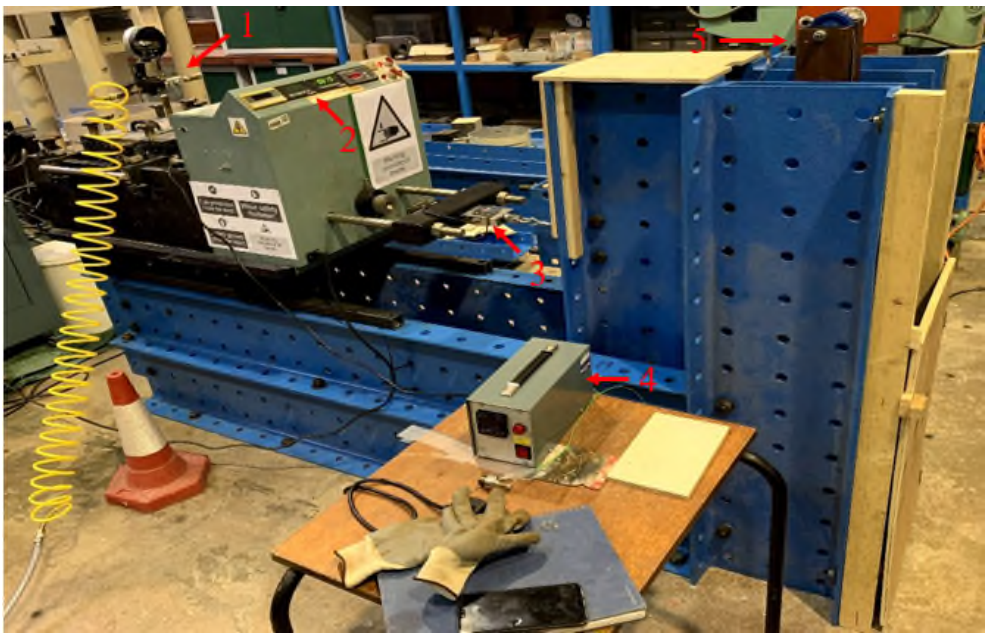

1. Normal stress loading system 2. Shear load and horizontal displacement gauges 3. Load cell 4. PID temperature controller 5. Pulley

(b) Front view

1. Drainpipe 2. Water bath 3. Bottom shear box 4. Side wall 5. Upper shear box 6. Power wire to heater mat

(c) Rear view

Figure 4.2 The photos of the real developed apparatus

4.2.2 shear stress system

The shear stress system is composed of top and bottom shear boxes, pyramid tooth gripping plate (Figure 4.3), shear rods, clamping bar, loading plate, steel wires, pulleys and hanger for dead weights, as presented in Figure 4.1. In the shearing process, the top shear box with internal dimension 300 mm in width by 300 mm in length by 100 mm in height is fixed on the sidewalls of the direct shear apparatus. The bottom shear box with internal dimension 300 mm in width by 400 mm in length by 100 mm in height is housed in a water bath. The lower box assembly is connected to the shear rod, which is free to move horizontally through the bearing rail underneath the bottom shear box. A pulley system is connected to the end of the shear rod using a hook. The pulley system is composed of steel wires, two fixed pulleys and a hanger for dead weights. One fixed pulley is parallel with the shear rod to guarantee the bottom shear box is only subjected to horizontal load from dead weights, as shown in Figure 4.1. During the tests, dead weights were added to the hanger to impose horizontal stress on the bottom shear box. When the horizontal displacement of the bottom shear box reaches the predetermined maximum value, the protection plate installed on the reaction frame is able to prevent further horizontal displacement of the bottom shear box and avoid the damage of the apparatus.

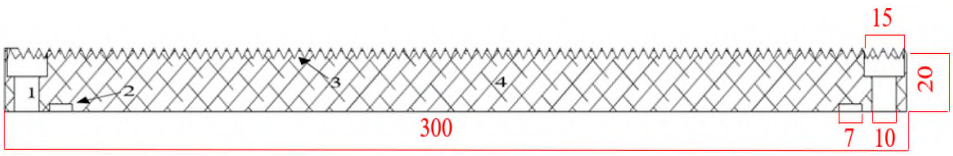

1.Counter borehole 2. Groove for rubber O-ring 3. Pyramid tooth gripping 4. Upper aluminium heater plate

Figure 4.3 Schematic diagram of the profile for the pyramid tooth gripping (mm)

Effective gripping of geosynthetics is necessary to transfer shear stress to the soil-geosynthetics interface. In this device, a clamping bar and the pyramid-tooth gripping plate are adopted to grip geosynthetics. The clamping bar is on

the leading edge of the bottom shear box to clamp the geosynthetics on the bottom shear box. The pyramid-tooth gripping plate is machined on the upward surface of the aluminium heating plate, as shown in Figure 4.3. The height of the pyramid-tooth is 4 mm, and the angle of the tips of the pyramid-tooth is 60°. The width and length of the pyramid-tooth are 3 mm and 4 mm, respectively. During the tests, the sharp tips of the pyramid-tooth penetrated the geosynthetics to resist the relative displacement between the geosynthetics and the bottom shear box. It guarantees all horizontal displacement during testing is because of the relative horizontal displacement between soil and the underlying geosynthetics, the lower shear box and the heating plate assembly, as shown in Figure 4.4.

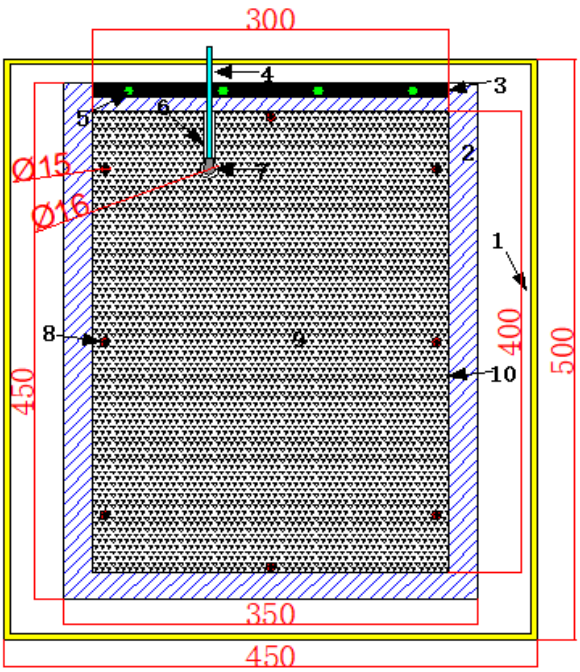

1.Water bath 2.Lower shear box 3.Clamping bar 4.Soft tube 5. Fixing screw 6.Channel 7. Sealing threaded elbow 8. Counterbore screw 9. Heater plate 10. Pyramid teeth gripping

Figure 4.4 The plan view schematic diagram of the lower shear box and heating elements (mm)

4.2.3 Heating system

The heating system for the direct shear device consists of an aluminium lower block with an internal heater mat, Type-T thermocouple controlled using a PID temperature controller. The heater mat is the heat source, 300 mm in length by 200 mm in width, with supply voltage 240 v ac, the peak temperature of 300 ℃, and power rating 240 W, and is housed inside the aluminium heating plate. The aluminium heating plate is placed in the bottom shear box underneath the soil-geosynthetics interface. Selection of aluminium as the raw material for the heating plate is because it can transfer the heat from the heater mat to soil-geosynthetics interfaces quickly because of its good thermal conductivity (Sposito, 1995). The aluminium heating plate is composed of separable upper and bottom parts with width 300 mm by length 400 mm by height 20 mm and width 300 mm by length 400 mm by height 30 mm, respectively, which is fixed together by fastening the counterbore screw in the 8 counterbore holes around the circumference of the heating plate, being presented in Figure 4.5 (a). The upward surface of the upper part is machined to pyramid tooth gripping to prevent the sliding of geosynthetics, and the downward surface is adhered by the heater mat, as shown in Figure 4.5 (b). Meanwhile, when the upper and bottom parts are fastened together, there is a groove with 200 mm in length by 20 mm in width by 300 mm in height in the bottom part for placing the heater mat, as shown in Figure 4.5 (c). The photos of the real heating plate are presented in Figure 4.6. The temperature of the heater mat is controlled by the PID temperature controller by adjusting the voltage of the power wire connected to the heater mat based on the signal from the K-type thermocouple. If the input measured temperature is lower than the targeted value, the PID temperature controller increases the voltage of the power wire connected to the heater mat to increase the temperature, if the input measured temperature is higher than the targeted value, the PID temperature controller decreases the voltage of the power wire to decrease the temperature, forming a close loop.

There are three reasons for heating the soil-geosynthetics interfaces from the underneath of the geosynthetics. The first one is that, during the tests, normal

stress was applied from the top of the soil specimen. If the heating system was installed on the top of the soil layer, the distribution of normal stress in the soil sample may be influenced to cause deviations in the experimental results. Secondly, if the heating system was installed on the top of the soil layer, it needs to take a long time to transfer heat to the soil-geosynthetics interfaces to reach the targeted temperature, which may result in the insufficient drying on the interfaces due to the limitation of experimental time. However, the primary purpose of this apparatus is to investigate the mechanical properties of soil-geosynthetics interfaces subjected to drying-wetting/thermal cycles and elevated temperature, thus, heating the interfaces from the bottom can allow the temperature of soil-geosynthetics interfaces to quickly reach the targeted value to sufficiently dry the interfaces. Thirdly, according to the existing literature, the measured temperature of cover systems in some landfills is higher than the ambient temperature due to the elevated temperature of the underlying wastes, and the prevailing direction of heat flow in the cover systems is upward (Yeşiller et al., 2005).

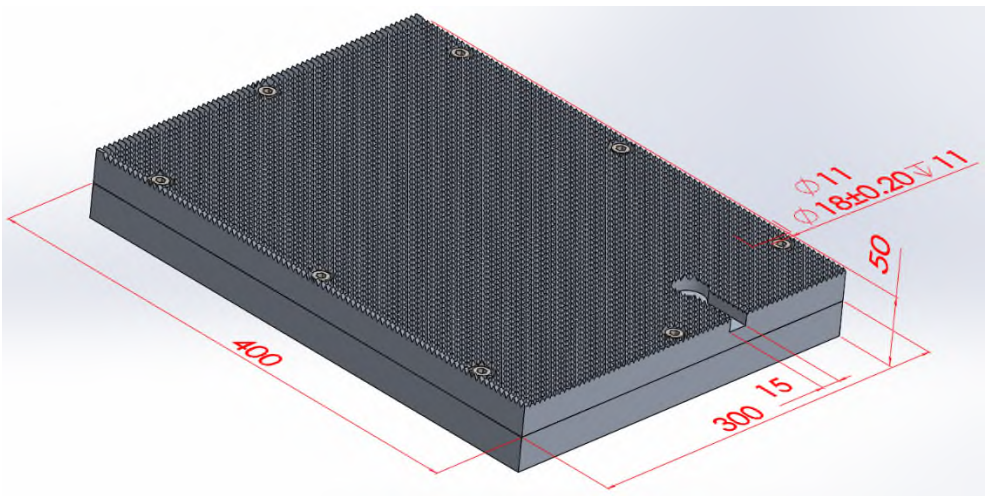

(a) The global view

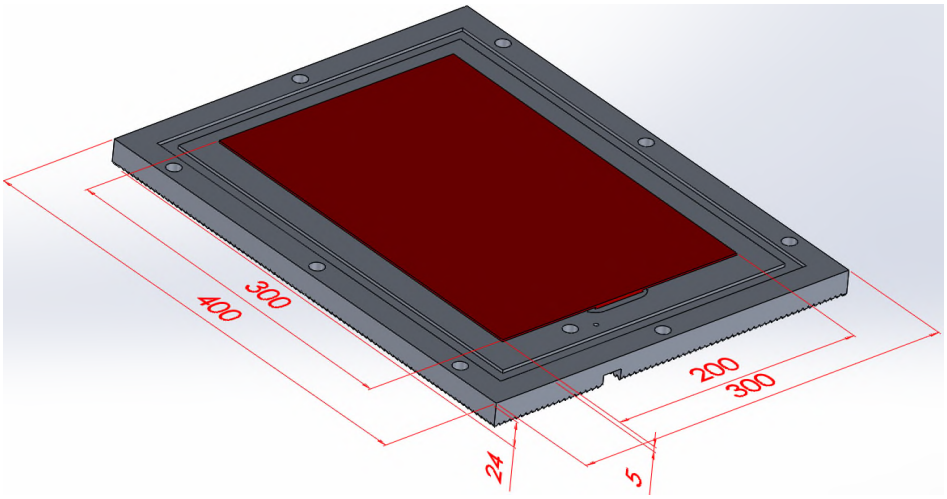

(b) The downward side of the upper part

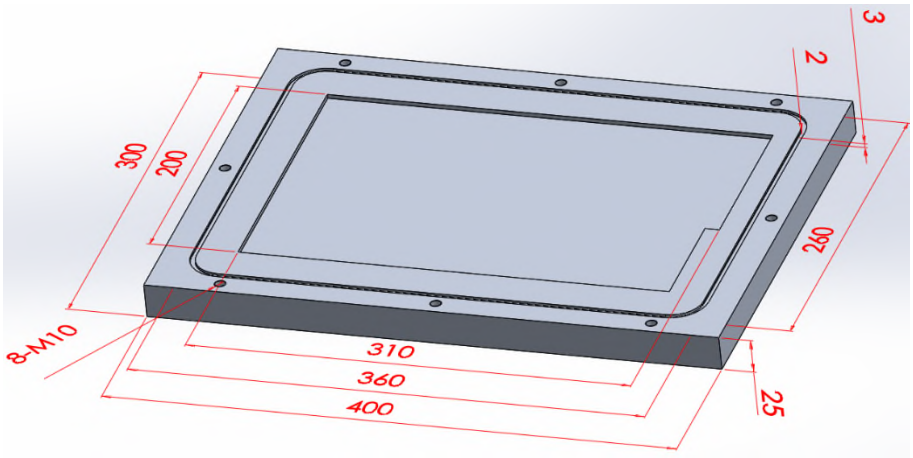

(c) The bottom part

Figure 4.5 The schematic diagram of the heating plate (mm)

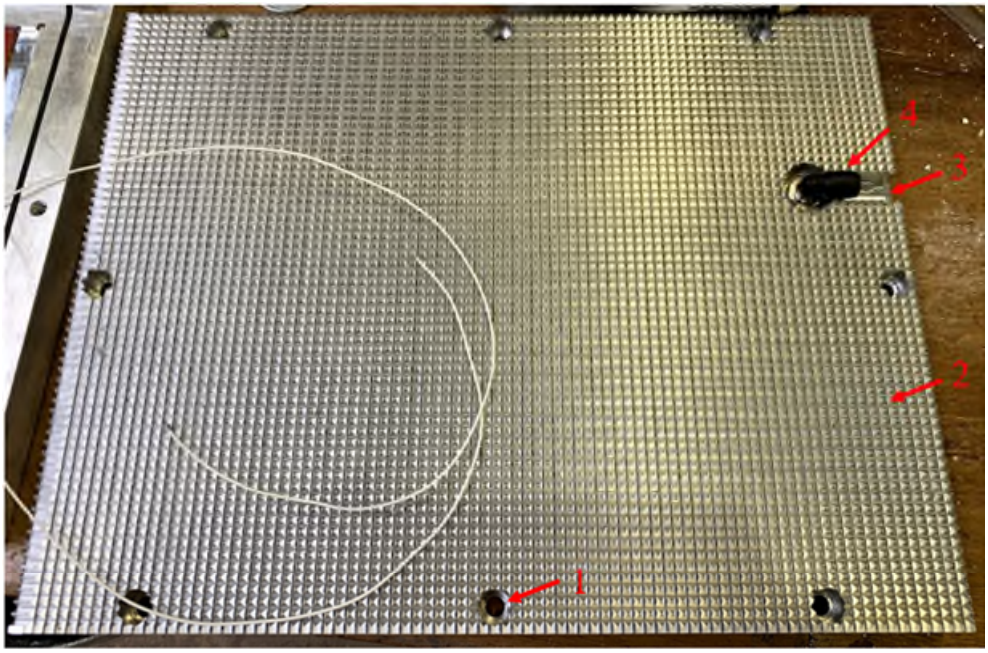

1. Counterbore hole 2. Pyramid teeth gripping 3. Channel 4. Sealing threaded elbow

(a)The upward side of the upper part

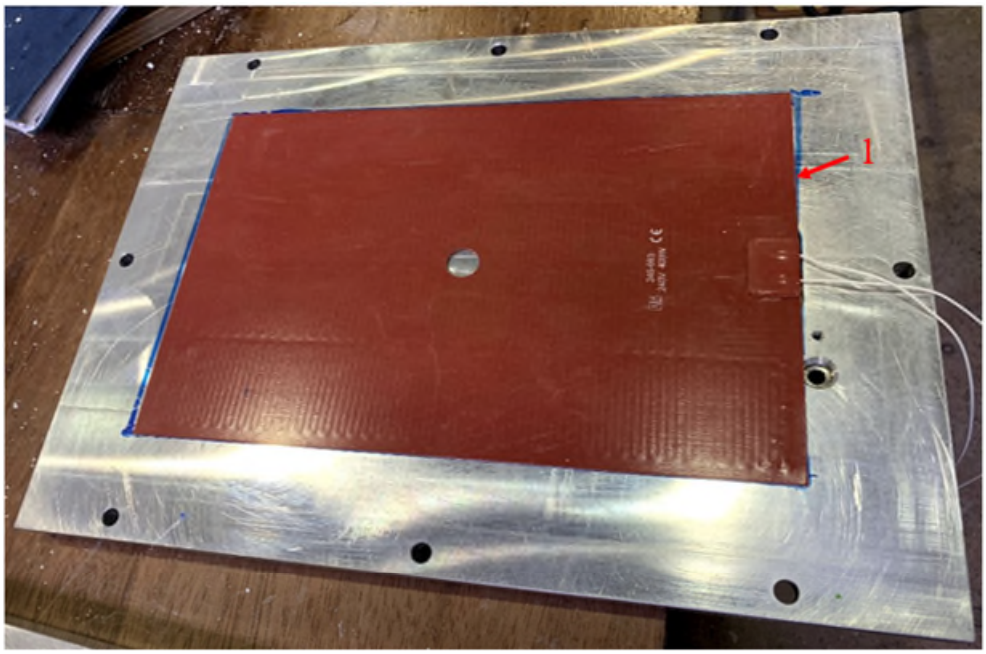

1.Heater mat

(b)The downward side of the upper part

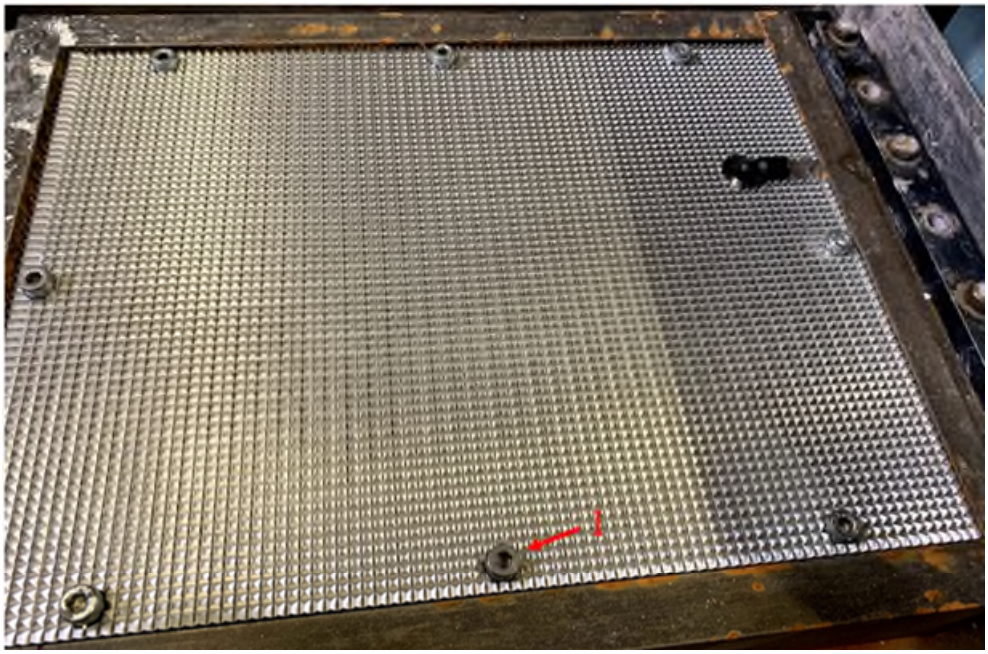

1. Counterbore screw

(c)The heating plate in the bottom shear box

Figure 4.6 The photos of the real heating plate

4.2.4 Data recording and control system

The data recording and control system consists of horizontal displacement transducer, normal stress gauge, T-type thermocouple, load cell, PID temperature controller, as well as shear stress and horizontal displacement gauges. The normal stress is measured and displayed via the mechanical normal stress dial. The horizontal displacement of the bottom shear box is measured using a single 100 mm linear potentiometer positioned at the front of the bottom shear box, as shown in Figure 4.1. The imposed horizontal shear load on the bottom shear box is measured adopting an S-type load cell with the load capacity of 4 kN. The sealed tip insulated Type-T thermocouple and the PID temperature controller are adopted to monitor and regulate the temperature of the soil-geosynthetics interface. The calibration curves for the S-type load cell, horizontal displacement sensor (linear potentiometer) and Type-T thermocouple are presented in Figure 4.7. The measured real-time horizontal displacement, shear load and temperature of the soil-geosynthetics interfaces are displayed in the shear load and horizontal displacement gauges and PID temperature controller, respectively. The displayed real-time

horizontal displacement, shear load and temperature of the interfaces are recorded by a camera that is placed in front of the shear load and horizontal displacement gauges and PID temperature controller, as shown in Figure 4.8. The photo of the test is presented in Figure 4.9. The reason why choosing a camera to record the experimental data is because the camera can record the whole process of the tests and film what actually happens to record more information of the tests. For example, during the tests, the camera can film the movement of shear rod that is connected to the bottom shear box to provide intuitional records of the relative displacement speed between soil and geosynthetics during the shearing process. In comparison, the data logger only can record the pure experimental data at low frequencies (given the length of tests) and cannot capture the nature of sudden movements.

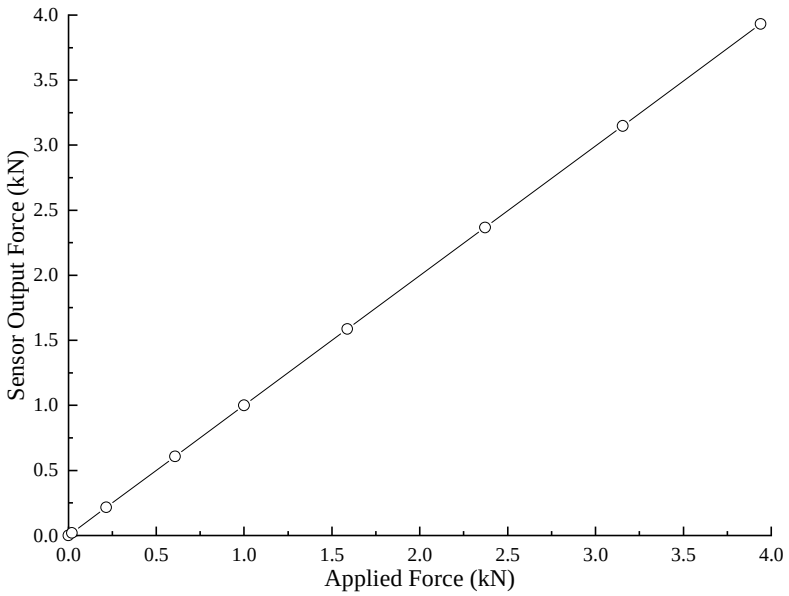

(a) S-type load cell

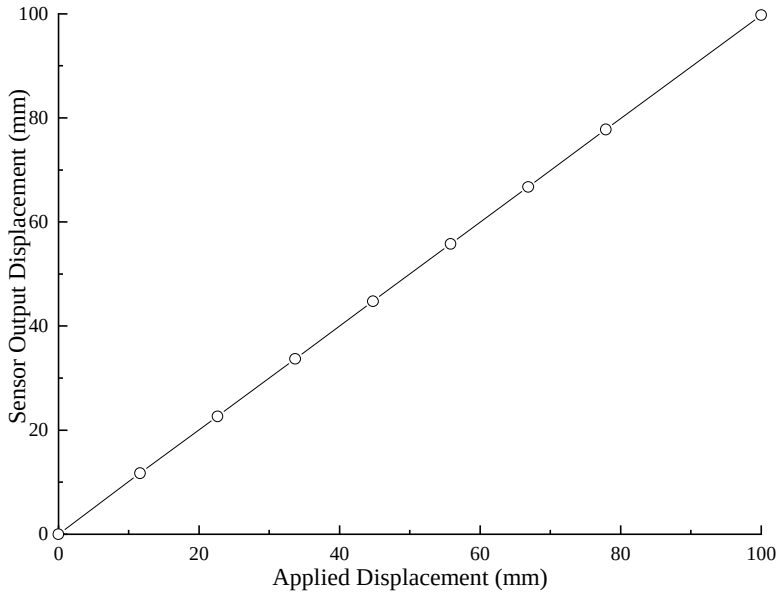

(b) Horizontal displacement sensor

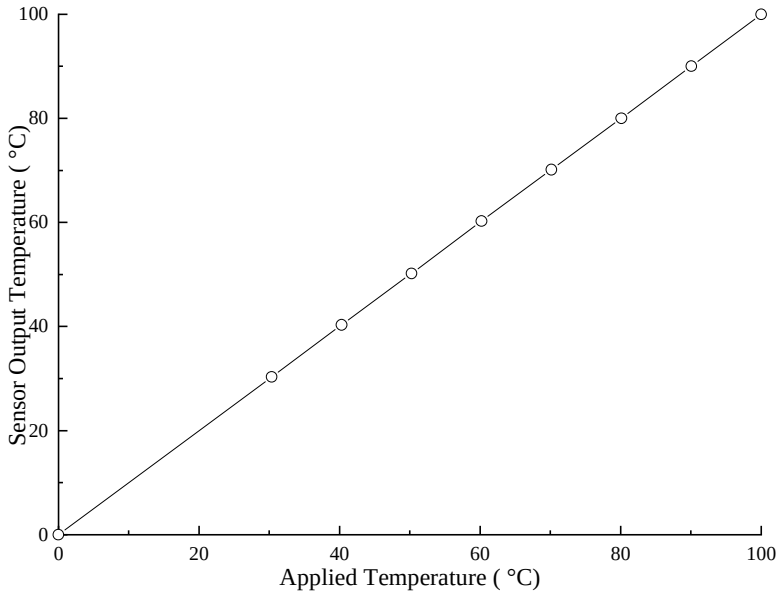

(c)Type-T thermocouple

Figure 4.7 Calibration curves

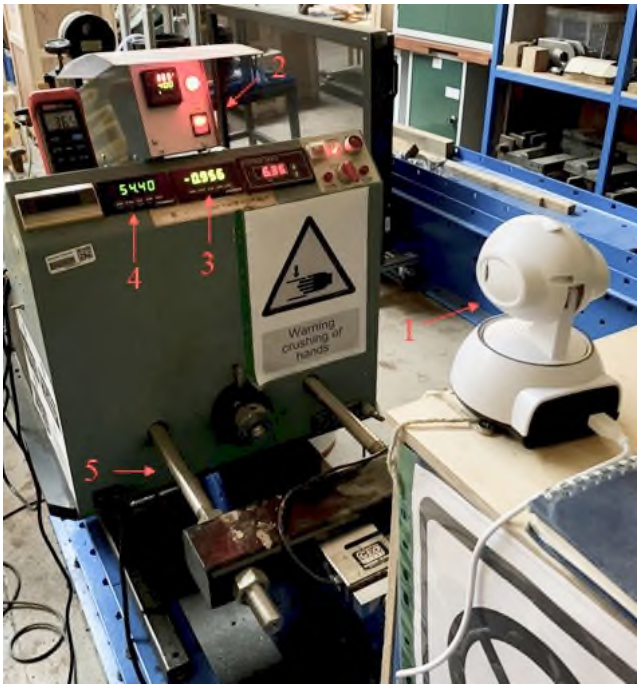

1.Camera 2. PID temperature controller 3. Shear stress gauge 4. Horizontal displacement gauge 5. Shear rod

Figure 4.8 The experimental data recording system

1. Shear load and horizontal displacment gauges 2. PID temperature controller 3. Shear rod 4. Load cell 5. Camera

Figure 4.9 The photo of the test

4.3 Type of tests

Whilst displacement-controlled testing can give the strength of an interface, it does not allow the in-situ conditions to be applied whilst other environmental factors are altered, whereas the stress-controlled apparatus presented in this research facilitates this. The stress-controlled shear tests on soil-geosynthetics interfaces that the modified apparatus is able to conduct can be classified into two kinds: i) rapid loading shear tests or ii) creep shear tests. In rapid loading shear tests, the shear load is continually increased until the soil-geosynthetics interface fails. In the creep shear tests, the soil-geosynthetics interface is subjected to consistent shear stress till the soil-geosynthetics interface fails or the test is terminated. The apparatus can be utilized to conduct the rapid loading shear tests and creep shear tests under different temperatures. Additionally, to replicate the real *in-situ* conditions, such as climatic change, etc., the apparatus also allows soil-geosynthetics interfaces to conduct creep shear tests or rapid loading shear tests during or after drying-wetting cycles/thermal cycles, respectively. These are achieved by submerging the soil-geosynthetics interfaces in water to wet and dry them with high temperature to simulate the process of wetting-drying cycles/ thermal cycles, respectively.

The preparation work of the stress-controlled rapid loading shear tests and creep shear tests, including installing soil sample and GDL, the compaction of soil sample, measuring moisture content of soil sample, adjusting the gap between the upper and bottom shear boxes, follows ASTM D5321 (ASTM, 2014). Due to the limitation of experimental equipment, in the existing literature, the research about the stress-controlled rapid loading shear tests and creep shear tests on soil-geosynthetics interfaces is rarely reported. There is a lack of corresponding standards for conducting the stress-controlled rapid loading shear tests and creep shear tests on soil-geosynthetics interfaces, let alone the standards for the stress-controlled tests subjected to environmental loadings. Hence, the main procedure of the stress-controlled tests on soil-GDL interfaces was determined by own experience and referring the relevant research about stress-controlled tests on geosynthetics, sand-geomembrane

interfaces, geosynthetics-geosynthetics interfaces, etc (Ghazizadeh and Bareither, 2018b; Liu and Martinez, 2014; Rhodes, 2019).

4.4 Validation tests

4.4.1 Test materials

4.4.1.1 Soil

Two types of soils were adopted in this research:(1) Kaolin Clay and (2) Mercia Mudstone Clay, both derived from the UK, the detailed properties of the adopted soil as shown in Section 3.4. The photos of the soil sample are presented in Figure 4.10. The reason for selecting the two types of soil is to investigate and compare the functionality of the modified apparatus on testing the interfaces between GDL and clayey soils with different plasticity.

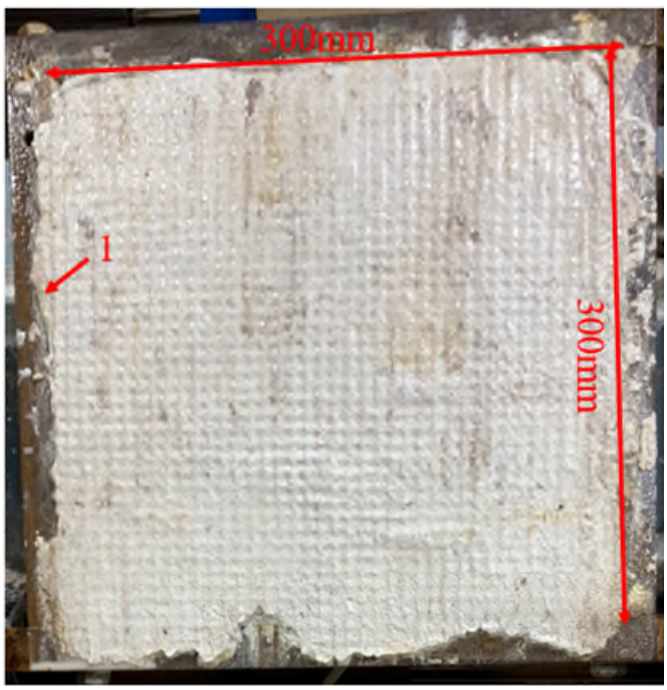

1.Upper shear box

(a)Kaolin Clay

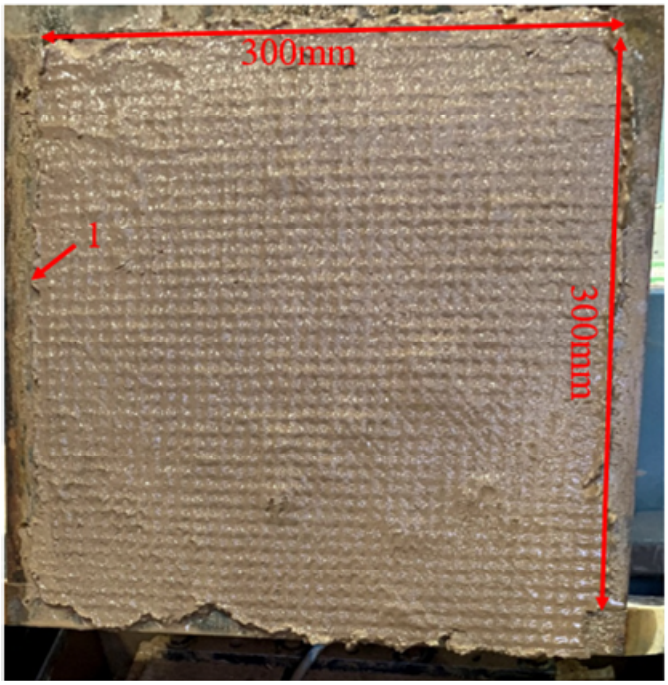

1. Upper shear box

(b)Mercia Mudstone Clay

Figure 4.10 Photos of soil sample

4.4.1.2 GDL

A proprietary Geocomposite Pozidrain Layer 6S250D/NW8 was adopted in this research. The GDL is composed of a single cuspate HDPE drainage core with a medium weight non-woven needle-punched and heat-treated staple fibre polypropylene geotextile filter thermally bonded on the dimple side and a lighter geotextile on the flat side. The schematic diagrams of the adopted GDL are shown in Figure 4.11, and the photos of the real GDL are shown in Figure 4.12. The GDL is often placed underneath the cover soil in landfills for drainage application, which is inevitable to be influenced by drying-wetting/thermals cycles and elevated temperature. The characteristics of the GDL are listed in Table 4.1.

(a) Cross-section of drainage core

1. Geotextile bonded on the dimple side 2. Drainage core 3. Geotextile bonded on the flat side

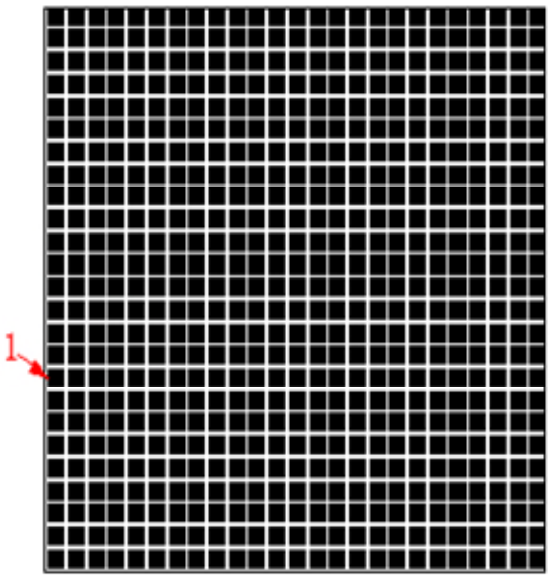

(b) Plan view of drainage core

1. Cuspate elements

Figure 4.11 Schematic diagrams of the adopted GDL

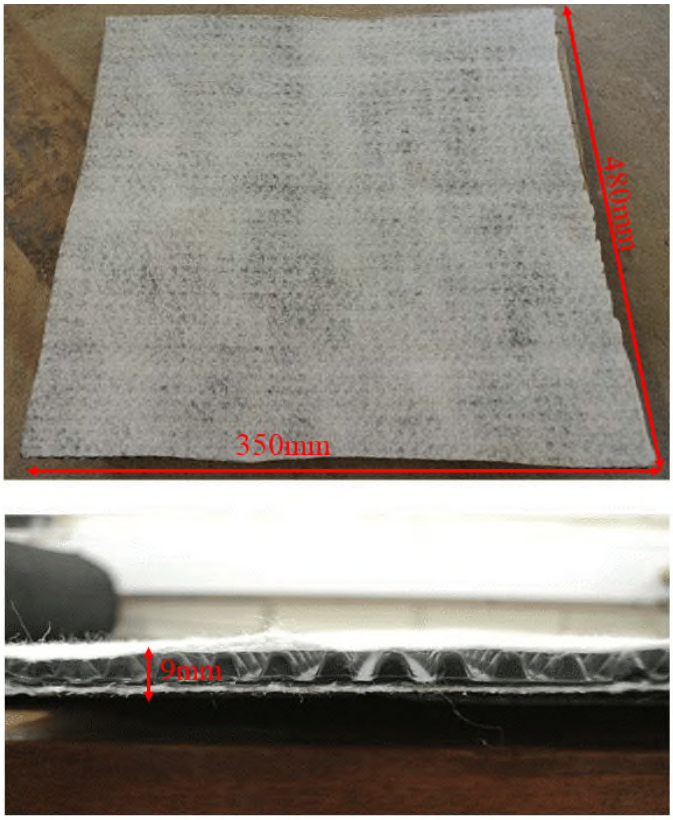

Figure 4.12 Photos of the real GDL (ABG.Ltd, 2020)

4.4.2 Preliminary sample preparation

Test samples were cut from a GDL roll, according to ASTM D 6072 (ASTM, 2008). The samples with 350 mm in width by 480 mm in length were cut so that shearing was carried out along the machine direction. The GDL was clamped to the leading edge of the lower shear box. After that, the upper shear box was filled with 13.02 kg or 13.50 kg of Mercia Mudstone Clay or Kaolin Clay at the optimum moisture content (11.8 % or 20 %) in three equal increments (25 mm height of each layer), respectively. The clay was then compacted adopting the light compaction method and each layer was compacted with 16 blows of a tamper. The total height of the Mercia Mudstone Clay or Kaolin Clay specimen above the GDL was 75 mm with density 1.93 g/cm^3 and 2.00 g/cm^3, respectively. The gap between the upper and bottom shear boxes was adjusted to maintain approximately 1 mm during the testing.

Table 4.1 The characteristics of the GDL

GDL properties	GDL	
Thickness of drainage core at 2kPa (mm)	6	
Drainage core type	Single direction cuspate core	
Mass per unit area (g/m^2)	840	
Tensile strength of machine direction (kN/m^2)	22	
Elongation at the peak of machine direction (%)	45	
CBR puncture resistance (N)	3750	
Geotextile properties	Bonded on the dimple side	Bonded on the flat side
Thickness at 2kPa (mm)	1.75	1.2
Tensile strength of machine direction (kN/m^2)	20	9.5
Pore size 090 (μm)	70	120
CBR puncture resistance (N)	3400	1600
Dynamic perforation cone drop (mm)	17	32

During the tests, the dimple side of HDPE drainage core for GDL is upward, and the pyramid-teeth were penetrated into the geotextile bonded on the flat side of HDPE drainage core to prevent the relative movement between GDL and the heating plate. After testing, the geotextile bonded on the flat surface of the drainage core was peeled to observe the flat surface of the drainage core. It was found that there was no obvious indention in the flat side of the drainage core, which indicates that the pyramid-teeth did not deeply penetrate into the drainage core and cause local elongation. Since the pyramid-teeth did not penetrate through the drainage core of GDL, the influence of the interaction between the soil sample in the upper shear box and the pyramid-

teeth of the heating plate on the experimental results can be ignored. This can be attributed to that, in the research, the adopted normal stress is relatively low (less than 50 kPa) and the low normal stress cannot impose enough pressure to allow the pyramid-teeth to deeply penetrate into the drainage core of GDL. Additionally, after the tests, the parts of GDL that were clamped by the clamping bar was observed, and there was no elongation in the clamping area of the GDL. This may be attributed to that the adopted low normal stress leads to low peak shear strength of the soil-GDL interfaces. Thus, the maximum tensile force imposed on the GDL was small, which cannot result in noticeable elongation on the GDL.

4.4.3 Determination of experimental parameters

The shearing of all rapid loading shear tests was conducted via adding weights with a rate of 10 kg every 5 minutes. The loading rate was ascertained by conducting tests on Mercia Mudstone Clay-GDL interfaces with different loading rates, including 10 kg in 2 minutes, 10 kg in 5 minutes, 10 kg in 7 minutes, 10 kg in 10 minutes, and 10 kg in 15 minutes, the test results as shown in Figure 4.13.

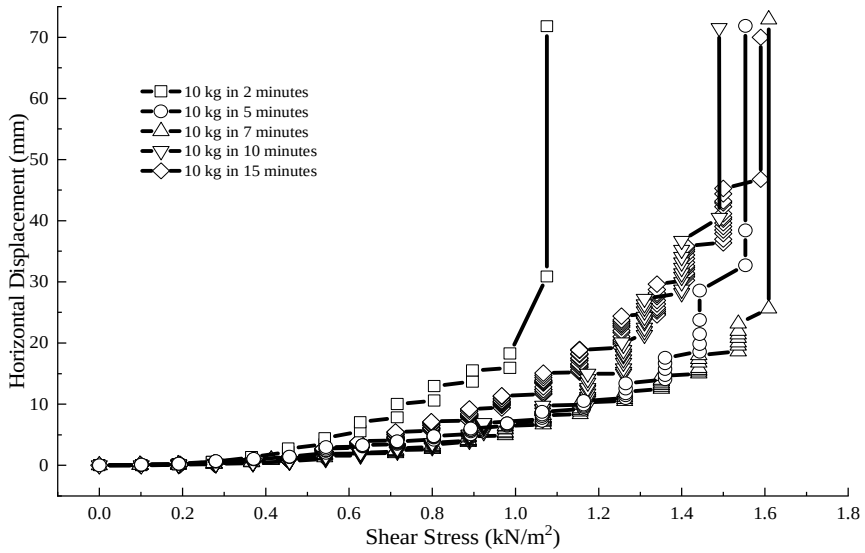

(a)Horizontal displacement-shear stress curves

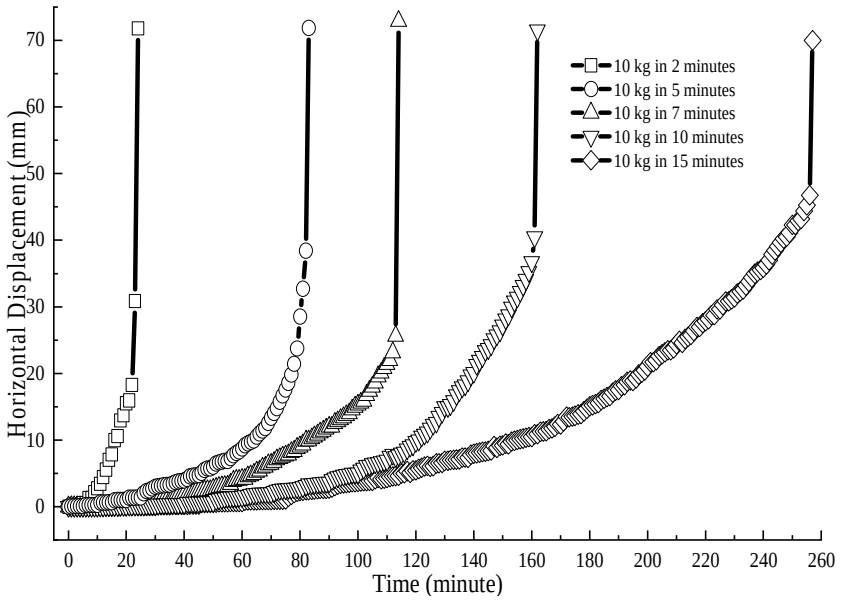

(b) Horizontal displacement-times curves

Figure 4.13 Experimental results for rapid loading shear tests on Mercia Mudstone Clay-GDL interfaces with different loading rates

Based on Figure 4.13, the horizontal displacement of the interfaces rises gradually with the increase in shear stress until the failure of interfaces. In general, the relationship curves between horizontal displacement and shear stress for tests with different loading rates are comparable, except for the test with a rate of 10 kg in 2 minutes. For the tests with different loading rates from 10 kg in 15 minutes to 10 kg in 5 minutes, they have negligible difference in the experimental results, with similar peak shear strength of around 17 kPa. However, the peak shear strength (12 kPa) of the test with 10 kg in 2 minutes loading rate is significantly lower than other tests. This may be attributed to that: when 10 kg in 2 minutes was adopted as the loading rate, owing to the rapid adding of dead weights, the hanger for placing dead weights was unstable, resulting in the specimen under 10 kg in 2 minutes loading rate being easy to fail under the effects of hanger vibration. Since, when the shear stress loading rate ranges from 10 kg in 5 minutes to 10 kg in 15 minutes, the impacts of shear stress loading rate on the peak shear strength of interfaces can be negligible, to allow time efficient testing 10 kg in 5 minutes was adopted as the loading rate. It also should be noted that, unlike the experimental results of displacement-controlled tests, no distinctive peaks

were observed in Figure 4.13 as once peak shear strength of interfaces is exceeded, failure ensues, much is the case in ultimate limit state failures in the field.

4.4.4 Performance of the shear stress system

To verify the performance of the shear stress loading system, three preliminary shear stress loading tests were carried out. In the preliminary experiments, 200 kg dead weights were gradually added on the hanger. The weight of added weights and the displayed force from load cell was recorded, as shown in Figure 4.14.

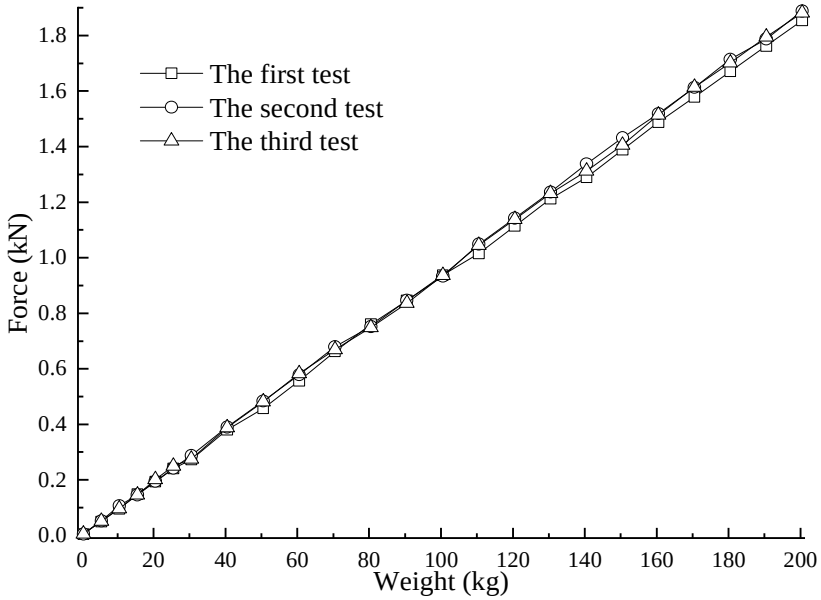

Figure 4.14 The performance of the shear stress loading system

Based on Figure 4.14, it can be seen that, for the three tests, the relationship curves between force and the weight of added dead weights are nearly linear. It indicates that the shear stress loading system has reliable stability, that is to say, the ratio between the weight of added dead weights and force is fixed, about 106.45:1. Additionally, the three curves are almost identical, which means the repeatability of the shear stress loading system is satisfied. Moreover, after calculating, the transfer efficiency of the shear stress loading system is around 94.61%. It demonstrates that 100 kg added dead weights can

impose 0.94 kN shear force on the specimens, which is acceptable in the research.

4.4.5 Performance of the heating system

Preliminary heating tests were conducted to assess the performance of the heating system, including (1) repeatability (2) temperature equilibration capability (3) stability. In order to simulate the real experiments, during the testing, the heating of soil-geosynthetics interfaces was initiated after consolidation for 24 hours, with a target temperature of 40 ℃. The interface was heated for 1000 minutes under the target temperature. After that, three repetitive tests were conducted under the same target temperature to evaluate the repeatability of the heating system. During the tests, the thermocouple was placed in the drainage core of the GDL to measure the temperature of the interface. Thus, the measured temperature from the thermocouple represents the actual temperature of soil-GDL interfaces. The measured temperature in elapsed time of the three tests is shown in Figure 4.15.

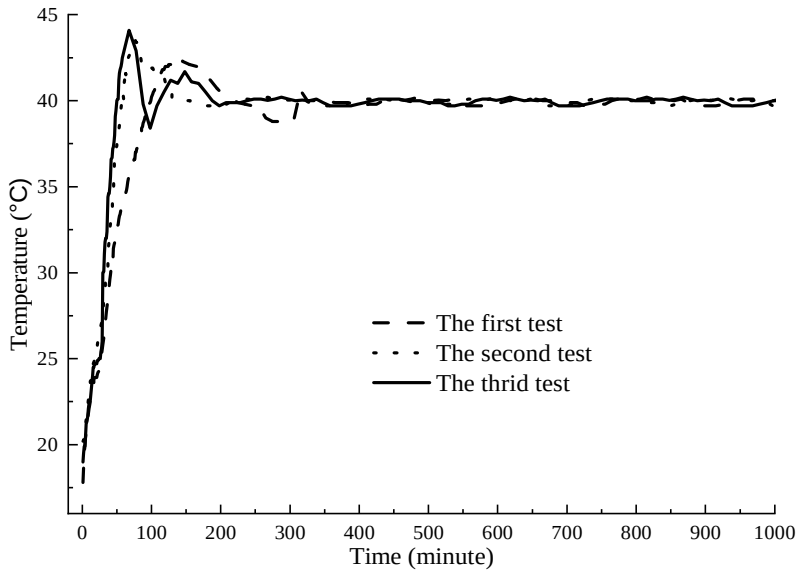

Figure 4.15 The measured temperature in elapsed time

Based on Figure 4.15, the change trends of the three curves are alike in

elapsed time, especially after they reach the targeted temperature. It demonstrates that the heating system has satisfied repeatability. More specifically, for the three curves, initially, they all rise rapidly over the targeted temperature. Then, they decrease gradually to the targeted temperature and keep stable. The lag times for the three tests are all less than 200 minutes. In this research, in the formal experiments, the heating duration is 24 hours, which is significantly higher than the lag time. Hence, the temperature equilibration ability for the heating system is acceptable. Additionally, it should be noticed that, after the lag time, the temperatures of the three tests all maintain at the consistent value of 40 ℃. Although there are some fluctuations around the targeted temperature, the fluctuations are negligible, with less than 0.3 ℃. It indicates that the modified apparatus can allow the shear deformation behaviour of soil-geosynthetics interfaces under temperature-changed environmental loadings, such as drying-wetting cycles, elevated temperature, and thermal cycles, to be investigated, with reliable performance.

4.4.6 Overall performance of the developed apparatus

The repetitive rapid loading shear tests were conducted with normal stress of 15 kPa, 25 kPa and 50 kPa, to simulate 0.75 m -2.5 m thickness of cover soils as is typical in UK practice. Repetitive standard rapid loading shear tests, under each normal stress, were conducted immediately after 24 hours consolidation and the experimental results were used to validate the repeatability of the modified apparatus. Shear deformation versus shear stress and elapsed time curves for the repetitive standard rapid loading shear tests on Mercia Mudstone Clay-GDL interfaces under different normal stresses are shown in Figure 4.16, respectively. In this research, in all the figures involving the shear stress of soil-GDL interfaces, the shear stress (kN/m^2) has been calculated by dividing the shear load (kN) by the contact area (0.3 m × 0.3 m) between soil and GDL.

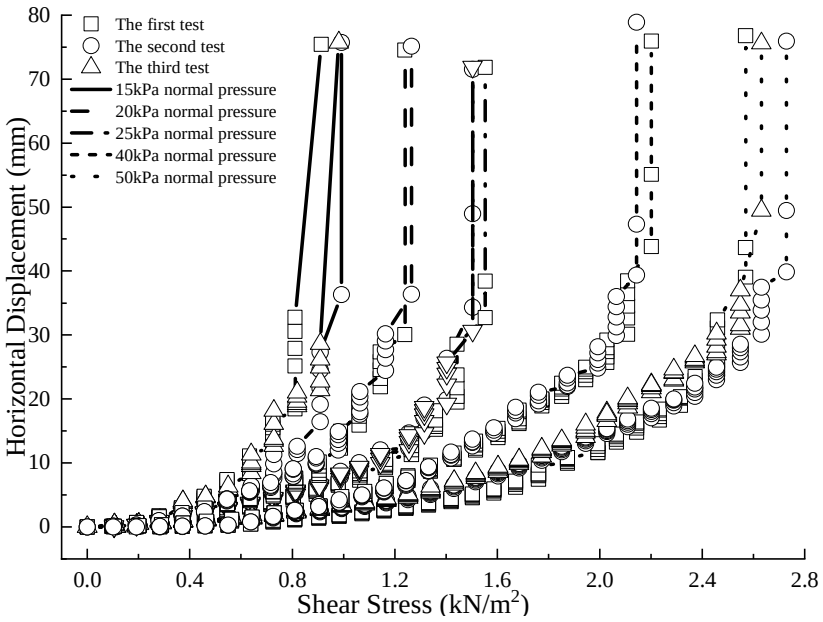

(a) Horizontal displacement versus shear stress

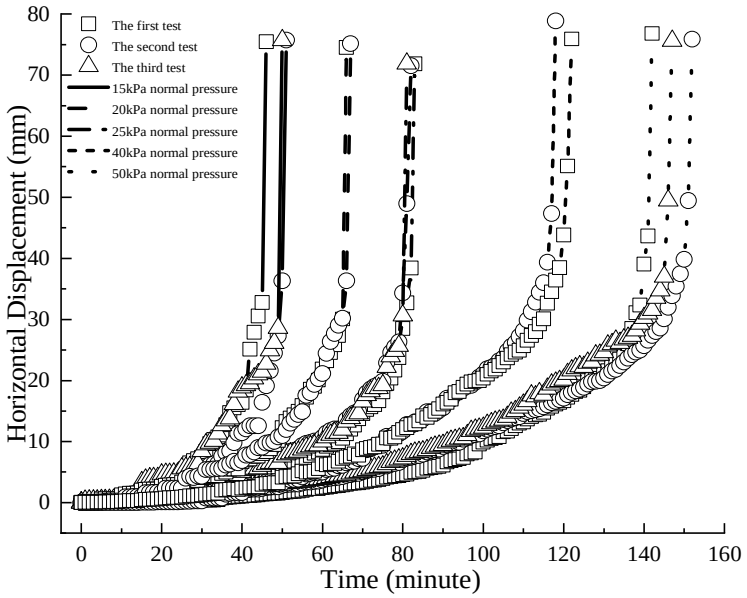

(b) Horizontal displacement in elapsed time

Figure 4.16 Experimental results of repetitive rapid shear loading tests on Mercia Mudstone Clay-GDL interfaces

Based on Figure 4.16, under each normal stress, the relationship curves of horizontal displacement versus shear stress and the curves of horizontal displacement in elapsed time for the three repetitive tests are similar, which indicates that the modified apparatus has satisfied repeatability. Moreover, it can be seen that the failure of the Mercia Mudstone Clay-GDL interfaces

happened suddenly with the loading of shear stress. For instance, for the first test under 15 kPa normal stress, at the 45th minute, the horizontal displacement is 33 mm, while in the next minute, it rises to 75 mm, indicating the failure of the specimen. Taking another example, for the first test under 50 kPa normal stress, at the 141st minute, the horizontal displacement is 44 mm, whereas it increases to 77 mm in the next minute, manifesting the failure of the interface.

According to the average peak shear strength under normal stress of 15 kPa, 25 kPa and 50 kPa, the Mohr-Coulomb strength lines of the specimens was obtained, as shown in Figure 4.17.

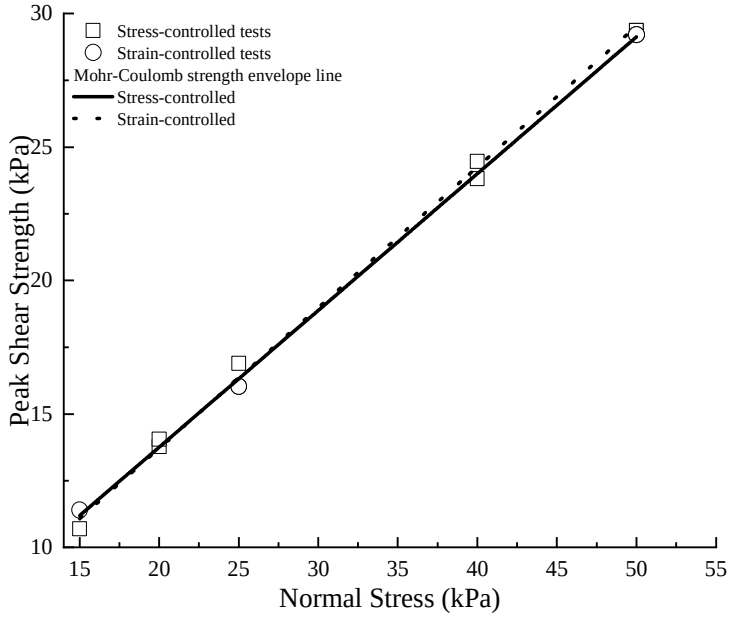

Figure 4.17 The Mohr-Coulomb strength line for repetitive rapid loading shear tests on Mercia Mudstone Clay-GDL interfaces

Based on Figure 4.17, the Mohr-Coulomb strength lines fit the experimental results well, with Coefficient of Determination R^2 equalling to 0.99. It indicates that the experimental results obtained from the modified apparatus conform to the Mohr-Coulomb Criterion well. In order to further validate the reliability of the modified apparatus, two repetitive rapid loading shear tests

were conducted under normal stress of 20 kPa and 40 kPa, respectively, the experimental results as shown in Figure 4.16. Their average peak shear strength was also calculated, respectively, as shown in Figure 4.17. According to Figure 4.17, the peak shear strength under normal stress of 20 kPa and 40 kPa is close to the Mohr-Coulomb strength lines and the conformity of the experimental results obtained from the developed apparatus to the Mohr-Coulomb criterion is further validated.

4.4.7 Comparison with the experimental results obtained by a conventional displacement-controlled apparatus

To validate the experimental results obtained by the bespoke apparatus against those obtained by a conventional displacement-controlled direct shear equipment, under normal stress of 15 kPa, 25 kPa and 50 kPa, the average shear stress and horizontal displacement of the three repetitive rapid loading shear tests on Mercia Mudstone Clay-GDL interfaces under the same shear loading time was calculated, respectively, as shown in Figure 4.18. Meanwhile, the rapid loading shear tests on Kaolin Clay-GDL interfaces under normal stress of 15 kPa, 25 kPa and 50 kPa were also conducted. The experimental outcomes of the displacement-controlled direct shear tests on Mercia Mudstone Clay-GDL interfaces and Kaolin Clay-GDL interfaces under normal stress of 15 kPa, 25 kPa and 50 kPa are drawn in Figure 4.18 to compare with the experimental results of the rapid loading shear tests on Mercia Mudstone Clay-GDL interfaces and Kaolin Clay-GDL interfaces, respectively. For the stress-controlled tests, shear stress is the independent variable that leads to the horizontal displacement of specimens. Thus, in this research, for the relationship curves between shear stress and horizontal displacement, shear stress is adopted as the *x*-axis (independent variable), and horizontal displacement is used as the *y*-axis (dependent variable). In order to be consistent with the stress-controlled tests, the horizontal displacement versus shear stress relationship curves of displacement-controlled tests also adopt shear stress as the *x*-axis and horizontal displacement as the *y*-axis.

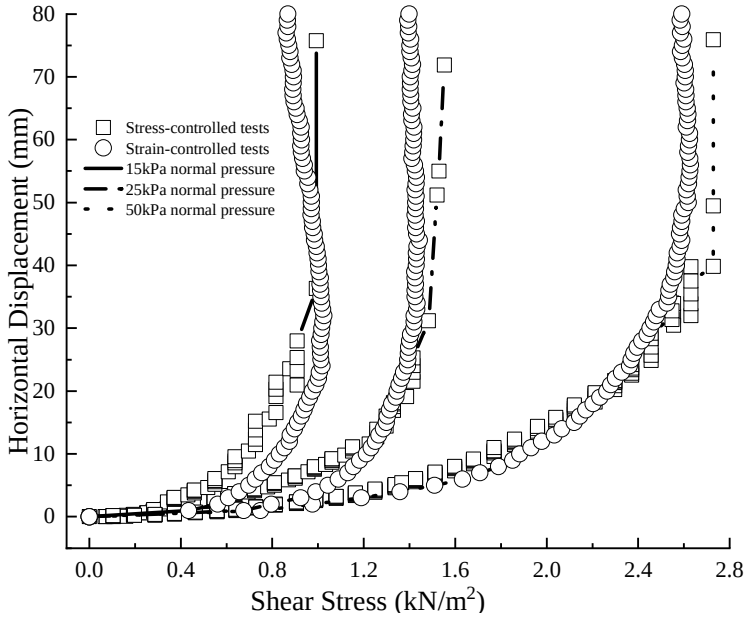

(a)Mercia Mudstone Clay

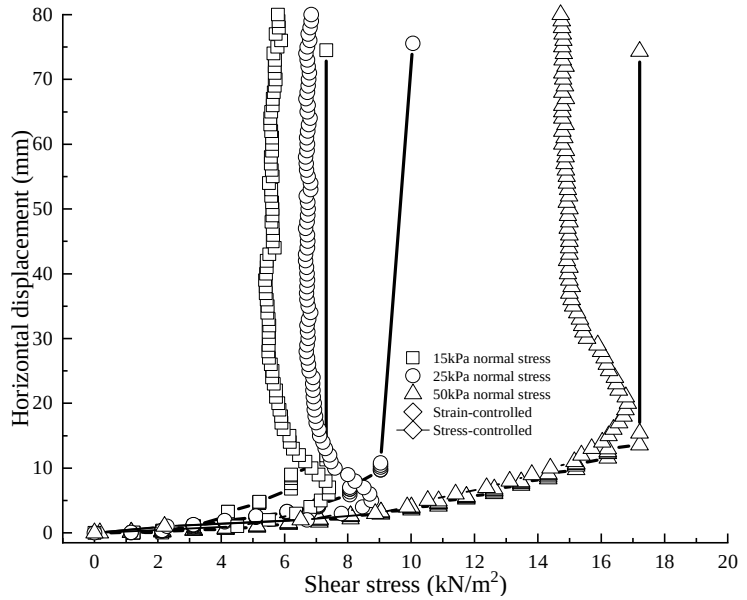

(b)Kaolin Clay

Figure 4.18 The results comparison between stress-controlled tests and displacement-controlled tests

Based on Figure 4.18, for both of Mercia Mudstone Clay- GDL interfaces and Kaolin Clay-GDL interfaces, the relationship curves between horizontal displacement and shear stress of the stress-controlled tests are similar to the curves of the displacement-controlled tests, respectively. Under the same normal stress, the peak shear strength of the displacement-controlled tests and

the stress-controlled tests is close, within 7 %, as shown in Figure 4.17. For example, under normal stress of 15 kPa and 50 kPa, the peak shear strength of Mercia Mudstone Clay – GDL interfaces for the stress-controlled tests is 10.7 kPa and 29.4 kPa, respectively, and the values for the displacement-controlled tests are 11.4 kPa and 29.2 kPa, respectively. The main difference between the curves of the stress-controlled tests and the displacement-controlled tests is that there is no post-peak stage in the stress-controlled tests as once peak is exceeded, failure ensues, much is the case in ultimate limit state failures in the field. Moreover, according to the Mohr-Coulomb strength line, the obtained cohesive force c and internal friction angle α of Mercia Mudstone Clay – GDL interfaces for the stress-controlled tests and the displacement-controlled tests are close, which is 3.17 kPa and 27.79°, 3.51 kPa and 27.11°, respectively. Additionally, in the displacement-controlled tests, for Mercia Mudstone Clay-GDL interfaces, after the peak shear stress, with the rise in horizontal displacement, the reduction in shear stress is slight, while, for Kaolin Clay -GDL interfaces, the reduction is remarkable, with an obvious post-strength being observed.

4.5 Summary

In this chapter, a temperature and stress-controlled direct shear apparatus was developed. By adopting this apparatus, a series of tests were carried out to validate the performance of the bespoke apparatus. The major conclusions are summarised as follows.

(1) The bespoke apparatus can allow the short-term and creep mechanical behaviour of soil-geosynthetics interfaces under environmental loadings, such as drying-wetting cycles, elevated temperature, and thermal cycles to be investigated, with reliable functionality.

(2) The whole performance of the bespoke temperature and stress-controlled shear apparatus was verified by conducting repetitive tests

and comparing the experimental outcomes obtained by the bespoke apparatus with the displacement-controlled equipment.

(3) In the rapid loading shear tests, the failure of the clayey soil-GDL interfaces happened suddenly once a shear stress threshold is exceeded, and the failure time and peak shear strength rise with the increases of normal stress, respectively.

(4) Unlike displacement-controlled testing, the stress-controlled apparatus allows in situ stress conditions to be applied (and varied if required) whilst other environmental conditions (temperature and saturation conditions) are altered.

(5) Unlike the conventional displacement-controlled apparatus, the developed stress-controlled apparatus cannot capture the post-peak stage of the shear stress-displacement curves as once peak shear stress is exceeded, failure ensues, much is the case in ultimate limit state failures in real engineering projects.

Chapter 5

Rapid loading shear tests on cover soil-GDL interfaces subjected to environmental loadings

5.1 Introduction

To obtain a better understanding on the short-term mechanical responses of clayey soil-GDL interfaces under environmental loadings, a series of rapid loading direct shear tests on clayey soil-GDL interfaces subjected to drying-wetting cycles, thermal cycles, drying-wetting cycle without heating and elevated temperature were performed using the bespoke stress and temperature-controlled large direct shear apparatus described in Chapter 4. The obtained experimental results allow for the impacts of the environmental factors on the short-term mechanical characteristics of clayey soil-GDL interfaces to be analysed and a corresponding detailed mechanism analysis is presented in Section 7.2.

5.2 Experimental program

In this study, rapid loading shear tests were conducted on two types of interfaces: Mercia Mudstone Clay-GDL interfaces and Kaolin Clay-GDL interfaces, respectively. Detailed properties of the adopted soil and GDL are presented in Section 3.4 and Section 4.4.1, respectively, and the preliminary preparation of specimens is introduced in Section 4.4.2. The rapid loading shear test refers to that, in the shearing process, the shear load is continually increased until the soil-GDL interface fails. As mentioned above, clayey soil-GDL interfaces are often used in the cover systems of waste containment facilities. In the UK, the general thickness of cover soil overlying the installed GDL is 1 m to 2 m and the normal stress on the clay-GDL interfaces imposed by the overlying cover soil is 20 kPa to 40 kPa. To represent the regular normal stress range imposed by the overlying cover soil, this research adopts the normal stress ranging from 15 kPa to 50 kPa, which simulates the

overlying cover soil with thickness ranging from approximately 0.75 m to 2.5 m. The shearing was initiated after 24 hours consolidation, with the soil-GDL interfaces submerged in water and adding weights at the rate of 10 kg every 5 minutes, which was ascertained through trial and error. The tests conducted as part of this investigation can be summarised into the following groups:

(1) **Standard rapid loading shear tests**: the tests were carried out under normal stress of 15 kPa, 20 kPa, 25 kPa, 40 kPa and 50 kPa, respectively, at room temperature (22 ℃).

(2) **Tests under elevated temperatures**: the process of the tests was almost the same with the standard tests, except that the whole process of the tests was conducted at an elevated temperature of 40 ℃ using the heating system under normal stress of 15 kPa, 25 kPa and 50 kPa, respectively.

(3) **Tests subjected to drying-wetting cycles**: in the tests, after 24 hours consolidation, the drying process was initiated. Water in the external shear box was discharged, and the heating system was turned on to dry the interface at a constant temperature of 40 ℃ for 24 hours. After that, the wetting process was started. The heating system was turned off, and water was poured into the external shear box to submerge the specimen for 24 hours. This accounts for a single drying-wetting cycle. The cycle was repeated until the required number was reached. Then, the shearing process was conducted on the soil-GDL interface with being submerged by water. In this research, tests after 0,1 and 3 drying-wetting cycles were implemented under normal stress of 15 kPa, 25 kPa and 50 kPa, respectively. After the drying cycle, the moisture content of Mercia Mudstone Clay and Kaolin Clay specimens in the top shear box was measured. A significant fall in soil moisture content during the drying process was observed, with about 40 % and 30 % less than those of the Mercia Mudstone Clay and Kaolin Clay specimens without experiencing drying cycles,

respectively.

(4) **Tests subjected to thermal cycle**: to investigate the sole impact of heating on the short-term mechanical behaviour of soil-GDL interfaces, tests subjected to thermal cycle were carried out. The procedure of the tests was almost the same with the tests subjected to drying-wetting cycles, except that during the drying process, the interfaces were heated to the temperature of 40 ℃ whilst being submerged in water. In this case, the tests after 1 thermal cycle were conducted under normal stress of 15 kPa, 25 kPa and 50 kPa, respectively.

(5) **Tests subjected to drying-wetting cycle without heating**: to explore the sole impact of drying on the short-term mechanical behaviour of soil-GDL interfaces, tests subjected to drying-wetting cycle without heating were carried out. The procedure of the tests was almost the same with the tests subjected to drying-wetting cycles, except that during the drying process, only water in the external shear box was discharged and the heating system remained switching off to dry the interface at room temperature of 22 ℃ for 7 days. In this case, the test after 1 drying-wetting cycle without heating was conducted under normal stress of 25 kPa. After the drying cycle without heating, the moisture content of Mercia Mudstone Clay and Kaolin Clay specimens in the top shear box was measured. A significant fall of moisture content in the soil sample during the drying process without heating was observed, with about 40 % and 30 % less than those of Mercia Mudstone Clay and Kaolin Clay specimens that did not experience drying cycle without heating, respectively, which was close to the reduction in the moisture content of Mercia Mudstone Clay and Kaolin Clay specimens experiencing the drying cycle with heating, respectively. This indicates that the drying effect of the drying cycle without heating on the soil samples was almost identical

to that of the drying cycle with heating.

(6) **Tests subjected to creep deformation**: in the tests, after 24 hours consolidation, a constant creep shear stress was imposed on soil-GDL interfaces under normal stress of 25 kPa for 5 days. After 5 days the rapid loading shearing process was initiated until failure of the interface. In this research, the imposed creep shear stress level was set as 50 %, 60 % and 70 % of the peak shear strength of the interfaces under 25 kPa normal stress (17.22 kPa for Mercia Mudstone-GDL interfaces and 10.11 kPa for Kaolin Clay-GDL interfaces), respectively.

The selection of 24 hours drying time is due to the following reasons: in real landfills, during the drying process, except for the heat produced from the underlying wastes, the cover soil is also directly exposed to sunshine, which can result in a relatively fast decline in the moisture content of cover soil. However, in the laboratory tests, during the drying process, the clayey soil-GDL interfaces are only heated from the bottom, which may cause the falling rate of moisture content in soil to be slower than that in reality. Thus, in this research, a relatively long drying duration of 24 hours was adopted to increase the decreasing magnitude of moisture content for soil sample during drying cycles. Based on the measured moisture content of Mercia Mudstone Clay and Kaolin Clay specimens after drying cycles, a significant fall of moisture content for soil samples was observed, with about 40 % and 30 % less than those of Mercia Mudstone Clay and Kaolin Clay specimens without experiencing drying cycles, respectively.

The temperatures of the clayey soil-GDL interfaces in cover systems of waste containment facilities are mainly controlled by two factors: the ambient temperature and the elevated temperature in the underneath waste due to the exothermal reaction of waste biodegradation and hydration. According to existing reports (Yeşiller et al., 2005), the maximum temperature of cover

systems in waste containment facilities can reach up to 40 ℃. Hence, to simulate an extreme situation, in this work, the temperature of 40 ℃ is adopted during the drying and heating cycles of the tests, respectively.

5.3 Results and analysis

5.3.1 Impacts of normal stress

The relationship curves between the horizontal displacement of Mercia Mudstone Clay/ Kaolin Clay - GDL interfaces against the shear stress and loading time are drawn in Figure 5.1 and Figure 5.2, respectively.

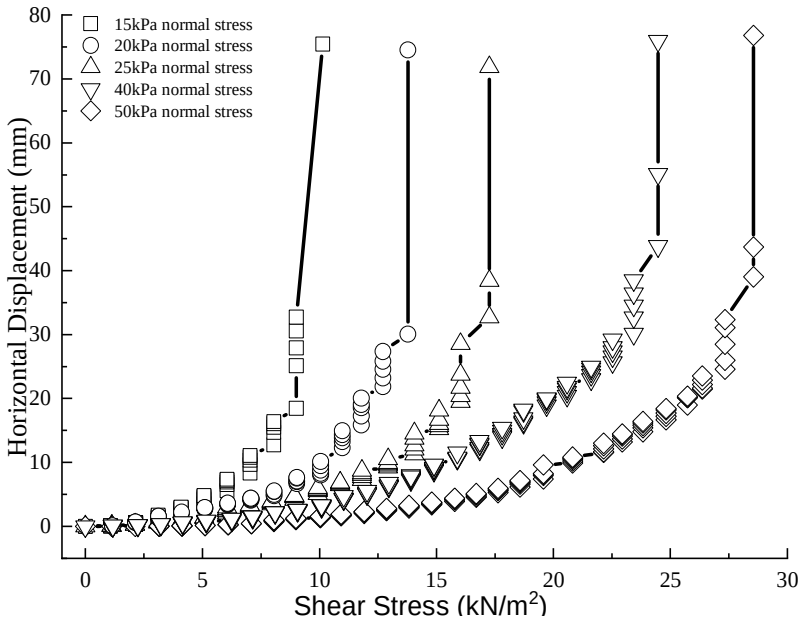

(a)Stress-horizontal displacement curves

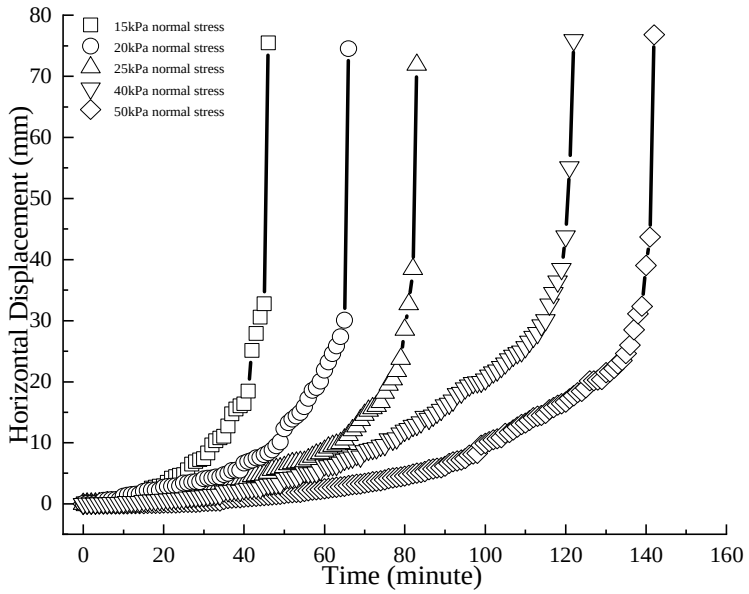

(b)Horizontal displacement in elapsed time

Figure 5.1 Tests on Mercia Mudstone Clay-GDL interfaces under different normal stress

Based on Figure 5.1, the peak shear strength and failure time of Mercia Mudstone Clay-GDL interfaces rise gradually with the rise in normal stress, respectively. For example, when the normal stress is increased from 15 kPa to 50 kPa, the peak shear strength and failure time increase by around 81 % and 208 %, respectively. This indicates that, under large vertical confining pressure, the stability of Mercia Mudstone Clay-GDL interfaces is stronger than that under low vertical confining pressure.

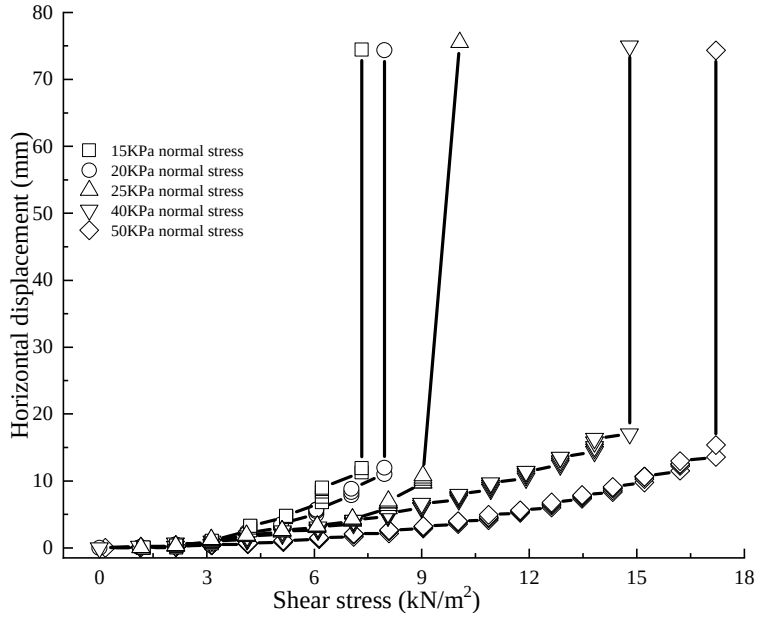

(a)Stress-horizontal displacement curves

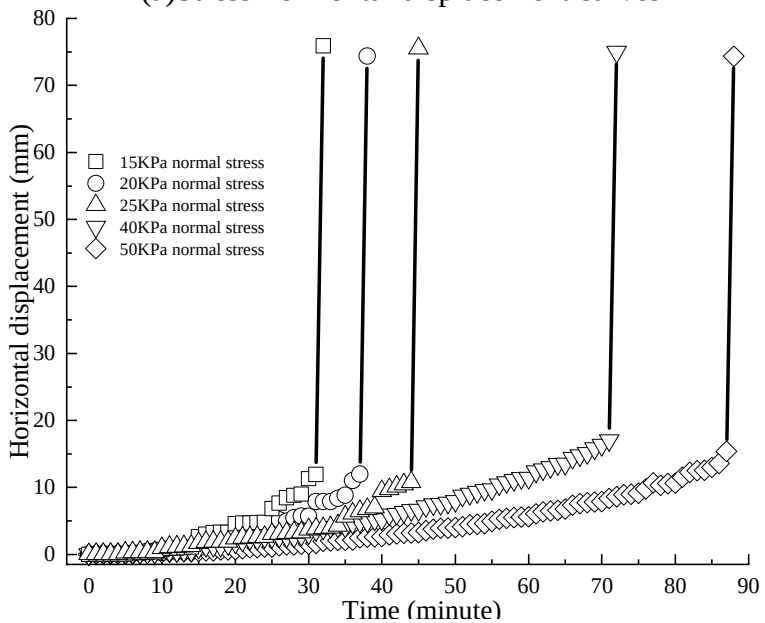

(b)Horizontal displacement in elapsed time

Figure 5.2 Tests on Kaolin Clay-GDL interfaces under different normal stresses

According to Figure 5.2, the peak shear strength and failure time of Kaolin Clay-GDL interfaces are lower than those of Mercia Mudstone Clay-GDL interfaces, respectively. As with Mercia Mudstone Clay-GDL interfaces, the peak shear strength and failure time of Kaolin Clay-GDL interfaces increase with the increase of normal stress, respectively. However, the influence of

normal stress on Kaolin Clay-GDL interfaces is less than that on Mercia Mudstone Clay-GDL interfaces, as shown in Figure 5.3. For instance, when normal stress is elevated from 20 kPa to 50 kPa, the peak shear strength and failure time of Mercia Mudstone Clay-GDL interfaces rise by approximately 116 % and 131 %, respectively. Meanwhile, for Kaolin Clay- GDL interfaces, they rise by 107 % and 115 %, respectively. Additionally, under the same shear stress, in elapsed time, the variation of horizontal displacement of Mercia Mudstone Clay-GDL interfaces is larger than that of Kaolin Clay-GDL interfaces. For example, under 25 kPa normal stress, for Mercia Mudstone Clay-GDL interfaces, during the last shear stress level of 1.44 kN/m^2 before failure, the horizontal displacement rises by 46.50 %, whilst for Kaolin Clay-GDL interfaces, during the last shear stress level of 0.81 kN/m^2 before failure, the horizontal displacement increases by 11.31 %. This indicates that the viscidity of Mercia Mudstone Clay-GDL interfaces is greater than that of Kaolin Clay-GDL interfaces. Moreover, it is worth noting that, Mercia Mudstone Clay-GDL interfaces can remain stable over a large horizontal displacement, whilst for Kaolin Clay-GDL interfaces, small deformation can lead to sudden failure. For instance, under normal stress of 40 kPa, for Mercia Mudstone Clay-GDL interfaces, at the 121^{st} minute, the horizontal displacement is 55.09 mm, in the next minute, it increases by 37.81 % to 75.92 mm, indicating the failure of the interface. In comparison, for Kaolin Clay-GDL interfaces, at the 71^{st} minute, this value is 17.02 mm, and rises by 340.54 % to 74.98 mm over the next minute, manifesting the failure of the interface. These results demonstrate that the ductility of Mercia Mudstone Clay-GDL interfaces is larger than that of Kaolin Clay-GDL interfaces and Kaolin Clay-GDL interfaces are more brittle than Mercia Mudstone Clay - GDL interfaces.

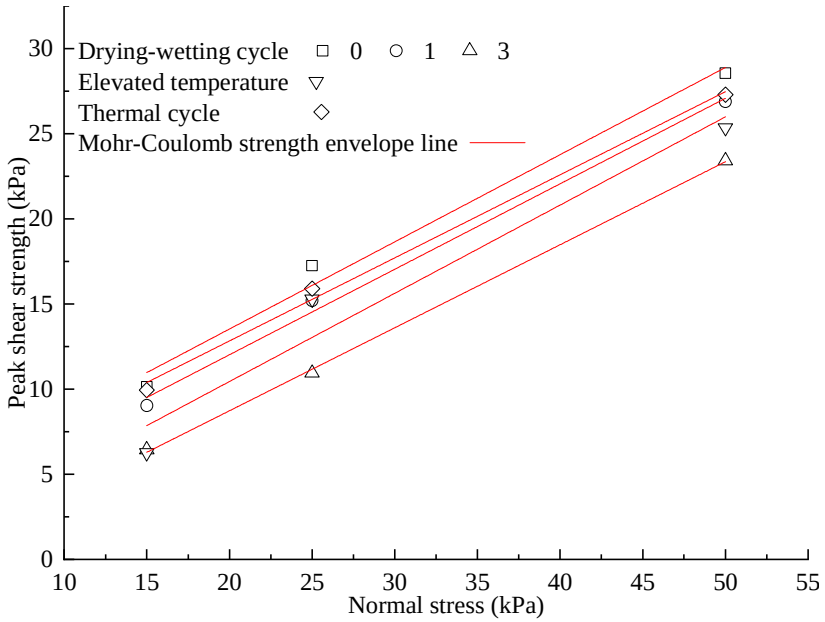

(a)Mercia Mudstone Clay-GDL interface

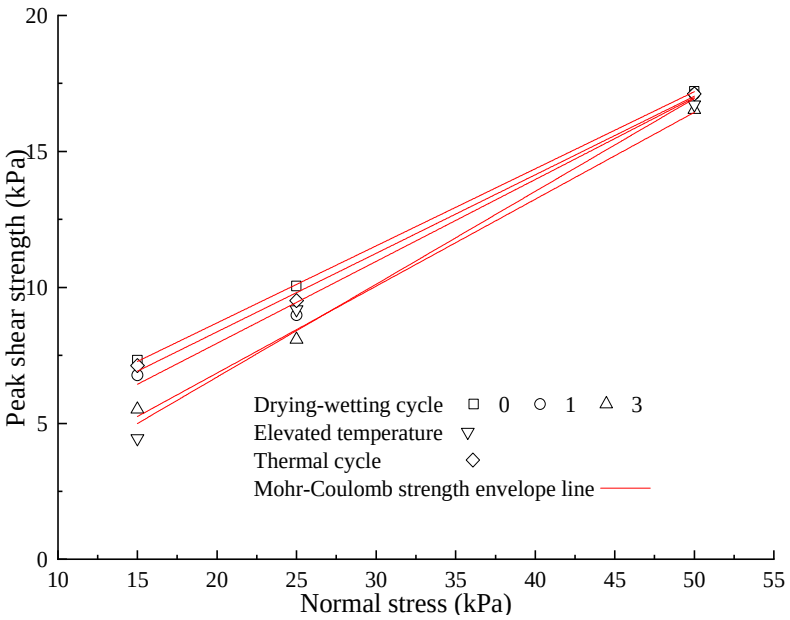

(b) Kaolin Clay-GDL interface

Figure 5.3 The peak shear strength of clayey soil-GDL interfaces

5.3.2 Impacts of creep deformation

The relationship curves between horizontal displacement of Mercia Mudstone Clay/ Kaolin Clay -GDL interfaces subjected to creep deformation against shear stress and loading time are drawn in Figure 5.4 and Figure 5.5,

respectively.

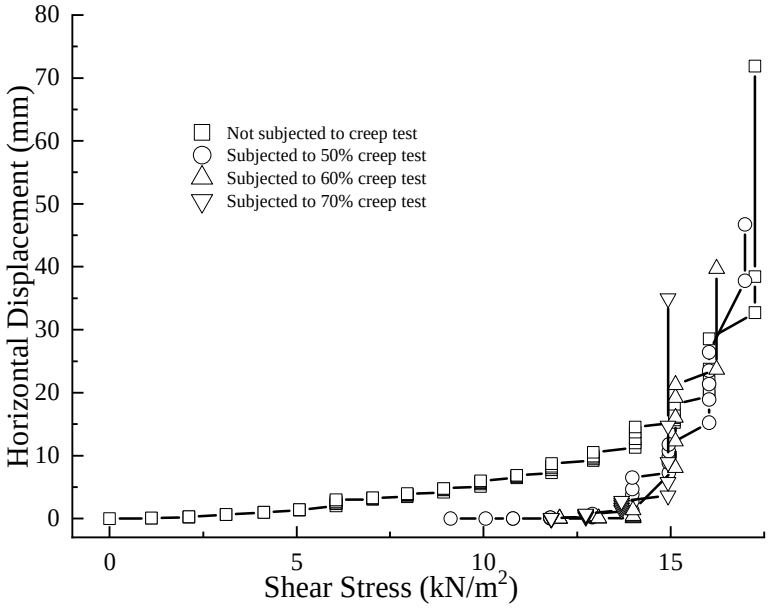

(a) Stress-horizontal displacement curves

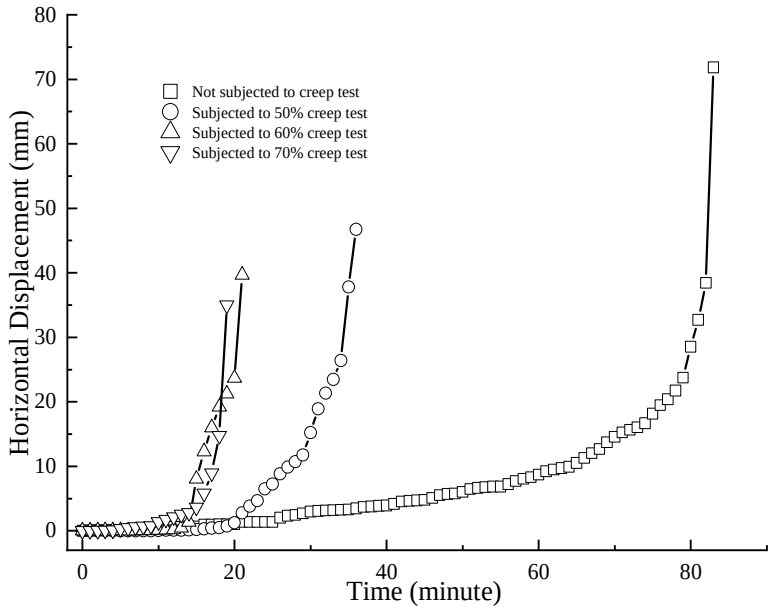

(b)Horizontal displacement in elapsed time

Figure 5.4 Tests on Mercia Mudstone Clay -GDL interfaces subjected to creep deformation

Based on Figure 5.4 and Figure 5.5, the creep deformation of both Mercia

Mudstone Clay/Kaolin Clay-GDL interfaces does not have considerable impact on their respective peak shear strengths. The peak shear strength of the specimens without and with creep deformation under different creep shear stress levels is close. However, the failure time of specimens experiencing creep deformation is lower than that without experiencing creep deformation.

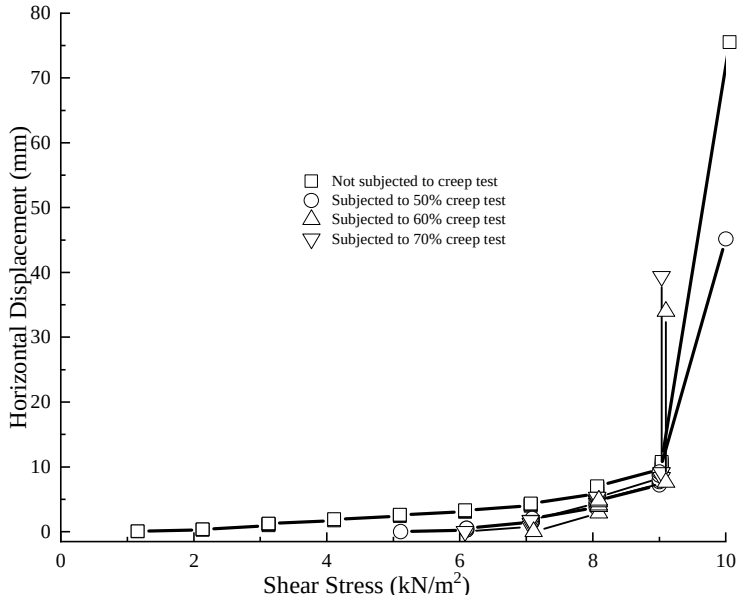

(a) Stress-horizontal displacement curves

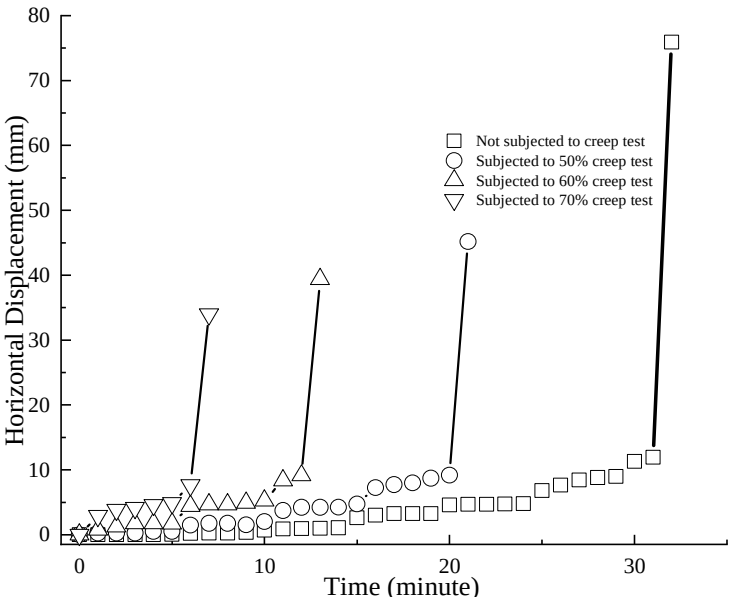

(b)Horizontal displacement in elapsed time

Figure 5.5 Tests on Kaolin Clay -GDL interfaces subjected to creep deformation

5.3.3 Impacts of temperature

The relationship curves between horizontal displacement of Mercia Mudstone Clay/ Kaolin Clay-GDL interfaces at different temperatures against shear stress and loading time are drawn in Figure 5.6 and Figure 5.7, respectively.

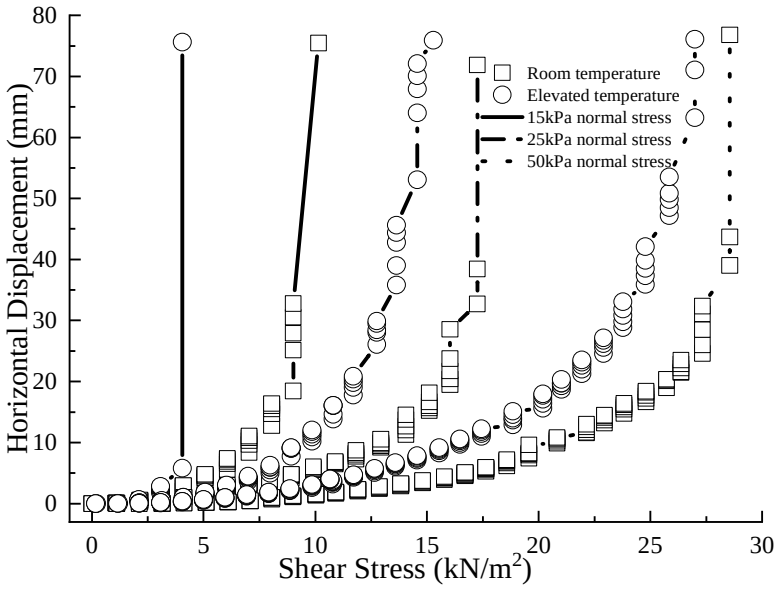

(a) Shear stress-horizontal displacement curves

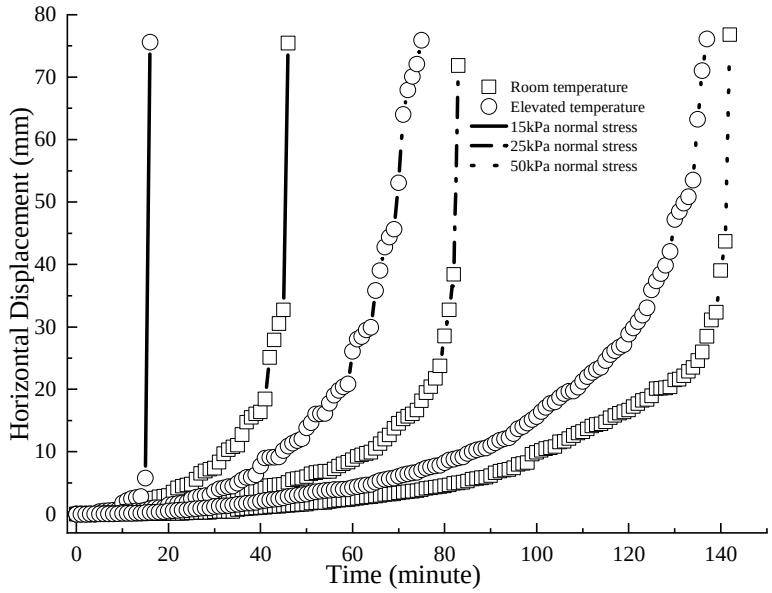

(b)Horizontal displacement in elapsed time

Figure 5.6 Tests on Mercia Mudstone Clay -GDL interfaces at different temperatures

Based on Figure 5.6, the horizontal displacement of Mercia Mudstone Clay - GDL interfaces at elevated temperature is higher than that of room temperature (22 ℃). More specifically, the disparity between them gradually rises with the ascent in shear stress and loading time. Moreover, at elevated temperature, the peak shear strength and failure time of interfaces are lower than those at room temperature. Under low normal stress, the difference between the peak shear strength/failure time at elevated temperature and room temperature is larger than that under high normal stress, respectively. This is presented in Figure 5.3. For instance, under 15 kPa normal stress, the peak shear strength and failure time of the specimen at room temperature are 60.13 % and 65.21 % greater than those at elevated temperature, respectively. In comparison, under 50 kPa normal stress, these values are 5.48 % and 3.52 %, respectively. Furthermore, the impacts of normal stress on the peak shear strength and failure time of the specimens at elevated temperature are larger than those at room temperature. For instance, when normal stress is increased from 15 kPa to 50 kPa, the peak shear strength and failure time of the specimens at room temperature increases by 181 % and 208 %, respectively. Meanwhile, for the specimens at elevated temperature, these values are 567.30 % and 756.25 %, respectively.

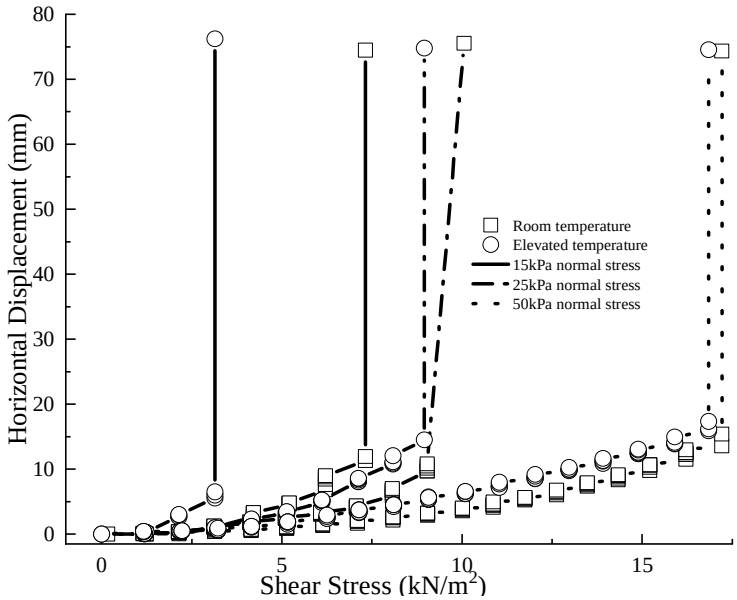

(a) Shear stress-horizontal displacement curves

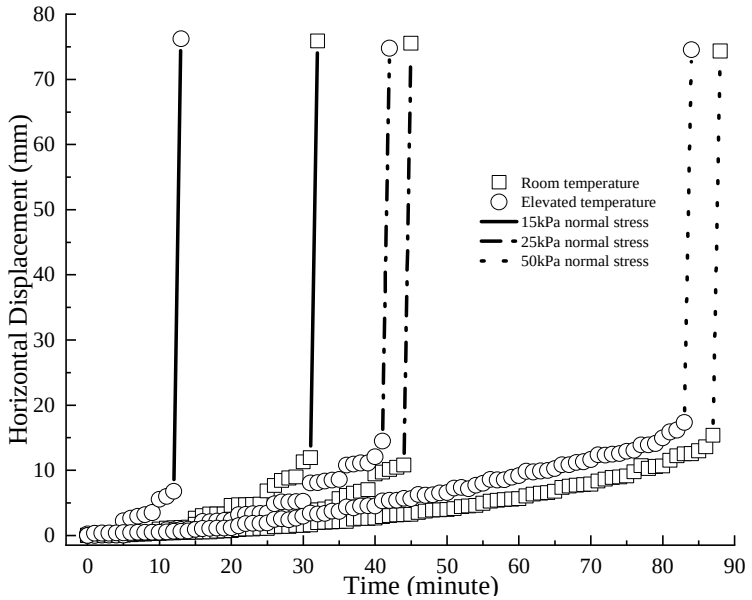

(b)Horizontal displacement in elapsed time

Figure 5.7 Tests on Kaolin Clay-GDL interfaces subjected at different temperatures

Based on Figure 5.7, similar to Mercia Mudstone Clay-GDL interfaces, the horizontal displacement of Kaolin Clay-GDL interfaces at elevated temperature is higher than that at room temperature. Moreover, as with Mercia Mudstone Clay-GDL interfaces, with the rise of temperature, the peak shear strength and failure time of Kaolin Clay-GDL interfaces decrease, and the decreasing magnitude under low normal stress is larger than that under high normal stress, respectively. However, the falling amplitude of Kaolin Clay-GDL interfaces was lower than that of Mercia Mudstone Clay-GDL interfaces, as shown in Figure 5.3. For example, under 50 kPa normal stress, for Kaolin Clay-GDL interfaces, with the rise in temperature, the peak shear strength and failure time fall 2.13 % and 2.54 %, respectively. Meanwhile, for Mercia Mudstone Clay-GDL interfaces, these values are 5.49 % and 3.52 %, respectively. Furthermore, similar to Mercia Mudstone Clay-GDL interfaces, the peak shear strength and failure time of Kaolin Clay-GDL interfaces at elevated temperature are more sensitive to the rise in normal stress than those at room temperature.

5.3.4 Impacts of drying-wetting cycles

The relationship curves between horizontal displacement of Mercia Mudstone Clay/ Kaolin Clay-GDL interfaces subjected to drying-wetting cycles against shear stress and loading time are drawn in Figure 5.8 and Figure 5.9, respectively.

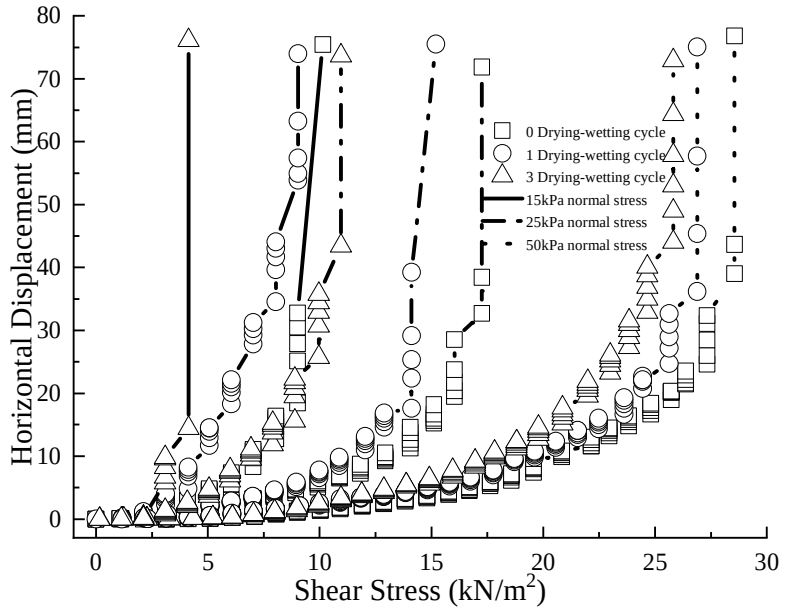

(a)Shear stress-horizontal displacement curves

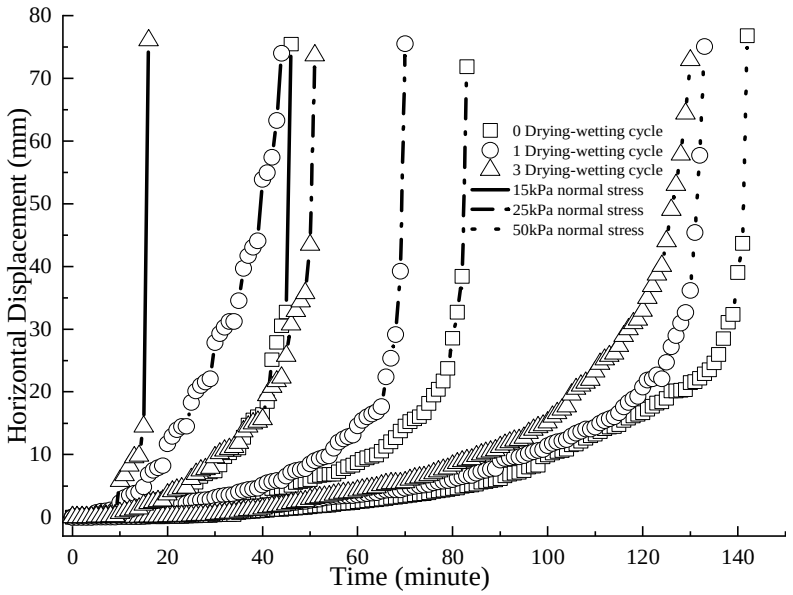

(b)Horizontal displacement in elapsed time

Figure 5.8 Tests on Mercia Mudstone Clay-GDL interfaces subjected to different drying-wetting cycles

Based on Figure 5.8, the horizontal displacement of Mercia Mudstone Clay-GDL interfaces with a high number of drying-wetting cycles is higher than those with a low number. More specifically, the difference between them increases gradually with the increase in shear stress and loading time. Taking the specimens under 50 kPa normal stress as an example, when the shear stress is 1.52 kN/m^2 at the 80^{th} minute, the horizontal displacement for the specimen subjected to 3 drying-wetting cycles is 37.14 % and 81.75 % higher than those of specimens subjected to 1 and 0 cycle, respectively. In comparison, when shear stress is 2.21 kN/m^2 at the 120^{th} minute, these values are 58.62 % and 97.54 %, respectively. Moreover, during drying-wetting cycles, the peak shear strength and failure time of the specimens gradually decrease. The extent of this decline under low normal stress is larger than that under high normal stress. This is presented in Figure 5.3. For example, under 25 kPa normal stress, the peak shear strength and failure time of original Mercia Mudstone Clay-GDL interfaces fall by 10.95 % and 4.34 %, 59.14 % and 65.21 % when subjected to 1 and 3 drying-wetting cycles, respectively. In comparison, under 50 kPa normal stress, these values are 5.83 % and 6.33 %, 9.57 % and 8.45 % when subjected to 1 and 3 cycles, respectively. Furthermore, the impact of normal stress on the peak shear strength and failure time of the specimens subjected to drying-wetting cycles are larger than that of the original specimens. For instance, when normal stress is increased from 15 kPa to 50 kPa, the peak shear strength and failure time of the original specimens increase by 181 % and 208 %, respectively, whilst for the specimens subjected to 3 cycles, these values are 523 % and 712 %, respectively.

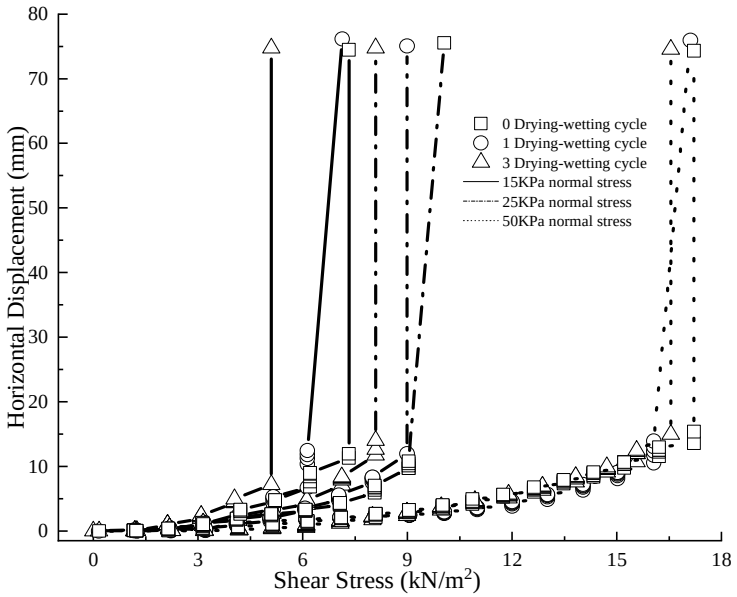

(a)Shear stress-horizontal displacement curves

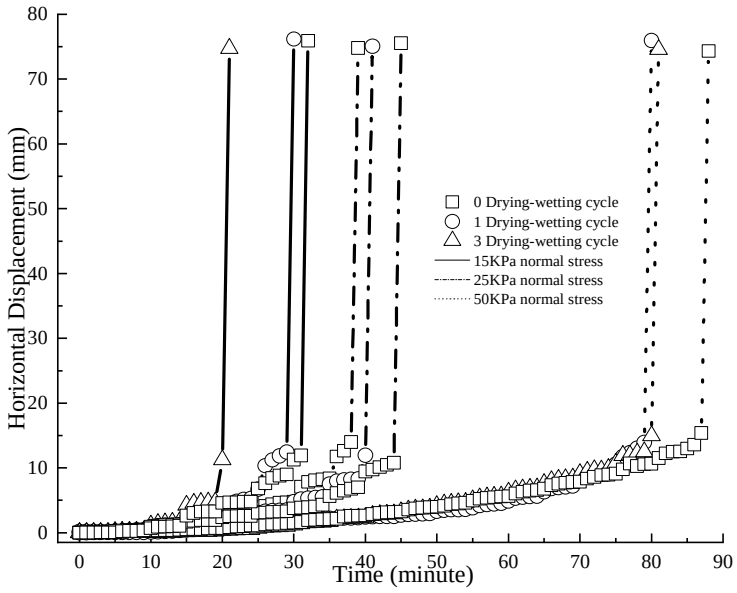

(b)Horizontal displacement in elapsed time

Figure 5.9 Tests on Kaolin Clay-GDL interfaces subjected to different drying-wetting cycles

Based on Figure 5.9, similar to Mercia Mudstone Clay-GDL interfaces, the horizontal displacement of Kaolin Clay-GDL interfaces with a high number of drying-wetting cycles is higher than those of a low number. However, unlike Mercia Mudstone Clay-GDL interfaces, the difference between the

horizontal displacement of Kaolin Clay-GDL interfaces with a high number of drying-wetting cycles and those with a low number does not rise markedly with the increase in shear stress and loading time. Taking the specimens under 50 kPa normal stress as an example, when shear stress is 0.90 kN/m^2 at the 46^{th} minute, the horizontal displacement for the specimen subjected to 3 drying-wetting cycles is 1.14 % and 1.5 % higher than those subjected to 1 and 0 cycle, respectively. In comparison, when shear stress is 1.32 kN/m^2 at the 74^{th} minute, these values are 1.62 % and 1.94 %, respectively. Moreover, as with Mercia Mudstone Clay-GDL interfaces, the peak shear strength and failure time of Kaolin Clay-GDL interfaces decrease gradually during drying-wetting cycles. The extent of this decrease under low normal stress is larger than that of under high normal stress, as shown in Figure 5.3. However, compared to Mercia Mudstone Clay-GDL interfaces, the falling amplitude of Kaolin Clay-GDL interfaces is lower. For example, under 25 kPa normal stress, the peak shear strength and failure time of original Kaolin Clay-GDL interfaces fall by 10.11 % and 8.88 %, 19.55 % and 13.33 % after 1 and 3 drying-wetting cycles, respectively. In comparison, for Mercia Mudstone Clay-GDL interfaces, these values are 11.91 % and 15.66 %, 36.38 % and 38.55 % after 1 and 3 cycles, respectively. Furthermore, similar to Mercia Mudstone Clay-GDL interfaces, the peak shear strength and failure time of Kaolin Clay-GDL interfaces subjected to drying-wetting cycles are more sensitive to the rise in normal stress than that of original specimens.

5.3.5 Impacts of thermal cycle

The relationship curves between horizontal displacement of Mercia Mudstone Clay / Kaolin Clay-GDL interfaces subjected to thermal cycle against shear stress and loading time are drawn in Figure 5.10 and Figure 5.11, respectively.

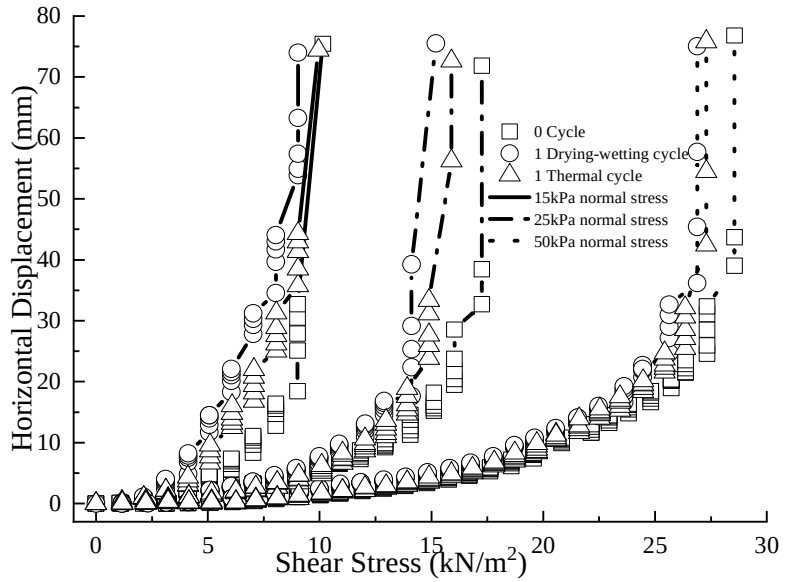

(a) Shear stress-horizontal displacement curves

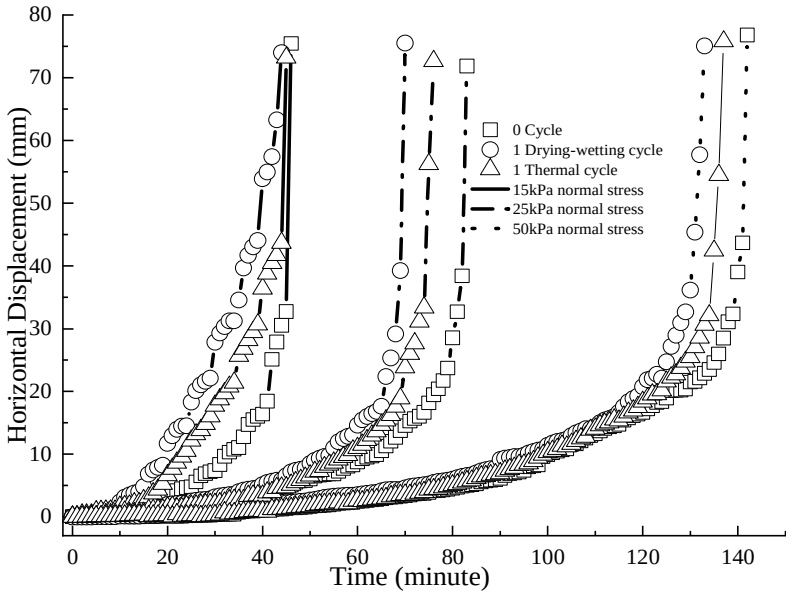

(b)Horizontal displacement in elapsed time

Figure 5.10 Tests on Mercia Mudstone Clay -GDL interfaces subjected to thermal cycle

Based on Figure 5.10, the horizontal displacement of Mercia Mudstone Clay-GDL interfaces subjected to 1 thermal cycle is higher than that of the original specimens but lower than those subjected to 1 drying-wetting cycle. Moreover, during the thermal cycle, the decline in peak shear strength and

failure time was observed. The decreasing amplitudes are lower than those during 1 drying-wetting cycle, respectively, as shown in Figure 5.3. For instance, under 25 kPa normal stress, after 1 thermal cycle, the peak shear strength and failure time of Mercia Mudstone Clay-GDL interfaces fall 7.85 % and 8.43 %, respectively. Whilst after 1 drying-wetting cycle, these percentages are 11.91 % and 15.66 %, respectively.

Based on Figure 5.11, similar to Mercia Mudstone Clay-GDL interfaces, the horizontal displacement of Kaolin Clay-GDL interface subjected to 1 thermal cycle is lower than those subjected to 1 drying-wetting cycle and higher than that of the original specimens. Moreover, as with Mercia Mudstone Clay-GDL interfaces, during the thermal cycle, the decreasing amplitudes of peak shear strength and failure time for Kaolin Clay-GDL interfaces are lower than those during 1 drying-wetting cycle, respectively. This is presented in Figure 5.3. However, the decreasing amplitudes of Kaolin Clay-GDL interfaces during the thermal cycle are lower than those of Mercia Mudstone Clay-GDL interfaces. For instance, under 50 kPa normal stress, for Kaolin Clay-GDL interfaces, the peak shear strength and failure time reduce by 1.42 % and 2.27 %, respectively, whist for Mercia Mudstone Clay-GDL interfaces, these numbers are 4.43 % and 3.52 %, respectively.

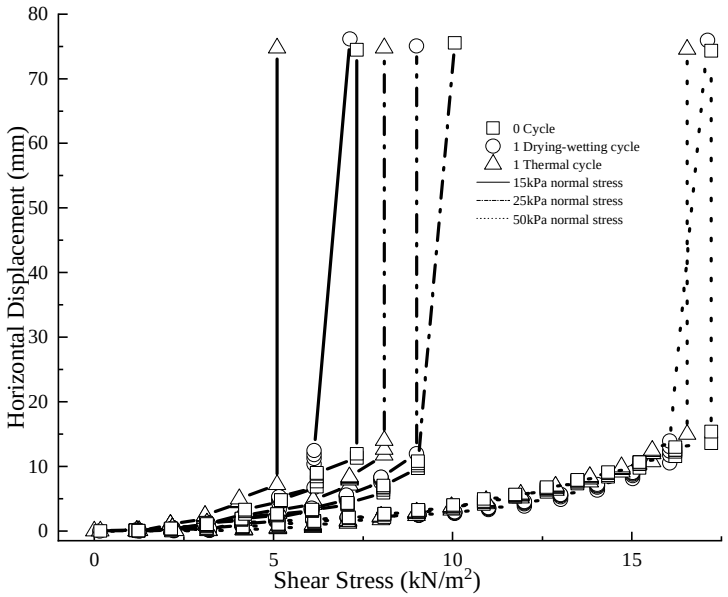

(a) Shear stress-horizontal displacement curves

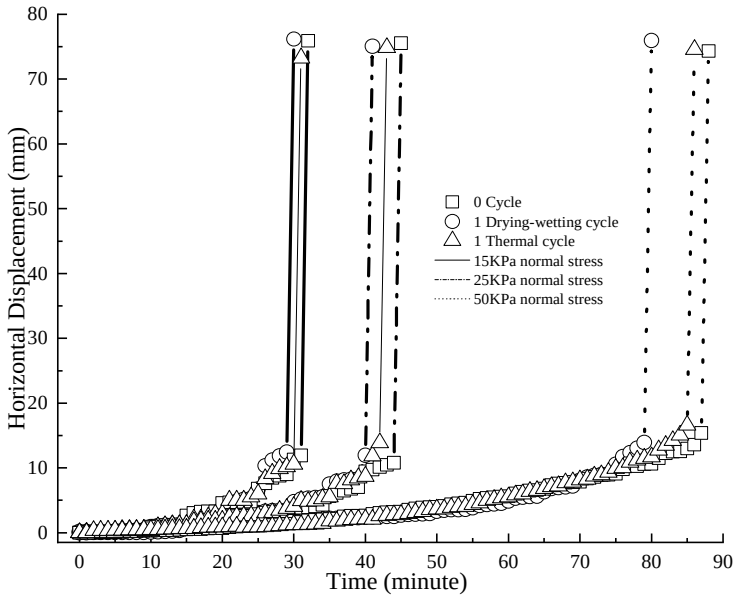

(b)Horizontal displacement in elapsed time

Figure 5.11 Tests on Kaolin Clay -GDL interfaces subjected to thermal cycle

5.3.6 Impacts of drying-wetting cycle without heating

The relationship curves between horizontal displacement of Mercia Mudstone Clay/ Kaolin Clay-GDL interfaces subjected to drying-wetting cycle without heating against shear stress and loading time are drawn in Figure 5.12 and Figure 5.13, respectively.

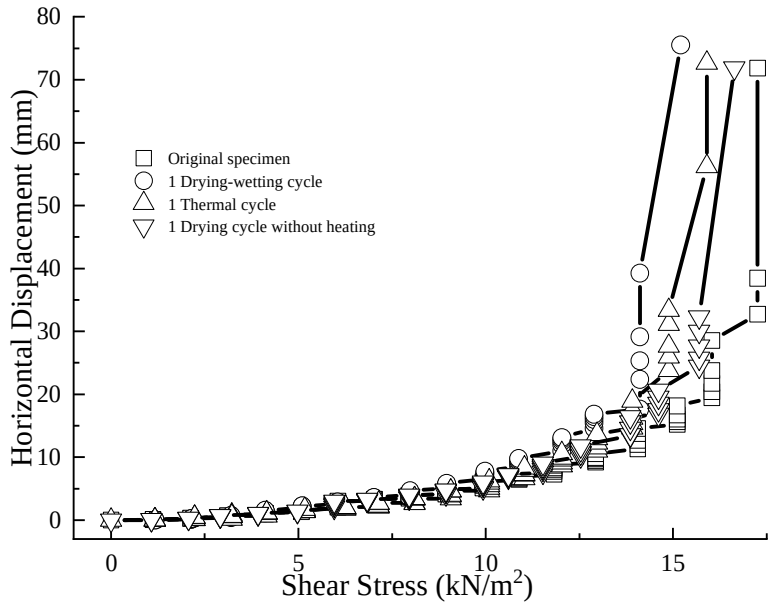

(a) Shear stress-horizontal displacement curves

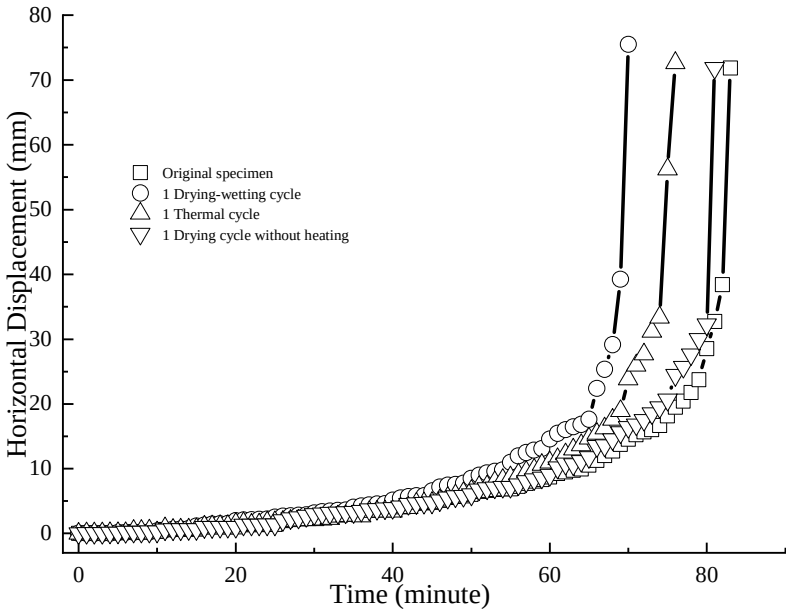

(b)Horizontal displacement in elapsed time

Figure 5.12 Tests on Mercia Mudstone Clay -GDL interfaces subjected to drying-wetting cycle without heating under 25 kPa normal stress

Based on Figure 5.12, the horizontal displacement of Mercia Mudstone Clay-GDL interfaces subjected to 1 drying-wetting cycle without heating is higher than that of the original specimen but lower than those subjected to 1 thermal cycle. Moreover, compared to the original specimen, the decrease in peak

shear strength and failure time of the specimen subjected to 1 drying-wetting cycle without heating was observed. However, the decreasing amplitudes are lower than those that are subjected to 1 drying-wetting cycle with heating and 1 thermal cycle, respectively. For instance, under 25 kPa normal stress, after 1 thermal cycle, the peak shear strength and failure time of Mercia Mudstone Clay-GDL interfaces fall by 7.85 % and 8.43 %, respectively. Meanwhile, after 1 drying-wetting cycle without heating, these values are 3.74 % and 2.46 %, respectively. This indicates that the impacts of drying alone on the peak shear strength and failure time of Mercia Mudstone Clay-GDL interfaces is small, which is lower than those of sole heating and drying with heating, respectively.

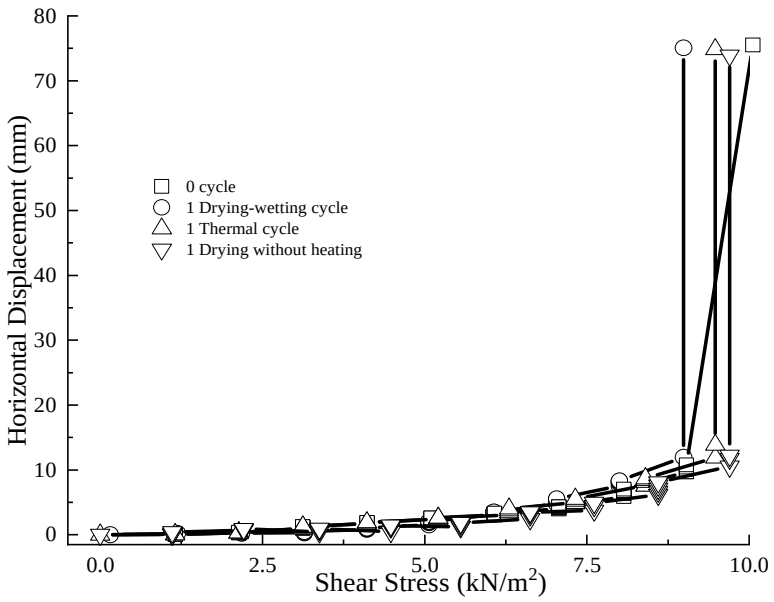

(a) Shear stress-horizontal displacement curves

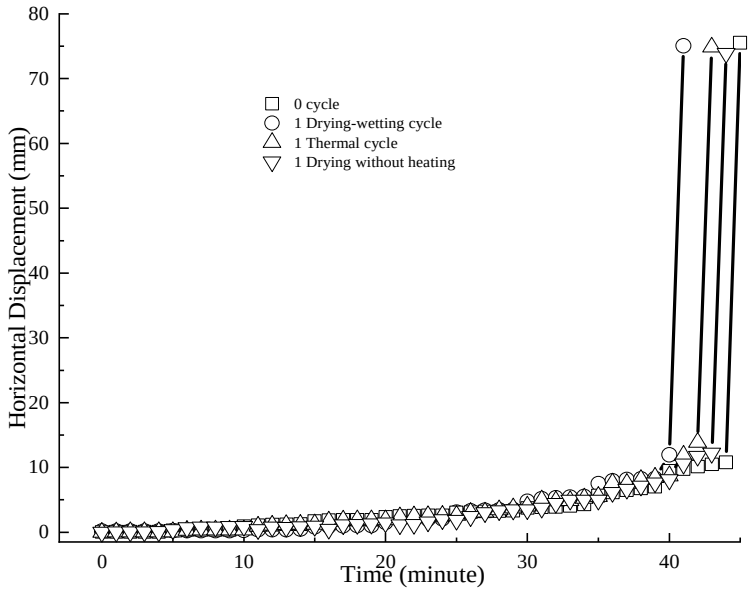

(b) Horizontal displacement in elapsed time

Figure 5.13 Tests on Kaolin Clay -GDL interfaces subjected to drying cycle without heating under 25 kPa normal stress

Based on Figure 5.13, similar to Mercia Mudstone Clay-GDL interfaces, the horizontal displacement of Kaolin Clay-GDL interfaces subjected to 1 drying-wetting cycle without heating is higher than that of the original specimen but lower than those subjected to 1 thermal cycle. Moreover, as with Mercia Mudstone Clay-GDL interfaces, compared with the original specimen, the decrease in peak shear strength and failure time of the Kaolin Clay-GDL interface subjected to 1 drying-wetting cycle without heating was observed. However, the decreasing amplitudes are lower than those of the specimens subjected to 1 drying-wetting cycle with heating and 1 thermal cycle, respectively. This indicates that the impacts of drying alone on the peak shear strength and failure time of Kaolin Clay-GDL interfaces is small, which is lower than those of sole heating and drying with heating, respectively. Additionally, the decreasing amplitudes of peak shear strength and failure time of Kaolin Clay-GDL interfaces during drying-wetting cycle without heating are lower than those of Mercia Mudstone Clay-GDL interfaces, respectively. For instance, under 25 kPa normal stress, for Kaolin Clay-GDL interfaces, the peak shear strength and failure time reduce by 3.5 % and 2.22 %, respectively, whilst, for Mercia Mudstone Clay-GDL interfaces,

these figures are 3.74 % and 2.46 %, respectively.

5.3.7 Interface shear strength parameters

According to Mohr-Coulomb strength criterion, cohesive forces (a) and internal friction angles (δ) of the clayey soil-GDL interfaces were obtained by fitting of Mohr-Coulomb strength lines, as presented in Figure 5.3. The attained parameters are tabulated in Table 5.1 (Lambe and Whitman, 1991).

Based on Table 5.1, the cohesive force and internal friction angle of Mercia Mudstone Clay-GDL interfaces are higher than those of Kaolin Clay-GDL interfaces, respectively. The difference of internal friction angle between them is larger than that of cohesive force. For example, the cohesive force of the original Mercia Mudstone Clay-GDL interface is 8.94 % higher than that of the Kaolin Clay-GDL interface. Whereas in terms of internal friction angle, it is 80.25 %. Additionally, during drying-wetting cycles, for both interfaces, the cohesive force reduced gradually, whilst a slight increase in the internal friction angle was observed. This demonstrated that the impact of drying-wetting cycles on the cohesive force is slightly larger than that on the internal friction angle. For instance, after 3 drying-wetting cycles, the cohesive force of Mercia Mudstone Clay-GDL interfaces and Kaolin Clay-GDL interfaces declines by 69.30 % and 84.76 %, respectively. Meanwhile, these percentages are 2.63 % and 12.70 %, respectively, in terms of the internal friction angle. Moreover, it should be noted that the impacts of thermal cycle on the strength parameters are less than those of drying-wetting cycles. Taking Mercia Mudstone Clay-GDL interfaces as an example, the cohesive force and internal friction angle change 39.81 % and 1.43 %, respectively after one drying-wetting cycle, whereas these figures are 6.68 % and 0.95 %, respectively, after one thermal cycle. With the increase in temperature, the internal friction angle increases slightly for both interfaces, whereas a decrease was observed in the cohesive force. The difference in cohesive force and internal friction angle between the original interfaces and the interfaces

at elevated temperature are greater than those between the original interfaces and interfaces subjected to drying-wetting/thermal cycles, respectively. A detailed mechanism analysis is presented in Section 7.2.

Table 5.1 The shear strength parameters of the specimens

		Original specimen	1 Drying-wetting cycle	3 Drying-wetting cycle	1 Thermal cycle	Elevated temperature
Mercia Mudstone Clay-GDL interface	Cohesive force a (kPa)	3.29	1.98	1.01	3.07	0.14
	Internal friction angle δ (°)	29.22	29.64	29.99	29.50	29.96
Kaolin Clay-GDL interface	Cohesive force a (kPa)	3.02	1.92	0.46	2.58	0.10
	Internal friction angle δ (°)	16.21	17.24	18.27	16.50	19.53

5.4 Summary

In this chapter, a series of rapid loading shear tests were carried out on clayey soil-GDL interfaces subjected to environmental loadings using the bespoke temperature and stress-controlled large direct shear apparatus. According to the experimental outcomes, the impacts of drying-wetting cycles, thermal cycle, drying-wetting cycle without heating, elevated temperature, normal stress, soil type and creep deformation on the short-term mechanical characteristics of clayey soil-GDL interfaces were investigated. A detailed mechanism analysis is presented in Chapter 7. The main conclusions are summarised as follows:

(1) The ductility of Mercia Mudstone Clay-GDL interfaces is higher than

that of Kaolin Clay-GDL interfaces. The Mercia Mudstone Clay-GDL interfaces can remain stable under a large horizontal displacement, whilst small deformation can lead to the sudden failure of Kaolin Clay-GDL interfaces. This indicates that Kaolin Clay-GDL interfaces are more brittle than Mercia Mudstone Clay-GDL interfaces.

(2) The peak shear strength and failure time of the interfaces subjected to drying-wetting cycles and elevated temperature are more sensitive to the rise in normal stress than that of the original specimens.

(3) Under low normal stress, the peak shear strength and failure time of clayey soil-GDL interfaces are more sensitive to drying-wetting cycles and elevated temperature than those under high normal stress, respectively.

(4) Compared to the original specimens, interfaces subjected to drying-wetting cycles, thermal cycles and elevated temperature, have lower peak shear strength.

(5) The peak shear strength of Mercia Mudstone Clay-GDL interfaces is higher than that of Kaolin Clay-GDL interfaces. Additionally, the detrimental impacts of drying-wetting cycles, thermal cycles and elevated temperature on the peak shear strength of Mercia Mudstone Clay-GDL interfaces are greater than those of Kaolin Clay-GDL interfaces, respectively.

(6) The peak shear strength and failure time of the clayey soil-GDL interfaces subjected to 1 drying-wetting cycle is lower than those subjected to 1 thermal cycle, respectively.

(7) The decreasing magnitudes of peak shear strength and failure time of clayey soil-GDL interfaces subjected to 1 drying-wetting cycle without heating are lower than those subjected to 1 drying-wetting

cycle with heating and 1 thermal cycle, respectively. This indicates that the detrimental impacts of drying without heating on the short-term mechanical properties of clayey soil-GDL interfaces is lower than those of sole heating and drying with heating, respectively.

Chapter 6

Creep tests on cover soil-GDL interfaces subjected to environmental loadings

6.1 Introduction

To obtain a better understanding about the creep mechanical responses of clayey soil-GDL interfaces under environmental loadings, in this chapter, a series of creep shear tests on clayey soil-GDL interfaces subjected to drying-wetting cycles, drying-wetting cycle without heating and thermal cycles were performed using the self-designed stress and temperature-controlled large direct shear apparatus. The obtained experimental results allow for the impacts of environmental factors on the creep mechanical characteristics of clayey soil-GDL interfaces to be analysed and a corresponding detailed mechanism analysis is presented in Section 7.3.

6.2 Experimental program

Creep shear tests were carried out on two types of interfaces: Mercia Mudstone Clay-GDL interfaces and Kaolin Clay-GDL interfaces, subjected to environmental loadings such as drying-wetting cycles, thermal cycles, and drying-wetting cycle without heating, using the aforementioned bespoke stress and temperature-controlled large direct shear apparatus. Detailed properties of the adopted soil and GDL are presented in Section 3.3 and Section 4.4.1, respectively, and the preliminary preparation of specimens is introduced in Section 4.4.2. The creep shear tests were conducted under normal stress of 25 kPa (representative of approximately 1.25 m of cover soils) that was taken at the middle normal stress range of those for the rapid loading tests and a value typical in the UK practice when allowing for top soil and vegetation. For all the creep shear tests, initially, 24 hours consolidation was conducted, and then dead weights were added to the hanger until reaching

the targeted creep shear stress level. A detailed introduction of the conducted tests is as follows:

(1) **Creep tests subjected to drying-wetting cycles**: In the tests, six different levels of creep shear stress: 50 %, 60 %, 70 %, 80 %, 90 % and 95 % of the peak shear strength for Mercia Mudstone Clay-GDL interfaces and five different levels of creep shear stress: 80 %, 70 %, 60 %, 50 %, and 40 % of the peak shear strength for Kaolin Clay-GDL interfaces were adopted, respectively. The peak shear strength was determined by conducting three standard rapid loading shear tests under 25 kPa normal stress. The average value of peak shear strength for the three repetitive tests was adopted as the reference for the creep shear tests (17.22 kPa for Mercia Mudstone Clay-GDL interfaces and 10.11 kPa for Kaolin Clay-GDL interfaces). During the tests, after 24 hours consolidation, the interfaces were initially imposed by corresponding creep shear stress, with being submerged in water. If the horizontal displacement of clayey soil-GDL interfaces has not reached the maximum value (80 mm) after 4 days from imposing the creep shear stress, drying-wetting cycles were imposed on the interfaces. The drying process was conducted before the subsequent wetting process. During the drying process, water in the external shear box was discharged and the heating system was turned on to dry the interfaces at a constant temperature of 40 ℃ for 24 hours. After that, the wetting process was carried out, where the interfaces were fully submerged in water for 24 hours at the room temperature (22℃). This is one number of drying-wetting cycle. In this research, three numbers of drying-wetting cycles were conducted for each test. After the drying cycle, the moisture contents of Mercia Mudstone Clay/ Kaolin Clay specimens in the top shear box were measured. A significant fall in the moisture content of soil samples during the drying process was observed, with about 40 % and 30 % less than those of Mercia Mudstone Clay and Kaolin Clay specimens without experiencing drying cycles, respectively.

(2) **Creep tests subjected to thermal cycles**: In order to further explore the variation mechanism of creep mechanical behaviour of interfaces during drying-wetting cycles and explore the individual impact of elevated temperature on the creep mechanical behaviour of interfaces, creep shear tests on clayey soil-GDL interfaces subjected to thermal cycles were conducted. Mercia Mudstone Clay-GDL interface samples were subjected to thermal cycles under 25 kPa normal stress with creep stress levels of 70 %, 80 % and 90 % of the peak shear strength. Meanwhile, Kaolin Clay-GDL interfaces were placed under 25 kPa normal stress and creep stress levels of 70 % and 80 % of the peak shear strength. The procedure of the creep tests subjected to thermal cycles was almost identical to the creep tests during drying-wetting cycles, with the exception that, unlike the drying cycles, during the heating cycles, the interfaces were heated to 40 ℃ whilst being submerged in water. In this research, three numbers of thermal cycles were conducted on the tests, respectively.

(3) **Creep tests subjected to drying-wetting cycles without heating**: To research the individual impacts of drying on the creep mechanical behaviour of interfaces, creep tests on clayey soil-GDL interfaces subjected to drying-wetting cycles without heating under 25 kPa normal stress with the creep stress level 70 % of the peak shear strength were carried out for Mercia Mudstone Clay-GDL interfaces. For Kaolin Clay-GDL interfaces, tests under 25 kPa normal stress with the creep stress level 60 % of the peak shear strength were conducted. The procedure of the creep tests subjected to drying-wetting cycles without heating was almost the same with the creep tests during drying-wetting cycles with heating, except that during the drying cycle without heating, only water in the external shear box was discharged and the heating system is kept off to dry the interfaces at the room temperature of 22 ℃ for 7 days. In this case, the number of drying-wetting cycle without heating was 1. After the

drying cycle without heating, the moisture contents of Mercia Mudstone Clay/ Kaolin Clay samples in the top shear box were measured. A significant decrease in moisture content of the soil samples during the drying cycle without heating was observed. The moisture content of Mercia Mudstone Clay experiencing drying cycle without heating was about 40 % less than that without experiencing drying cycles without heating. For Kaolin Clay, this figure was around 30 %. These are close to the reducing magnitudes of the moisture content for Mercia Mudstone Clay and Kaolin Clay specimens experiencing drying cycles with heating, respectively. This indicates that the drying effect of the drying cycle without heating on the soil samples is almost identical to that of the drying cycle with heating.

6.3 Results and analysis

6.3.1 Impacts of creep shear stress level

Figure 6.1 presents the creep shear deformation of Mercia Mudstone Clay-GDL interfaces during the whole test.

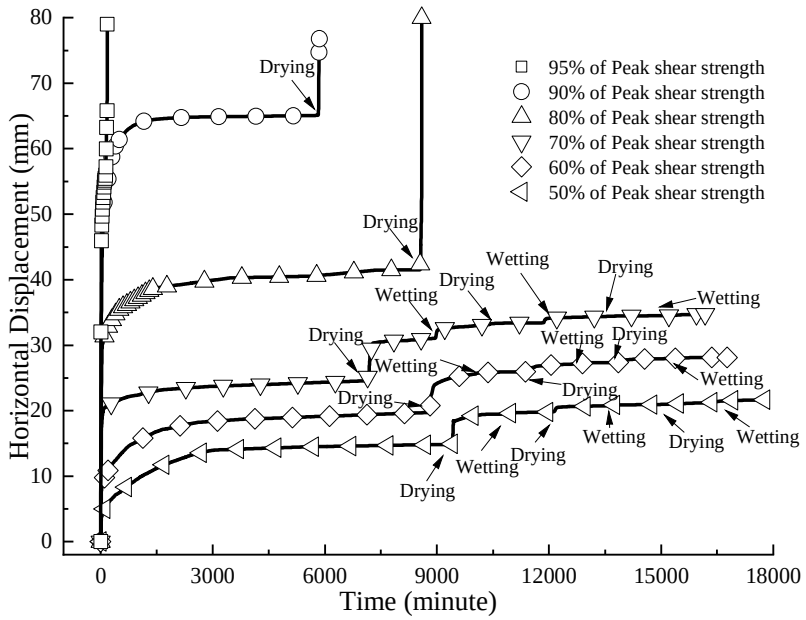

Figure 6.1 The shear creep deformation of Mercia Mudstone Clay-GDL interfaces during the whole test

Based on Figure 6.1, the creep shear stress level has large influences over the creep shear behaviour of Mercia Mudstone Clay - GDL interfaces. Horizontal displacements of Mercia Mudstone Clay-GDL interfaces under a high creep shear stress level are larger than those under a low creep shear stress level. Especially for specimen under 95% creep shear stress level, the horizontal displacement increases significantly to 79 mm before the drying-wetting cycles. This indicates the failure of the sample. Additionally, with the increase of creep shear stress level, the duration of the primary stage (in which the displacement increases with a diminishing displacement rate) is reduced. For example, under 50 % creep shear stress level, the horizontal displacement stabilises at around 14 mm at the 3150^{th} minute. In comparison, under 90 % creep shear stress level, the horizontal displacement stabilises at about 65 mm displacement at the 1500^{th} minute. Moreover, drying-wetting cycles have large effect on the creep shear deformation of Mercia Mudstone Clay-GDL interfaces. After the primary creep stage and before the beginning of drying-wetting cycles, the horizontal displacement of Mercia Mudstone Clay-GDL interfaces under a creep shear stress level lower than 95 % manages to stabilise, with a small change of the horizontal displacement in elapsed time. During the first drying cycle, the horizontal displacement rises significantly. Especially for the tests with creep shear stress levels of 90 % and 80 %, the first drying cycle causes the failure of the interfaces. When creep shear stress levels are 70 %, 60 %, and 50 %, respectively, during the first drying cycle, although the horizontal displacement rises remarkably, the horizontal displacement stabilises over a short time and the specimens do not fail. Compared to the first drying cycle, the following drying-wetting cycles have relatively small effect on the horizontal displacement of Mercia Mudstone Clay-GDL interfaces.

In order to analyse the creep shear deformation of the specimen under 95 % creep shear stress level in detail, the creep deformation of the specimens during the first 200 minutes is drawn in Figure 6.2.

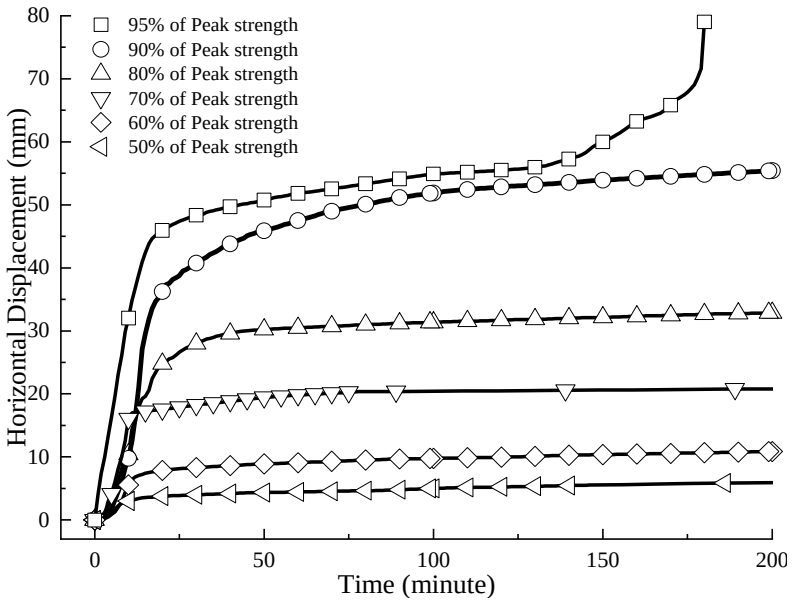

Figure 6.2 The shear creep deformation of Mercia Mudstone Clay-GDL interfaces during the first 200 minutes

Based on Figure 6.2, for the specimen under the 95 % creep shear stress level, during the primary creep stage, the horizontal displacement rises rapidly to 46 mm at the 19th minute. During the secondary creep stage, the horizontal displacement increases about 10 mm. Following this, the interface suddenly fails in the tertiary creep stage with a rapid rise in horizontal displacement. In total, for the specimen under the 95 % creep shear stress level, it takes around 180 minutes to fail. In comparison, for the specimens under a lower creep shear stress level (less than or equal to 90 %), after the significant rise of horizontal displacement during the primary creep stage, their horizontal displacement keeps stable during the secondary creep stage, and they do not experience the tertiary creep stage with a sharp increase until the beginning of the drying-wetting cycles. Moreover, by comparing with the variation trend of horizontal displacement in elapsed time for original Mercia Mudstone Clay-GDL interface in the rapid loading shear test under 25 kPa normal stress, as shown in Figure 5.1, the variation trend of horizontal displacement in elapsed time for the Mercia Mudstone Clay-GDL interface under 95 % creep shear stress level in creep tests is different. In the rapid loading shear test, the failure of specimens is very suddenly, which is more rapid and unanticipated

than that of the creep failure for the interface under 95 % creep shear stress level.

Figure 6.3 presents the creep shear deformation of Kaolin Clay-GDL interfaces during the whole test.

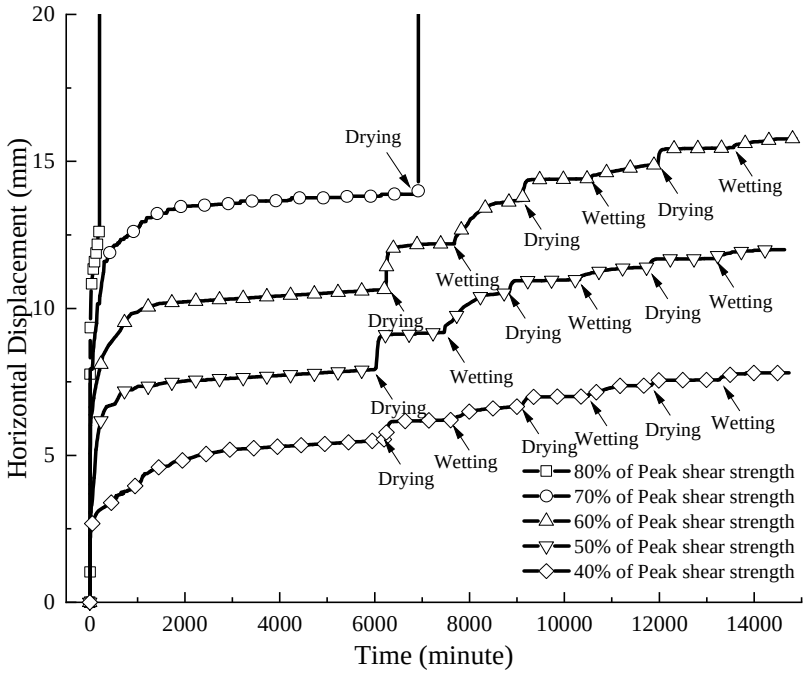

Figure 6.3 The creep shear deformation of Kaolin Clay-GDL interfaces during the whole tests

Based on Figure 6.3, similar to Mercia Mudstone Clay-GDL interfaces, the level of creep shear stress has significant impacts on the creep shear deformation of Kaolin Clay-GDL interfaces. The horizontal displacement of Kaolin Clay-GDL interfaces under a high creep shear stress level is higher than those under a low shear stress level. Especially for the Kaolin Clay-GDL interface under 80 % creep shear stress level, the sample fails before the beginning of drying-wetting cycles. In comparison, the Mercia Mudstone Clay-GDL interface remains stable under the 90 % creep shear stress level before the beginning of drying-wetting cycles, as shown in Figure 6.1. When the creep shear stress level is lower than or equal to 70 %, the interfaces become stable after the primary creep stage. Additionally, as with Mercia Mudstone Clay-GDL interfaces, the influence of drying-wetting cycles on the

creep deformation of Kaolin Clay-GDL interfaces are large. The impacts are more evident for interfaces under a high creep shear stress level than those under a low creep shear stress level. For example, during the first drying cycle, the horizontal displacement of the interface under 40 % creep shear stress level rises around 0.6 mm, whilst that under 60 % creep shear stress level rises about 2.5 mm. Especially for the interface under 70 % creep shear stress level, it comes to failure caused by the first drying cycle. In comparison, for Mercia Mudstone Clay-GDL interfaces, failure does not occur during the drying-wetting cycles when the creep shear stress level is less than or equal to 70 %. It is also worth noting that, the first drying-wetting cycle has a larger influence over the horizontal displacement than following cycles. Taking the interface under 50 % creep shear stress level as an example, during the first drying and first wetting cycle, the horizontal displacement increases by 2 mm and 1.4 mm, respectively. Meanwhile, during the second cycle, these values are 0.4 mm and 0.3 mm, respectively.

In order to analyse the creep shear deformation of samples under 80 % creep shear stress level in detail, the creep deformation of the specimens in the first 250 minutes was drawn in Figure 6.4.

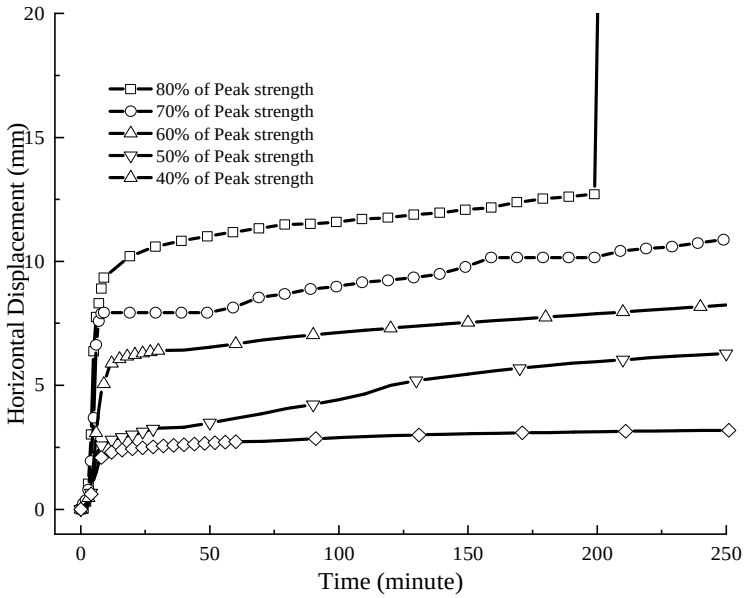

Figure 6.4 The creep shear deformation of Kaolin Clay-GDL interfaces in the first 250 minutes

Based on Figure 6.4, the Kaolin Clay-GDL interface under 80 % creep shear stress level experiences immediate elastic deformation after the loading of creep shear stress during the primary stage. This is similar to what is observed for Mercia Mudstone Clay-GDL interfaces under 95 % creep shear stress level. Following this, the creep deformation comes to the secondary creep stage where creep deformation stabilises. The failure of the Kaolin Clay-GDL interface occurs at around the 200^{th} minute during the tertiary creep stage and is more sudden than that of the Mercia Mudstone Clay-GDL interface. In comparison, the horizontal displacement of Kaolin Clay-GDL interfaces under a creep shear stress level less than or equal to 70 % stabilises during the secondary creep stage and does not experience the tertiary creep stage before the beginning of drying-wetting cycles.

6.3.2 Impacts of drying-wetting cycles

To further analyse the impact of drying-wetting cycles on the creep deformation of the interfaces, taking the beginning time of the first drying cycle as the 0 minute and the horizontal displacement at the beginning of the first drying cycle as 0 mm, curves about the horizontal displacement of Mercia Mudstone Clay-GDL interfaces under 70 %, 60 % and 50 % creep shear stress levels and Kaolin Clay-GDL interfaces under 60 %, 50 % and 40 % creep shear stress levels in elapsed time are drawn in Figure 6.5 and Figure 6.6, respectively.

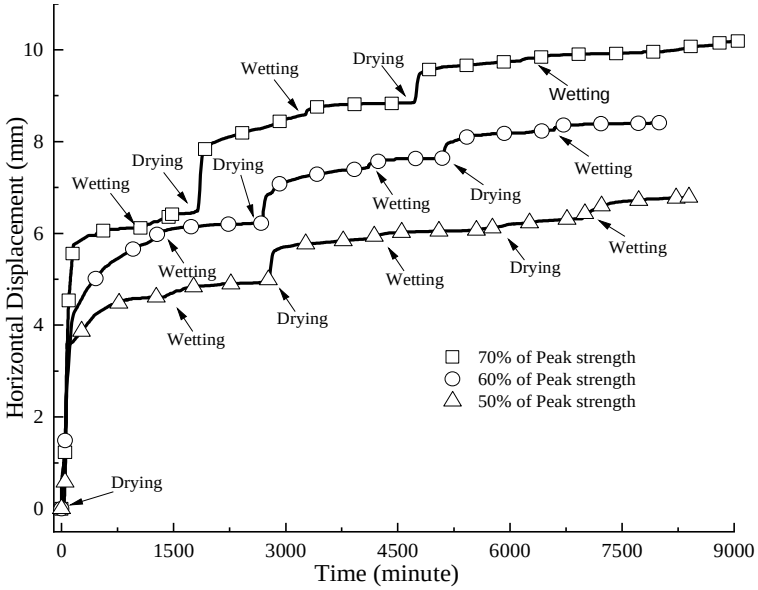

Figure 6.5 The creep shear deformation of Mercia Mudstone Clay-GDL interfaces during drying-wetting cycles

Based on Figure 6.5, the first drying cycle has the largest impact on the horizontal displacement of Mercia Mudstone Clay-GDL interfaces compared with the following drying cycles. Taking the interface under 70 % creep shear stress level as an example, the horizontal displacement rises 6 mm during the first drying cycle. In comparison, the rising magnitudes during the second and third cycles are 2 mm and 1 mm, respectively, which is about 3 and 6 times less than that of the first cycle, respectively. Additionally, the drying cycles have larger impacts on the horizontal displacement than that of the wetting cycles. For example, during the first drying cycle, the horizontal displacement for the interface under 60 % creep shear stress level rises approximately 6 mm, whilst during the first wetting cycle, it rises approximately 0.5 mm, which is around 12 times less than that of the first drying cycle. Meanwhile, the horizontal displacement during the second drying cycle increases approximately 1 mm, which is about 3 times higher than that of the second wetting cycle. For the third cycle, the horizontal displacement increases 0.5 mm during the drying process, which is 2 times higher than that of the wetting process. Furthermore, under a high creep shear stress level, increase in the horizontal displacement during the drying cycle is larger than that of a low creep shear stress level. For example, during the first drying cycle, the rise in

horizontal displacement for Mercia Mudstone Clay-GDL interfaces under creep shear stress levels of 70 %, 60 % and 50 % is 6 mm, 5.70 mm and 4.60 mm, respectively.

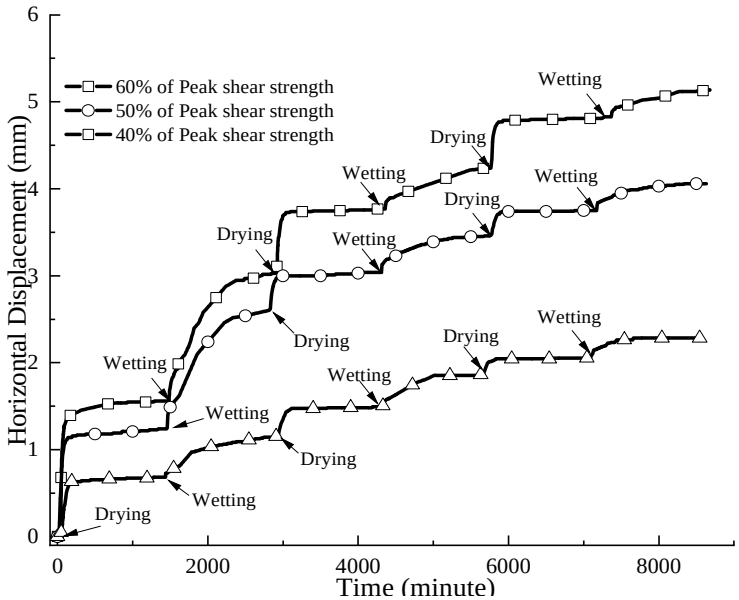

Figure 6.6 The creep shear deformation of Kaolin Clay-GDL interfaces during drying-wetting cycles

Based on Figure 6.6, as with Mercia Mudstone Clay-GDL interfaces, the first drying cycle and wetting cycle have the highest influence over the horizontal displacement of Kaolin Clay-GDL interfaces compared with the following drying and wetting cycles, respectively. Taking the Kaolin Clay-GDL interface under 60 % creep shear stress level as an example, the horizontal displacement rises by 1.5 mm and 1.4 mm during the first drying and first wetting cycle, respectively. Meanwhile, during the third drying cycle and wetting cycle, the value is 0.6 mm and 0.3 mm, respectively. Additionally, as with Mercia Mudstone Clay-GDL interfaces, the impact of drying cycles on the horizontal displacement of Kaolin Clay-GDL interfaces is larger than that of wetting cycles. However, compared to Mercia Mudstone Clay-GDL interfaces, wetting cycles have greater impacts on the creep deformation of Kaolin Clay-GDL interfaces. For the drying cycles, the opposite phenomenon is observed. For instance, under 50 % creep shear stress level, the horizontal displacement of Kaolin Clay-GDL interfaces increases about 2 mm during

the first drying cycle, whereas this is 4.6 mm for Mercia Mudstone Clay-GDL interfaces. In comparison, during the first wetting cycle, the horizontal displacement of Mercia Mudstone Clay-GDL interfaces and Kaolin Clay-GDL interfaces rises by 0.34 mm and 1.37 mm, respectively.

6.3.3 Impacts of thermal cycles

The above-mentioned analysis shows that drying cycles can lead to an increase of horizontal displacement for clayey soil-GDL interfaces and even can induce the failure of the clayey soil-GDL interfaces under a high creep shear stress level. However, the mechanism of this response remains uncertain due to the fact that during the drying cycles, there are two main variables that may cause the response. Besides drying, the elevated temperature also may result in large deformation of the clayey soil-GDL interface due to the presence of thermos-softening plastics. Both phenomena are of common occurrence in real landfill cover systems and have significant impacts on their performance. Hence, in this section, to explore the influences of elevated temperature and drying on the creep deformation of clayey soil-GDL interfaces, respectively, creep tests subjected to thermal cycles under creep shear stress levels of 90 %, 80 % and 70 % for Mercia Mudstone Clay-GDL interfaces and creep shear stress levels of 70 % and 60 % for Kaolin Clay-GDL interfaces were carried out. The procedure of creep tests subjected to thermal cycles was almost identical to the creep tests subjected to drying-wetting cycles. The only difference between them is that, unlike the drying cycles, for the creep tests subjected to thermal cycles, during the heating cycles, interfaces were submerged in water and both the interfaces and water were kept at 40 ℃ for 24 hours. The experimental results of the creep tests on Mercia Mudstone Clay-GDL interfaces subjected to thermal cycles and the corresponding creep tests subjected to drying-wetting cycles under the same creep shear stress level are plotted in Figure 6.7.

Based on Figure 6.7, for Mercia Mudstone Clay-GDL interfaces during thermal cycles, their horizontal displacement increases significantly during the first thermal cycle due to the increase of temperature. Especially for the

Mercia Mudstone Clay-GDL interfaces under creep shear stress levels of 90 % and 80 %, the interfaces fail during the first thermal cycle. This indicates that elevated temperature can lead to a noticeable increase in the horizontal displacement of Mercia Mudstone Clay-GDL interfaces during the creep deformation process. This can be considered as one of the factors that result in the increasing creep shear deformation during the drying cycle in the creep tests.

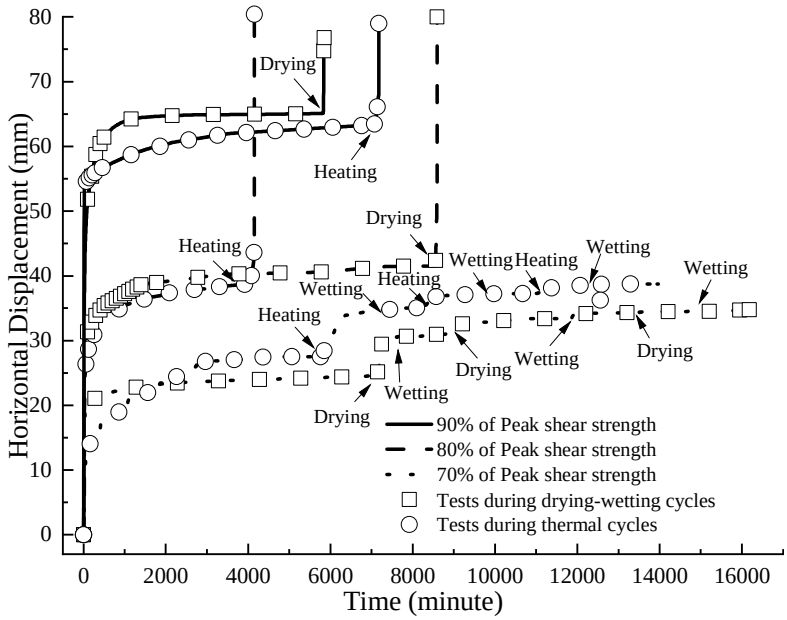

Figure 6.7 The influence of thermal cycles on creep behaviour of Mercia Mudstone Clay-GDL interfaces during the whole tests

In order to further determine that, during the drying cycles, the increase in creep shear deformation of Mercia Mudstone Clay-GDL interfaces is due to the combined impacts of elevated temperature and drying or the individual impact of the two factors, taking the beginning time of the first drying/thermal cycle as the 0 minute and the horizontal displacement at the beginning of the first drying/thermal cycle as 0 mm, the horizontal displacement of Mercia Mudstone Clay-GDL interfaces subjected to thermal cycles and that subjected to drying-wetting cycles under 70 % creep shear stress level in elapsed time is drawn in Figure 6.8.

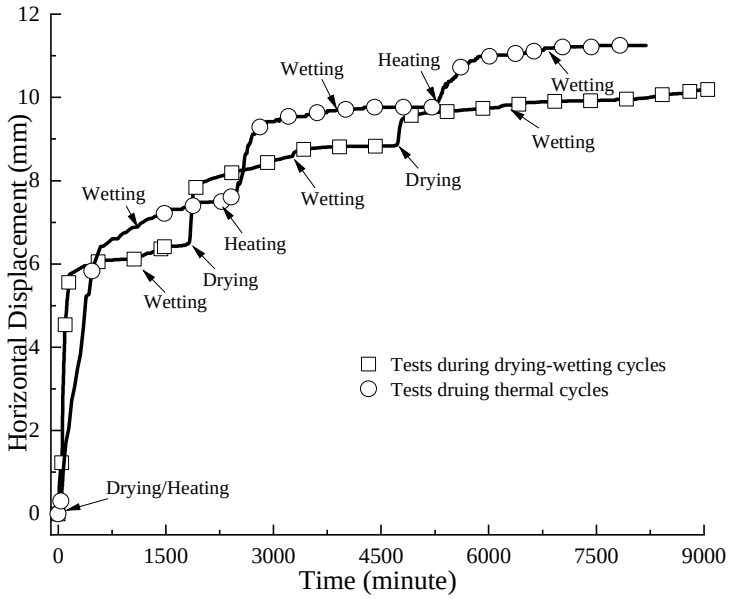

Figure 6.8 The impacts of thermal cycles on creep deformation of Mercia Mudstone Clay-GDL interfaces during drying-wetting/thermal cycles

Based on Figure 6.8, the increase in horizontal displacement during thermal cycles is higher than those during drying cycles. This can be attributed to the fact that Mercia Mudstone Clay-GDL interfaces were submerged in water. This softened the overlying clay sample, providing more lubrication between Mercia Mudstone Clay particles and Mercia Mudstone Clay-GDL interfaces, respectively. This led to a reduction in the shear resistance of Mercia Mudstone Clay-GDL interfaces. In comparison, during the drying cycles, the overlying clay sample was unsaturated. This led to the generation of suction in soil to enhance the shear resistance of the Mercia Mudstone Clay-GDL interfaces. For example, during the first and second thermal cycles, the horizontal displacement increases by 7 mm and 2.2 mm, respectively, which is around 1.4 mm and 0.20 mm higher than those during the first and second drying cycles, respectively. Additionally, it should be noted that, for the specimens in the creep tests subjected to thermal cycles, the increase of horizontal displacement during the wetting cycles is larger than that in the drying-wetting cycles. This could be attributed to the fact that, in the wetting cycles of the creep tests subjected to thermal cycles, although the heating system was turned off, initially the temperature of water was high. Therefore, the time taken for the interface and water to cool down to the room

temperature was longer than that in the creep tests subjected to drying-wetting cycles. Thus, due to the high temperature, the increase in the horizontal displacement of interfaces during the wetting cycles of the thermal cycles is larger than that of the drying-wetting cycles.

The experimental results of the creep tests on Kaolin Clay-GDL interfaces during thermal cycles and the corresponding creep tests subjected to drying-wetting cycles under the same creep shear stress levels are plotted in Figure 6.9.

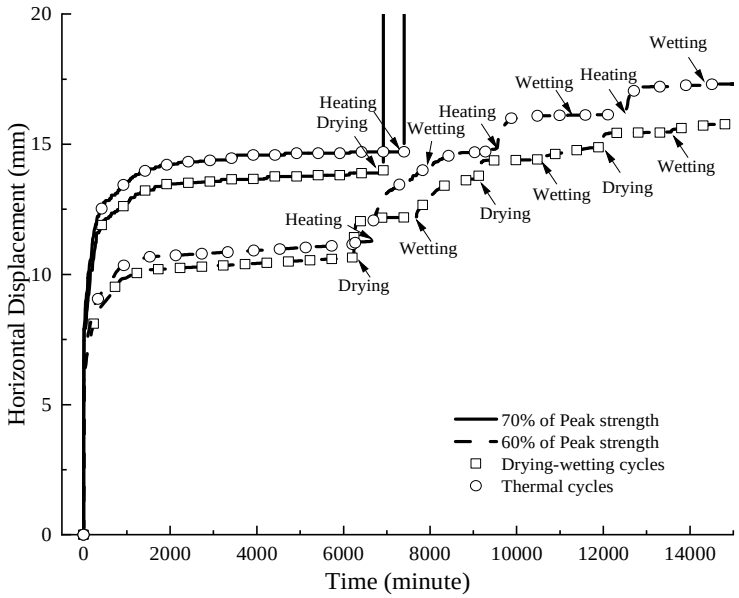

Figure 6.9 The influence of thermal cycles on creep behaviour of Kaolin Clay-GDL interfaces during the whole tests

Based on Figure 6.9, similar to Mercia Mudstone Clay-GDL interfaces, the horizontal displacement of Kaolin Clay-GDL interfaces increases markedly during the first thermal cycle. Especially for the Kaolin Clay-GDL interface under 70 % creep shear stress level, failure occurs in the first thermal cycle. However, for the Mercia Mudstone Clay-GDL interface at the same creep shear stress level, failure does not occur during the first thermal cycle. Regarding the Kaolin Clay-GDL interface under 60 % creep shear stress level, the first thermal cycle has the highest influence on the horizontal displacement. For example, during the first thermal cycle, the horizontal

displacement rises by around 2.9 mm, whereas during the third thermal cycle, this is about 1 mm. This demonstrates that elevated temperature is an important factor to result in the rise in the horizontal displacement of Kaolin Clay-GDL interfaces during creep deformation.

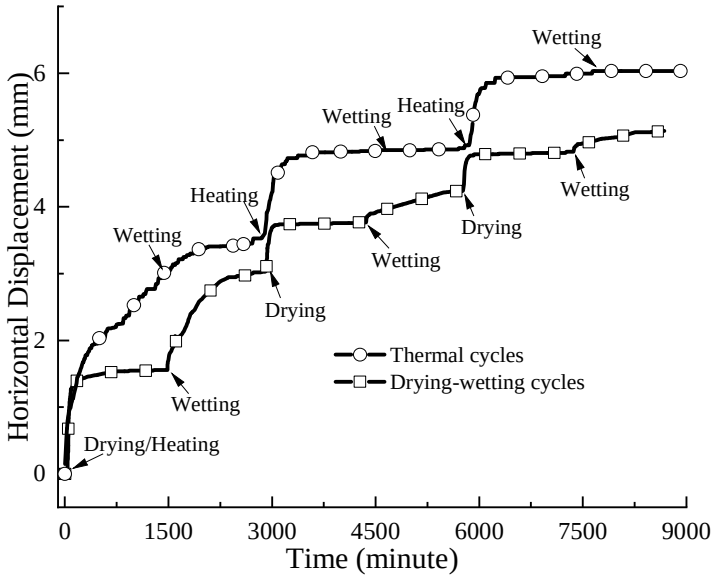

Figure 6.10 The impacts of thermal cycles on creep deformation of Kaolin Clay-GDL interfaces during drying-wetting/thermal cycles

Based on Figure 6.10, similar to Mercia Mudstone Clay-GDL interfaces, the rise in horizontal displacement of Kaolin Clay-GDL interfaces during the thermal cycles is always higher than those during the drying cycles. This can be attributed to the fact that during thermal cycles, the Kaolin Clay-GDL interfaces were submerged in water. This softened the overlying clay sample to provide more lubrication between Kaolin Clay particles and Kaolin Clay - GDL interfaces, respectively, reducing the shear resistance of Kaolin Clay-GDL interfaces. In comparison, during the drying cycles, the overlying clay sample was unsaturated. This led to the generation of suction in soil to enhance the shear resistance of Kaolin Clay-GDL interfaces. For example, during the first thermal cycle, the horizontal displacement rises by 2.9 mm, which is around 1.4 mm higher than that during the first drying cycle.

6.3.4 Impacts of drying cycles without heating

In this section, to further explore the action mechanism of drying cycles on the creep deformation of clayey soil-GDL interfaces and investigate the individual impacts of drying on the creep deformation of clayey soil-GDL interfaces, creep tests subjected to drying-wetting cycle without heating under the creep shear stress level of 70 % of peak shear strength for Mercia Mudstone Clay-GDL interfaces and the creep shear stress level of 60 % for Kaolin Clay-GDL interfaces were carried out, respectively. The procedure of the creep tests subjected to drying-wetting cycle without heating was almost identical to those subjected to drying-wetting cycles with heating. The only difference is that, for creep tests subjected to drying-wetting cycles without heating, during the drying cycles, only water in the external shear box was discharged and the heating system was kept off to dry the interfaces at the room temperature of 22 ℃ for 7 days. The experimental results of the creep tests on Mercia Mudstone Clay-GDL interfaces subjected to drying-wetting cycle without heating and the corresponding creep tests subjected to drying-wetting cycles with heating and thermal cycles under the same creep shear stress level are plotted in Figure 6.11.

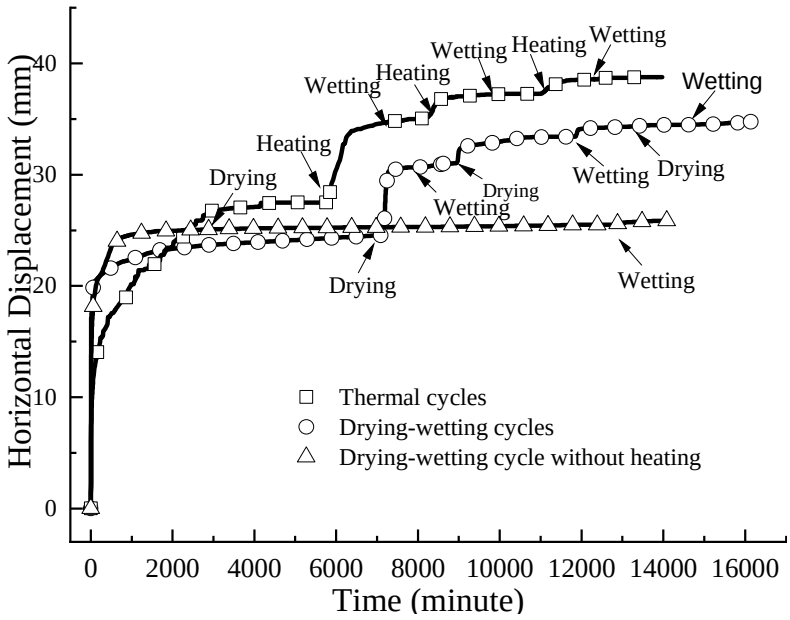

Figure 6.11 The influence of drying-wetting cycle without heating on creep behaviour of Mercia Mudstone Clay-GDL interfaces during the whole tests

Based on Figure 6.11, when the Mercia Mudstone Clay-GDL interface is subjected to drying cycles without heating, the horizontal displacement remains stable. Variation in the horizontal displacement of interfaces during drying cycles with heating and the heating processes of thermal cycles is significantly higher than that during the drying cycle without heating, respectively. This indicates that drying alone cannot lead to an apparent rise in horizontal displacement of Mercia Mudstone Clay-GDL interfaces during creep deformation, which has marginal attribution to the increase in creep shear deformation during drying cycles with heating in creep tests.

In order to further determine that, during drying cycles with heating, the increase in creep shear deformation of Mercia Mudstone Clay-GDL interfaces is due to the combined impacts of elevated temperature and drying, or individual impacts of the two factors, taking the beginning time of the first drying cycle without heating, drying cycle with heating and thermal cycle as the 0 minute, respectively, and the horizontal displacement at the beginning of the first drying cycle without heating, drying cycle with heating and the thermal cycle as 0 mm, respectively, the horizontal displacement of Mercia Mudstone Clay-GDL interfaces subjected to drying-wetting cycle without heating under the creep shear stress level of 70 % and the corresponding creep tests subjected to drying-wetting cycles with heating and thermal cycles under the same creep shear stress level in elapsed time is drawn in Figure 6.12.

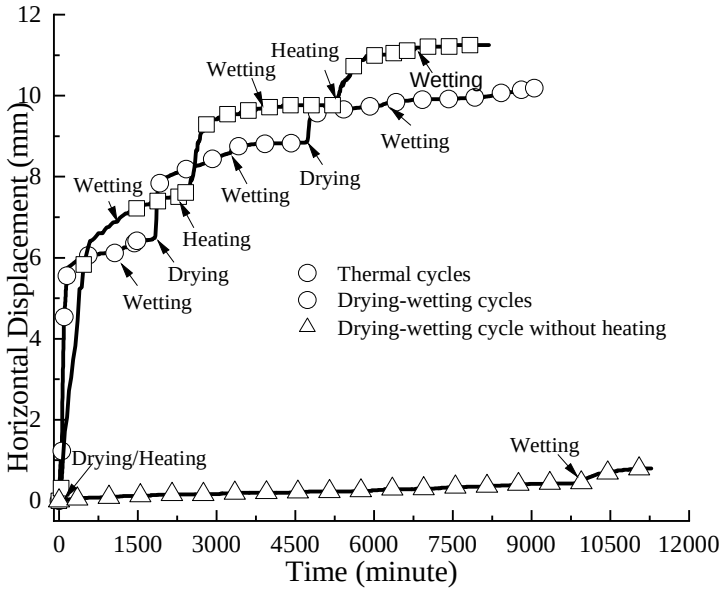

Figure 6.12 The impacts of drying-wetting cycle without heating on creep deformation of Mercia Mudstone Clay-GDL interfaces during drying-wetting/thermal cycles

Based on Figure 6.12, the rise in horizontal displacement during the drying cycle without heating is significantly lower than those during drying cycles with heating and the heating processes of thermal cycles. This can be explained that, in regard to the presence of thermos-softening materials, the stiffness (modulus) of HDPE drainage core and geotextile fibres for the GDL decreases at elevated temperature, which results in the softening of the drainage core and geotextile fibres, weakening the interlocking effects and skin friction between soil and GDL. Additionally, at elevated temperature, the viscosity of water in soil reduces, which increases the pore water pressure in soil to reduce its effective stress. This causes the reduction in the shear strength of soil (Bacas et al., 2015). Thus, owing to the decreasing shear resistance caused by elevated temperature, during the drying cycles with heating and thermal cycles, the variation in creep deformation of Mercia Mudstone Clay-GDL interfaces is larger than that during the drying cycle without heating. Regarding the specific variation amplitude of horizontal displacement, the horizontal displacement rises by 0.4 mm during the drying cycle without heating, whilst the value for the first heating process of thermal cycles and the first drying cycle with heating is 6.8 mm and 6.1 mm, respectively. This indicates that the impacts of drying alone on the rise in

horizontal displacement of Mercia Mudstone Clay-GDL interfaces during drying cycles with heating are marginal, with the main influence factor being elevated temperature. It also should be noted that there is an increase in horizontal displacement of the Mercia Mudstone Clay-GDL interface during the wetting cycle of drying-wetting cycle without heating. This may be due to the fact that drying-wetting cycles can result in a reduction in peak shear strength of Mercia Mudstone Clay. When Mercia Mudstone Clay-GDL interfaces were subjected to drying-wetting cycles without heating, the peak shear strength of Mercia Mudstone Clay above the GDL may reduce to weaken the interlocking effects between soil and GDL. This may result in the decrease in creep shear resistance of the interfaces to cause the increase in the horizontal displacement.

The experimental results of creep tests on Kaolin Clay-GDL interfaces during drying-wetting cycle without heating under the creep shear stress level of 60 % and the corresponding creep tests subjected to drying-wetting cycles with heating and thermal cycles under the same creep shear stress levels are plotted in Figure 6.13.

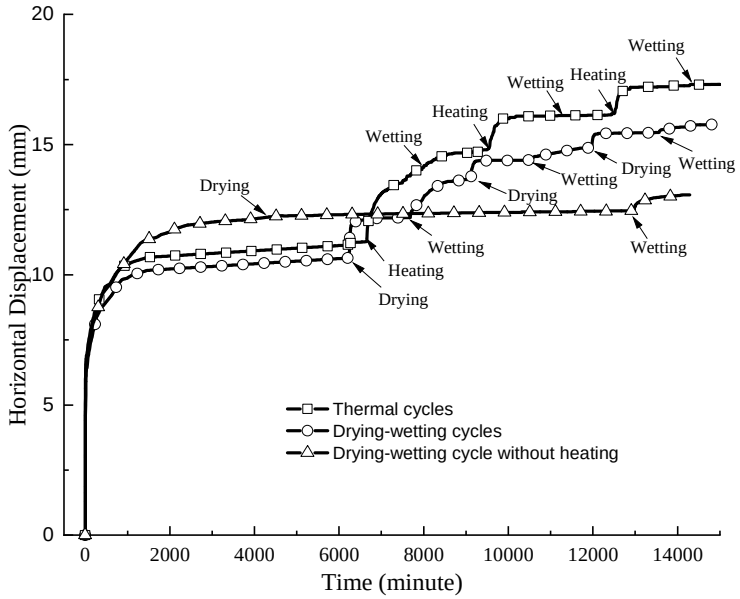

Figure 6.13 The influence of drying-wetting cycle without heating on creep behaviour of Kaolin Clay-GDL interfaces during the whole tests

Based on Figure 6.13, as with Mercia Mudstone Clay-GDL interfaces, for the Kaolin Clay-GDL interface subjected to drying-wetting cycle without heating, its horizontal displacement keeps stable during the drying cycle without heating. Variation in the horizontal displacement of the interfaces during the drying cycles with heating and during the heating processes of thermal cycles is significantly higher than that during the drying cycle without heating, respectively. This indicates that drying alone cannot lead to an apparent rise in horizontal displacement for Kaolin Clay-GDL interfaces during creep deformation, which has marginal influence on the increase in creep shear deformation of the interfaces during the drying cycles with heating in creep tests.

In order to further determine that, during drying cycles with heating, the increase in creep shear deformation of Kaolin Clay-GDL interfaces is due to the combined impacts of elevated temperature and drying or the individual impacts of the two factors, taking the beginning time of the first drying cycle without heating, drying cycle with heating and thermal cycle as the 0 minute, respectively, and the horizontal displacement at the beginning of the first drying cycle without heating, drying cycle with heating and thermal cycle as 0 mm, respectively, the horizontal displacement of Kaolin Clay-GDL interfaces subjected to drying-wetting cycle without heating under the creep shear stress level of 60 % and the corresponding creep tests subjected to drying-wetting cycles with heating and thermal cycles under the same creep shear stress level in elapsed time is drawn in Figure 6.14.

Based on Figure 6.14, similar to Mercia Mudstone Clay-GDL interfaces, the rise in horizontal displacement of Kaolin Clay-GDL interfaces during the drying cycle without heating is significantly lower than those during the drying cycles with heating and the heating processes of thermal cycles. This can be related to the same mechanism as that for Mercia Mudstone Clay-GDL interfaces. Regarding the specific variation amplitude of horizontal displacement, the horizontal displacement increases by 0.3 mm during the drying cycle without heating, whilst this increase during the first heating

process of thermal cycles and the first drying cycle with heating is 3.0 mm and 1.6 mm, respectively. This indicates that the impacts of drying alone on the increase in horizontal displacement of Kaolin Clay-GDL interfaces during drying cycles with heating is marginal and the main influence factor is elevated temperature. As with Mercia Mudstone Clay-GDL interfaces, there is an increase in horizontal displacement of the Kaolin Clay-GDL interface during the wetting cycle of drying-wetting cycle without heating. This can be ascribed to the same mechanism with that of Mercia Mudstone Clay-GDL interfaces.

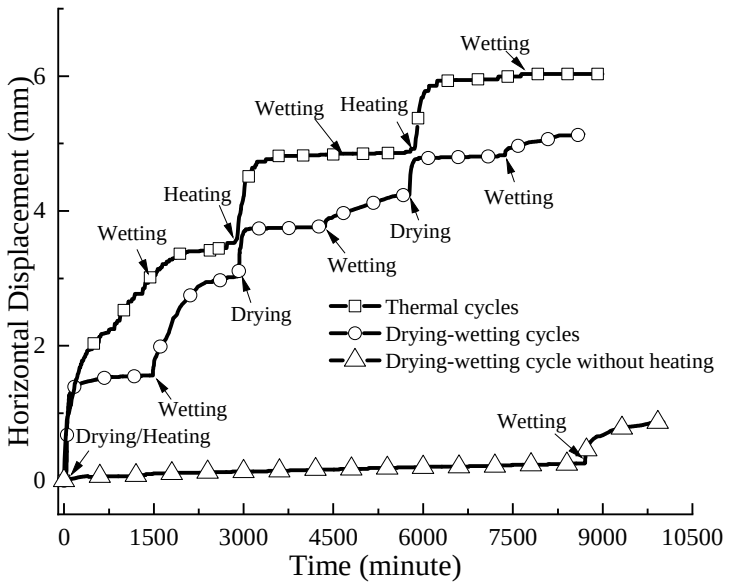

Figure 6.14 The impacts of drying-wetting cycle without heating on creep deformation of Kaolin Clay-GDL interfaces during drying-wetting/thermal cycles

6.3.5 Creep deformation rate of interfaces subjected to drying-wetting cycles

To explore the variation in creep deformation rate during drying-wetting cycles, the creep deformation rate of Mercia Mudstone Clay-GDL interfaces subjected to drying-wetting cycles in elapsed time is drawn in Figure 6.15.

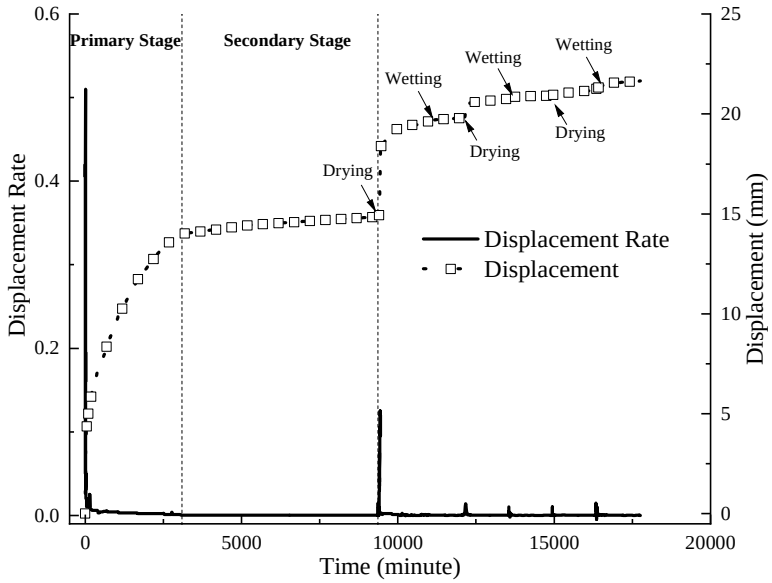

(a) 50 % creep shear stress level

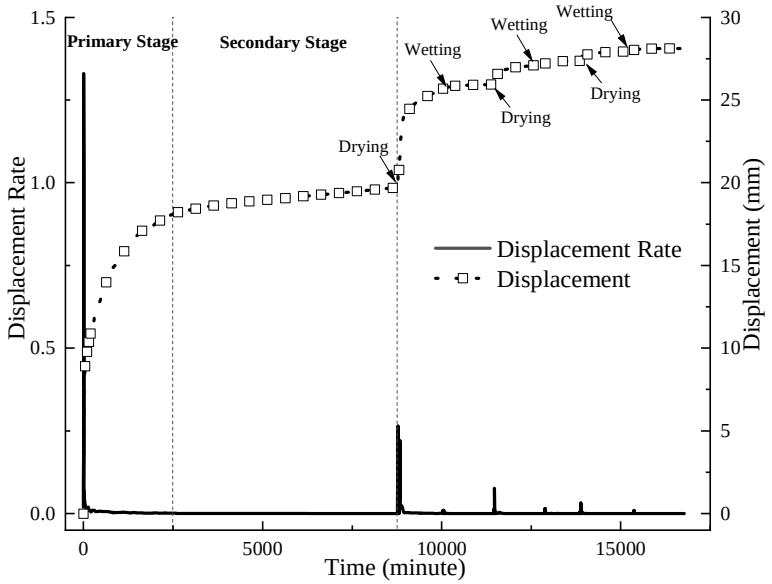

(b) 60 % creep shear stress level

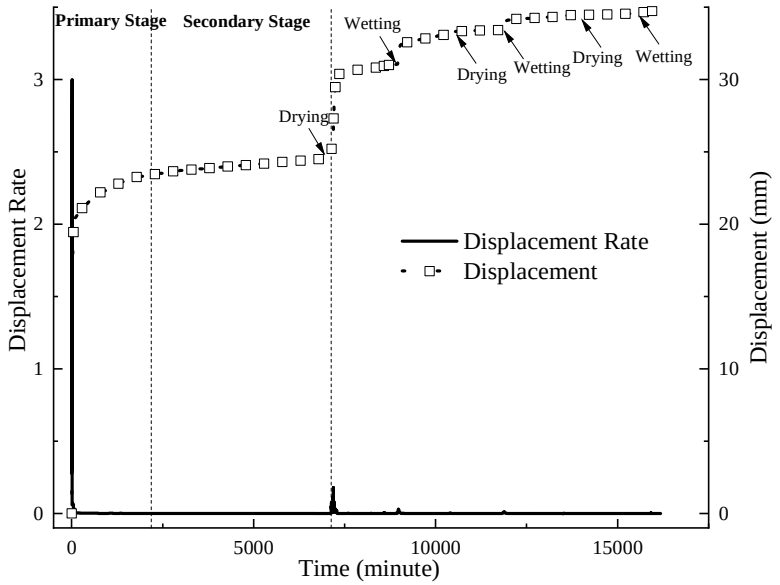

(c) 70 % creep shear stress level

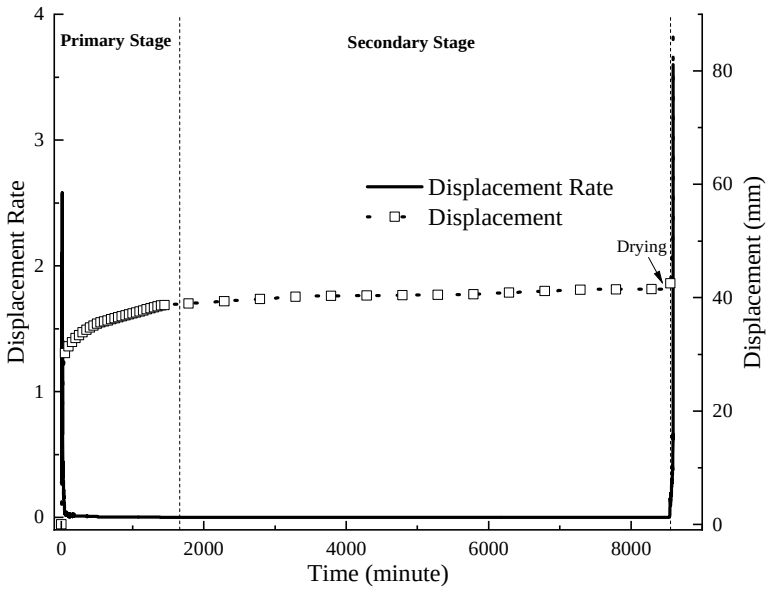

(d) 80 % creep shear stress level

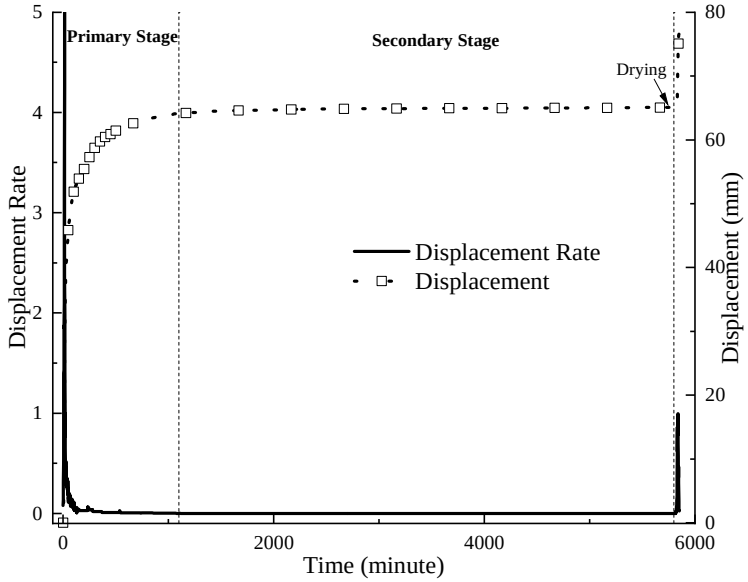

(e) 90 % creep shear stress level

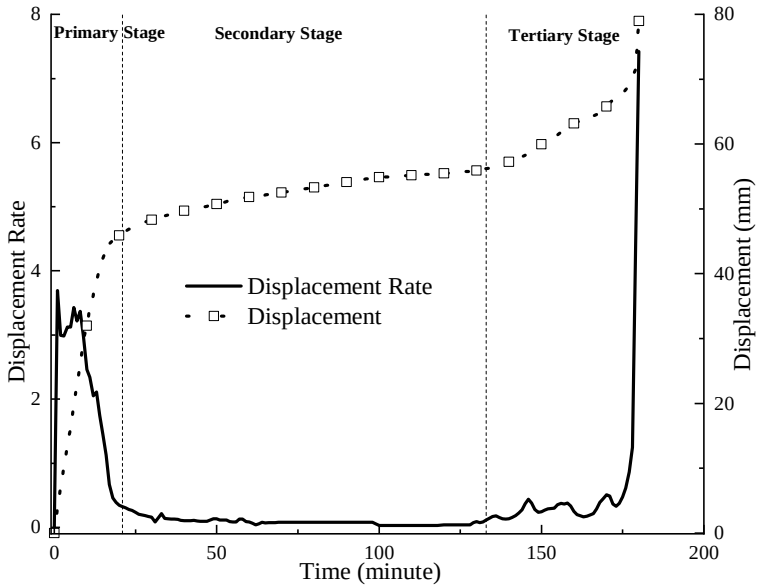

(f) 95 % creep shear stress level

Figure 6.15 Creep displacement rate of Mercia Mudstone Clay-GDL interfaces subjected to drying-wetting cycles

Based on Figure 6.15, the highest displacement rate generally occurs at the primary creep stage after creep shear stress was imposed, as shown in Figure 6.15 (a), (b), (c) and (e), or the failure of interfaces caused by drying and wetting cycles / creep shear stress, as shown in Figure 6.15 (d) and (f). More

specifically, for Mercia Mudstone Clay-GDL interfaces under 50 %, 60 %, 70 % and 90 % creep shear stress levels, the highest displacement rate takes place in the primary creep stage, and it rapidly reaches the peak value after imposing creep shear stress, then decreasing to a low value and keeping stable in the following primary and secondary creep stages. For Mercia Mudstone Clay-GDL interfaces under 80 % and 95 % creep shear stress levels, the largest displacement rate happens during the failure of interfaces. Overall, the highest displacement rate of the interfaces increases with the increase in creep shear stress level. Regarding the displacement rate during drying-wetting cycles, the highest displacement rate occurs during the first drying cycle, which rapidly reaches the peak value after the first drying loading and then reduces to a steady value. During the following drying-wetting cycles, the displacement rate slightly rises but the varying magnitudes are significantly lower than that of the first drying loading. Additionally, the rise in displacement rate due to the drying loadings is higher than that of the wetting loadings. By comparing the displacement rate of interfaces with diverse creep shear stress levels, it is found that under a high creep shear stress level, the increase in displacement rate due to drying cycles and wetting cycles is higher than those under a low creep shear stress level, respectively.

The creep displacement rate of Kaolin Clay-GDL interfaces subjected to drying-wetting cycles is illustrated in Figure 6.16.

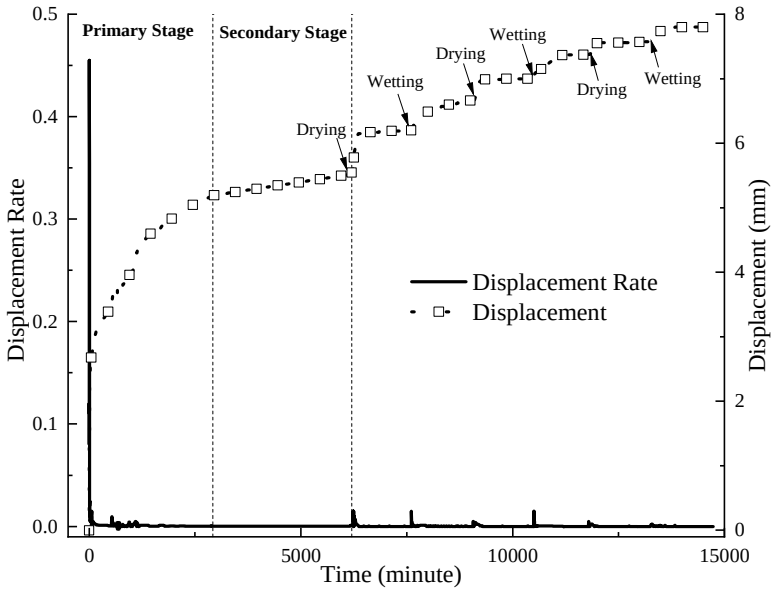

(a) 40 % creep shear stress level

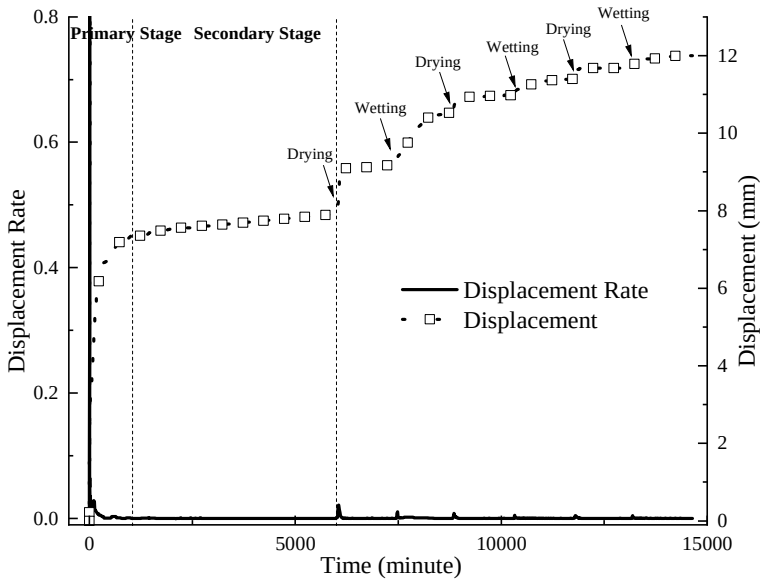

(b) 50 % creep shear stress level

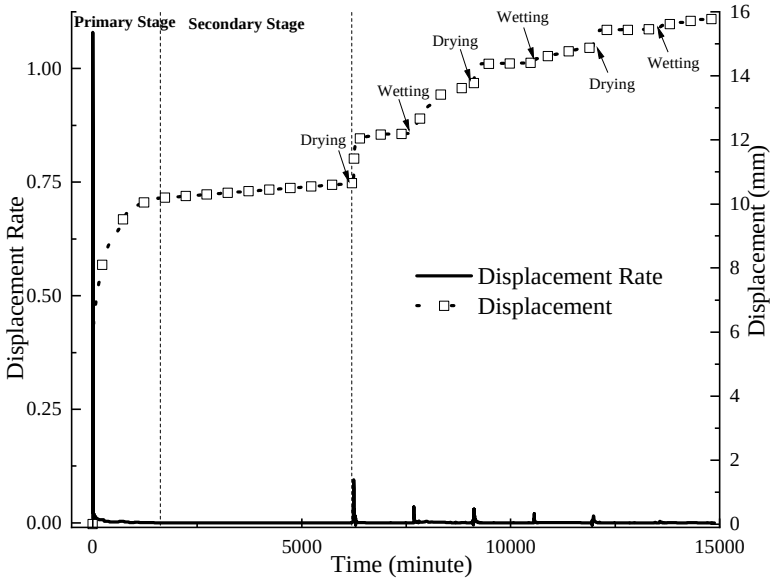

(c) 60 % creep shear stress level

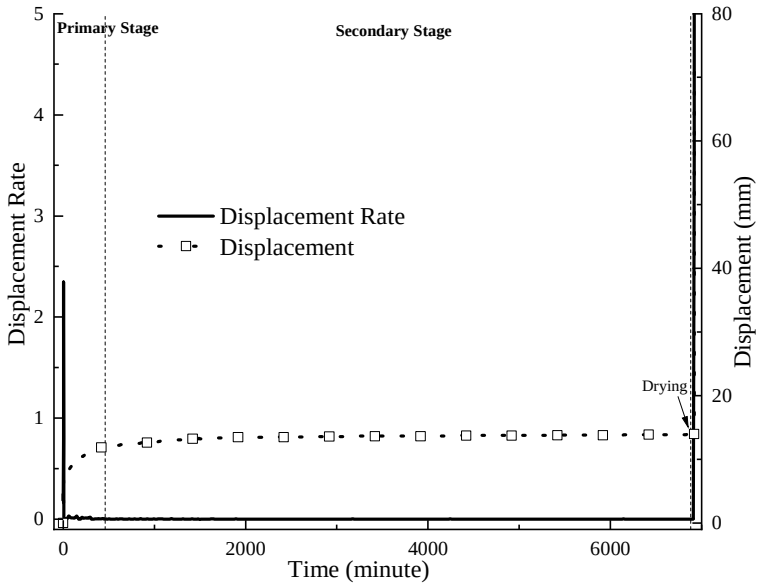

(d) 70 % creep shear stress level

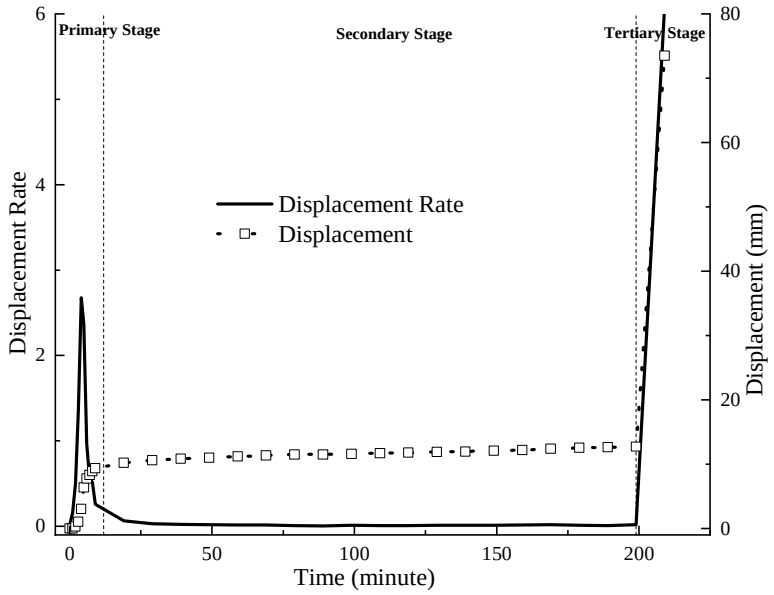

(e) 80 % creep shear stress level

Figure 6.16 Creep displacement rate of Kaolin Clay-GDL interfaces subjected to drying-wetting cycles

Based on Figure 6.16, similar to Mercia Mudstone Clay-GDL interfaces, the highest displacement rate for Kaolin Clay-GDL interfaces occurs at the primary creep stage after creep shear stress was imposed or the failure of the interfaces caused by the drying-wetting cycles or creep shear stress. More specifically, for interfaces under 40 %, 50 %, and 60 % creep shear stress level, the highest displacement rate occurs during the primary creep stage, and it rapidly reaches the peak value after the creep shear stress is imposed, then decreasing to a low value before stabilising. For interfaces under 70 % and 80 % creep shear stress levels, the largest displacement rate happens in the failure process of interfaces. Overall, the highest displacement rate of the interfaces increases with the increase in creep shear stress level. Under the same creep shear stress level, the highest displacement rates of Kaolin Clay-GDL interfaces are higher than those of Mercia Mudstone Clay-GDL interfaces, respectively. This can be attributed to the higher brittleness of Kaolin Clay-GDL interfaces than that of Mercia Mudstone Clay-GDL interfaces. In terms of the displacement rate during drying-wetting cycles, like Mercia Mudstone Clay-GDL interfaces, the highest displacement rate occurs

during the first drying cycle, which rapidly reaches the peak value after the first drying loading and then reduces to a steady value. During the following drying and wetting cycles, the displacement rate slightly rises, but the varying magnitudes are significantly lower than that of the first drying loading. By comparing the displacement rate of interfaces under diverse creep shear stress levels, it is found that the increase in displacement rate due to drying and wetting cycles under a high creep shear stress level is higher than those under a low creep shear stress level. However, unlike Mercia Mudstone Clay-GDL interfaces, the difference between the displacement rates during drying loadings and wetting loadings is not significant.

In Figure 6.16, when the time is at zero, the interface is in the initial state and there is no creep displacement; i.e. the creep displacement equals to 0 mm. Thus, in the 0 minute, the displacement rate of the interface is 0. Then, with the loading of creep shear stress, the creep displacement of the interface rises, which results in the rapid increase in displacement rate. After the displacement rate rises to the peak value, it gradually decreases to a low value. The above-mentioned general changing trends of displacement rate during the loading of creep shear stress are the same for the interfaces under different creep shear stress levels in Figure 6.16, with a small duration of the rise in displacement rate during the loading of creep shear stress (within 10 minutes). For the displacement rate-time relationship curves of interfaces under 40 %, 50 %, 60 % and 70 % creep shear stress level, as shown in Figure 6.16 (a), (b), (c) and (d), the scale of their horizontal axis (time) is more than 7000 minutes, which is far larger than the duration of the rise in displacement rate. Thus, in Figure 6.16 (a), (b), (c) and (d), initially the rising process of displacement rate is not showed clearly, which is overlapped with the decreasing process of displacement rate. In comparison, for the displacement rate-time relationship curve of the interface under 80 % creep shear stress level, as shown in Figure 6.16 (e), the scale of its horizontal axis (time) is around 200 minutes. The difference between the scale of horizontal axis (time) in Figure 6.16 (e) and the duration of the rise in displacement rate during the loading of creep shear stress is not as large compared with those of Figure

6.16 (a), (b), (c) and (d). Thus, in Figure 6.16 (e), initially the change of displacement rate is shown clearly.

6.3.6 Creep deformation rate of interfaces subjected to thermal cycles

The displacement rate of Mercia Mudstone Clay-GDL interfaces subjected to thermal cycles is presented in Figure 6.17.

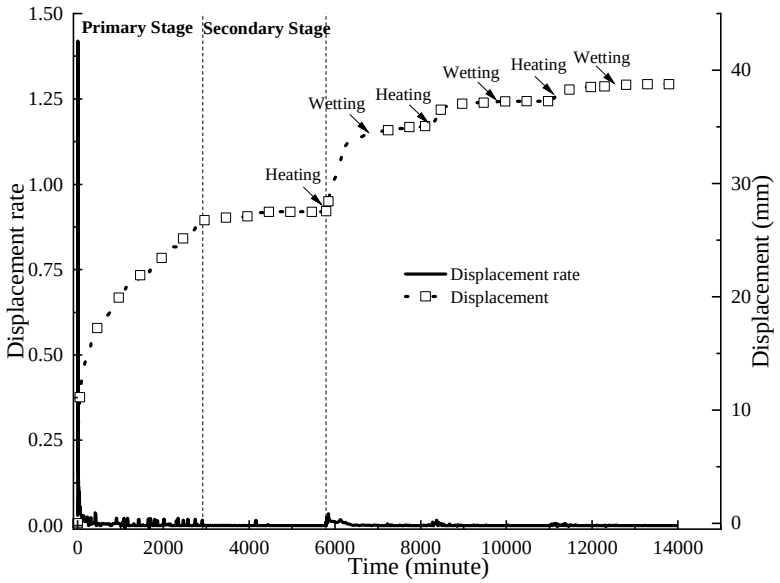

(a) 70 % creep shear stress level

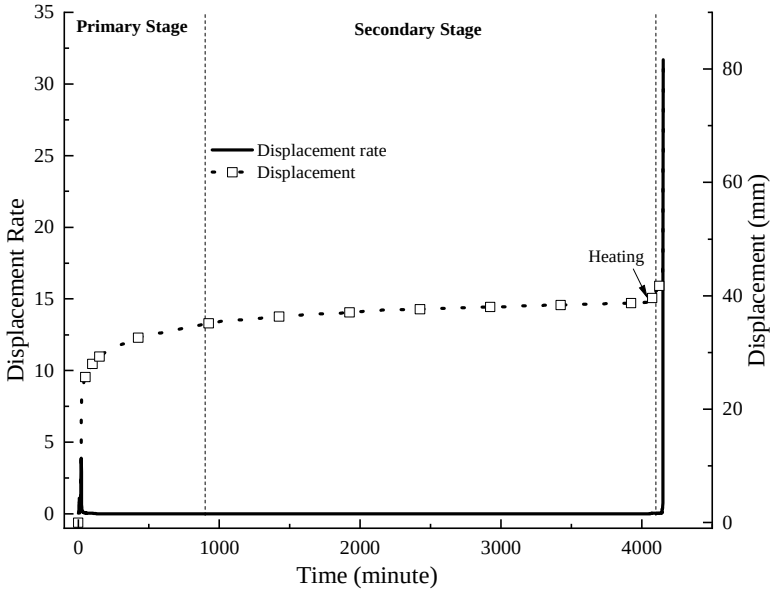

(b) 80 % creep shear stress level

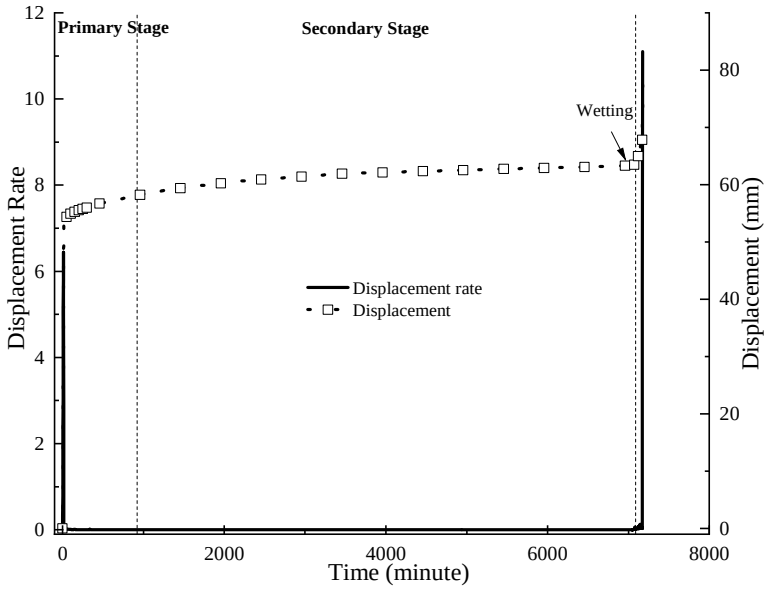

(c) 90 % creep shear stress level

Figure 6.17 Mercia Mudstone Clay-GDL interfaces subjected to thermal cycles

Based on Figure 6.17, the highest displacement rate of Mercia Mudstone Clay-GDL interfaces under 80 % and 90 % creep shear stress levels occurs during the first thermal cycle in which elevated temperature causes the rapid increase in the displacement rate and the failure of interfaces. Regarding the Mercia Mudstone Clay-GDL interface subjected to thermal cycles under 70 % creep shear stress level, although the peak displacement rate during each heating cycle is lower than that of the corresponding drying cycle of the interface subjected to drying-wetting cycles under the same creep shear stress level, the decreasing speeds in displacement rate during thermal cycles once reaching peak value are lower than those during the corresponding drying cycles, respectively. This demonstrates that the variation in displacement, due to heating cycles, is smoother and lasts a longer period than those caused by drying cycles. Additionally, the rise in displacement rate due to the first heating cycle is higher than those caused by the following heating cycles. Also, the increase in displacement rate due to the heating cycles is generally larger than those caused by the wetting cycles.

The displacement rate of Kaolin Clay-GDL interfaces during thermal cycles is presented in Figure 6.18.

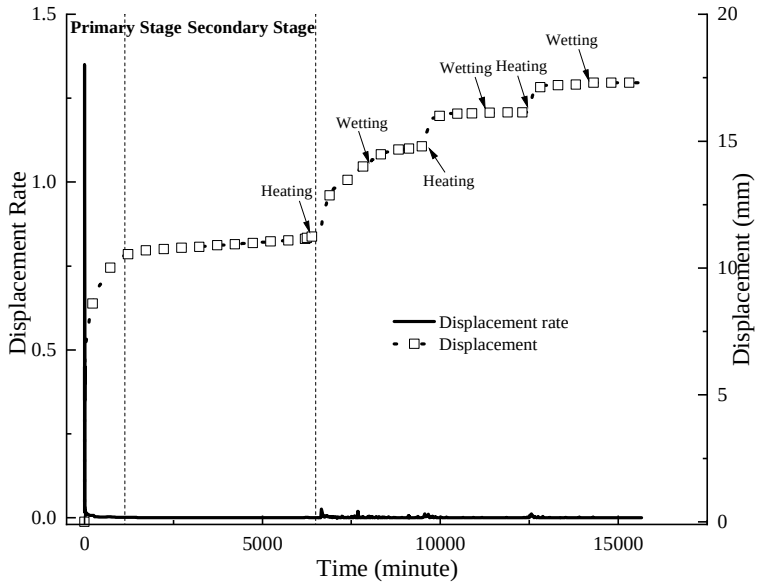

(a) 60 % creep shear stress level

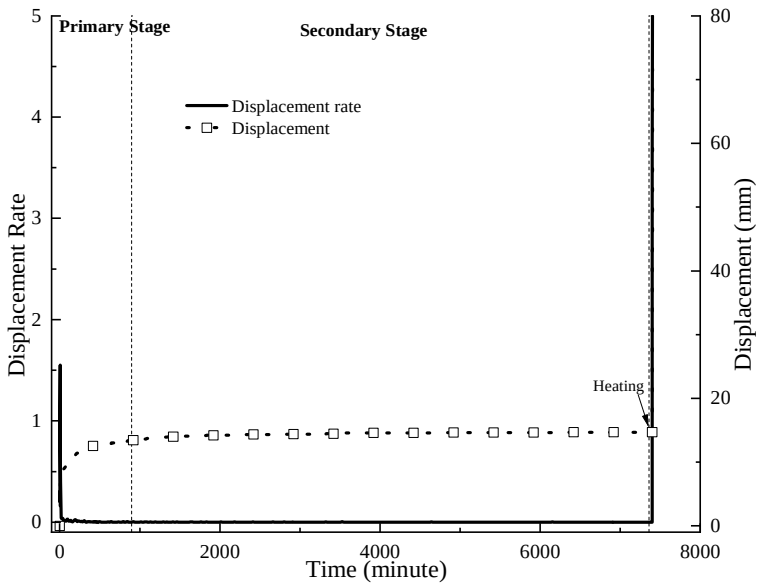

(b) 70 % creep shear stress level

Figure 6.18 Creep displacement rate of Kaolin Clay-GDL interfaces subjected to thermal cycles

Based on Figure 6.18, the highest displacement rate of the Kaolin Clay-GDL

interface under 70 % creep shear stress level occurs during the first thermal cycle, in which elevated temperature causes the rapid rise in displacement rate and the failure of the interface. Regarding the Kaolin Clay-GDL interface subjected to thermal cycles under 60 % creep shear stress level, similar to Mercia Mudstone Clay-GDL interfaces, although the peak displacement rate during each heating cycle is lower than that of the corresponding drying cycle of the interface subjected to drying-wetting cycles under 60 % creep shear stress level, the decreasing speeds of displacement rate during the heating cycles once reaching the peak displacement rate are lower than those of the corresponding drying cycles, respectively. This demonstrated that the variation in displacement due to heating cycles is smoother and lasts for a longer period than those caused by drying cycles. However, unlike Mercia Mudstone Clay-GDL interfaces, the displacement rate of Kaolin Clay-GDL interfaces during the first heating cycle has no significant difference to those during the following heating cycles. Furthermore, the rise in displacement rate of Kaolin Clay-GDL interfaces, due to the heating cycles, is generally close to those caused by the wetting cycles, respectively.

6.3.7 Creep deformation rate of interfaces subjected to drying-wetting cycle without heating

The creep displacement rate of Mercia Mudstone Clay-GDL interfaces during drying-wetting cycle without heating is presented in Figure 6.19.

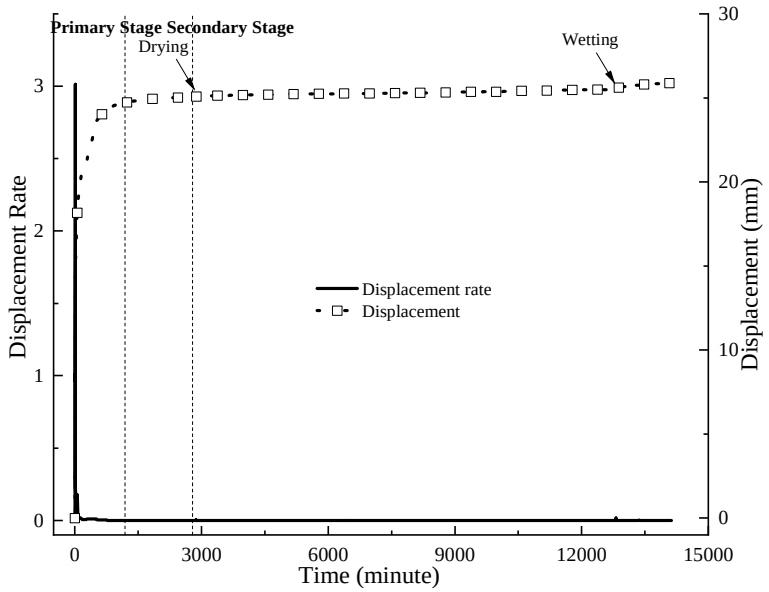

Figure 6.19 Mercia Mudstone Clay-GDL interfaces during drying-wetting cycle without heating

Based on Figure 6.19, the highest displacement rate occurs during the wetting cycle, which is significantly higher than that during the drying cycle without heating. In comparison to the displacement rate of Mercia Mudstone Clay-GDL interfaces during the drying cycles with heating and the heating process of thermal cycles, the rate during drying cycle without heating is lower. For example, the highest displacement rates during the first drying cycle with heating and the first heating process of the thermal cycle are 0.18 and 0.11, respectively, whilst the highest displacement rate during the first drying cycle without heating is around 0.005. This indicates that elevated temperature is the main reason of the increase in the creep deformation rate for Mercia Mudstone Clay-GDL interfaces and drying alone has marginal influence on the increase of the creep deformation rate.

The creep displacement rate of Kaolin Clay-GDL interfaces during drying-wetting cycle without heating is presented in Figure 6.20.

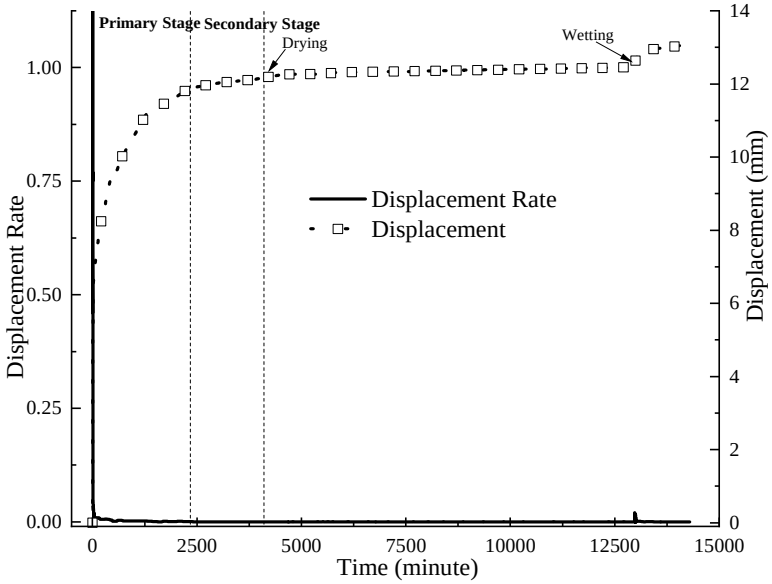

Figure 6.20 Kaolin Clay-GDL interfaces during drying-wetting cycle without heating

Based on Figure 6.20, similar to Mercia Mudstone Clay-GDL interfaces, the highest displacement rate occurs during the wetting cycle, which is significantly higher than that of the drying cycle without heating. By comparing the displacement rate of Kaolin Clay-GDL interfaces during the drying cycles with heating and the heating process of thermal cycles, the rate during drying cycle without heating is lower. For example, the highest displacement rates during the first drying cycle with heating and the first heating process of thermal cycles are 0.10 and 0.05 respectively, whilst the highest displacement rate during the first drying cycle without heating is around 0.001. This indicates that elevated temperature is the main reason for the increase in the creep deformation rate of Kaolin Clay-GDL interfaces and drying alone has marginal influence on the increase of the creep deformation rate.

6.4 Summary

In this chapter, a series of creep shear tests were carried out on clayey soil-GDL interfaces subjected to environmental factors using the bespoke temperature and stress-controlled large direct shear apparatus. According to

the experimental outcomes, the impacts of drying-wetting cycles, thermal cycles, drying-wetting cycle without heating, soil type and creep shear stress level on the creep mechanical characteristics of clayey soil-GDL interfaces were investigated. A detailed mechanism analysis is presented in Chapter 7. The main findings are summarised as follows:

(1) Mercia Mudstone Clay-GDL interfaces have larger creep shear resistance than that of Kaolin Clay-GDL interfaces. It is found that before drying-wetting cycles, the critical creep shear stress level, above which failure occurs, for Mercia Mudstone Clay-GDL interface is 95 %, while for Kaolin Clay-GDL interfaces, it is 80 %. During the drying-wetting cycles and thermal cycles, the critical creep shear stress level for Mercia Mudstone Clay-GDL interfaces is 80 %, while for Kaolin Clay-GDL interfaces, this is 70 %.

(2) Drying-wetting cycles and thermal cycles have large impacts on the creep behaviour of clayey soil-GDL interfaces, respectively. More specifically, the impacts of drying cycles and heating cycles on the horizontal displacement are considerably larger than that of wetting cycles, respectively. It is found that the first drying cycle and first heating cycle has the largest impacts on the horizontal displacement, compared to the following drying cycles and heating cycles, respectively. Additionally, the impacts of drying cycles and heating cycles on the horizontal displacement of interfaces under a high creep shear stress level is larger than those under a low creep shear stress level, respectively.

(3) The increase in horizontal displacement of clayey soil-GDL interfaces resulted from the heating process of thermal cycles is higher than those resulted from the drying cycles with heating. In comparison, the rise of horizontal displacement during the drying cycle without heating is significantly lower than both of those during the drying cycles with heating and during the heating processes of thermal cycles.

This indicates that drying alone cannot lead to an apparent increase in the horizontal displacement of Kaolin Clay-GDL interfaces during creep deformation, which has a marginal contribution to the increase in creep shear deformation during drying cycles with heating in the creep tests.

(4) The highest displacement rate generally occurs during the primary creep stage after creep shear stress is imposed or the failure process of interfaces caused by either drying-wetting cycles or creep shear stress. The highest displacement rate of interfaces increases with the increase in creep shear stress level. Additionally, the highest displacement rate of Kaolin Clay-GDL interfaces is higher than those of Mercia Mudstone Clay-GDL interfaces under the same creep shear stress level, respectively.

(5) In terms of the displacement rate during drying-wetting cycles and thermal cycles, the highest displacement rate occurs during the first drying cycle and the first heating cycle, respectively, which is significantly higher than those during following cycles, respectively. Additionally, the displacement rate during drying cycles and heating cycles is higher than those of wetting cycles, respectively.

(6) Under the same creep shear stress level, although the peak displacement rate during each heating cycle is lower than those of the corresponding drying cycles, the decreasing speeds of displacement rate during heating cycles once reaching the peak value are lower than those of the corresponding drying cycles, respectively. This illustrated that the variation in displacement during heating cycles is smoother and lasts for a longer period than that of drying cycles. Additionally, the displacement rate of the clayey soil-GDL interfaces during drying cycle without heating is lower than those during the drying cycles with heating and heating processes of thermal cycles, respectively. This

indicates that elevated temperature is the main reason for the increase in the creep deformation rate of clayey soil-GDL interfaces and drying alone has marginal influence on the increase of the creep deformation rate.

Chapter 7

Discussion

7.1 Introduction

This chapter discusses the research outcomes presented in Chapter 5 and Chapter 6 to provide an in-depth analysis of the research results. Initially, based on the results of rapid loading shear tests in Chapter 5, the interaction mechanism of clayey soil-GDL interfaces subjected to drying-wetting cycles, elevated temperature, thermal cycles and drying-wetting cycle without heating is presented to further investigate the influence of environmental factors on the short-term mechanical characteristics of clayey soil-GDL interfaces. Then, based on the results of creep tests in Chapter 6, the interaction mechanism of clayey soil-GDL interfaces subjected to drying-wetting cycles, thermal cycles and drying-wetting cycle without heating is presented to further investigate the influence of environmental factors on the creep mechanical characteristics of clayey soil-GDL interfaces.

7.2 Mechanism analysis associated with the impacts of environmental loadings on the short-term mechanical properties of interfaces

In this section, mechanisms analysis about the impacts of elevated temperature, thermal cycles, drying-wetting cycle without heating and drying-wetting cycles on mechanical properties of clayey soil-GDL interfaces during rapid loading shear tests in Chapter 5 are conducted to research the action mechanism of the environmental factors on the short-term mechanical properties of clayey soil-GDL interfaces.

Figure 7.1 depicts the detailed interaction mechanism between soil and GDL. According to Figure 7.1, the peak shear strength of clayey soil-GDL interfaces is mobilised from two components: the skin friction and the

interlocking effects between soil and GDL (Bacas et al., 2015). More specifically, initially, the soil specimen, nonwoven geotextile and drainage core are separate and after the compaction during the installation of soil, soil penetrates the geotextile and drainage core slightly. With normal stress loading, the soil and geotextile fabrics are further compressed around the drainage core and embedded into the cuspate elements of the drainage core, which enhances the interlocking effects between soil lumps and the drainage core to increase the peak shear strength of the interface. Especially under high normal stress, a large quantity of soil and geotextile fabrics can be embedded into the drainage core to provide larger interlocking effects between soil and GDL than that under low normal stress. Additionally, for the soil with high moisture saturation, it is softer and easier to be pushed into the geotextile and drainage core compared with soil with low moisture saturation (Othman, 2016). In this research, the tests were conducted in a submerged condition with 24 hours consolidation. Although the imposed normal stress was not very high, the long-time consolidation process allowed the saturated soil to be sufficiently pressed into the geotextile and drainage core, leading to the interlocking effects being an important factor to affect the peak shear strength of soil-GDL interfaces. Figure 7.2 presents the surface of the soil specimens after testing. The clear indentations caused by the cuspate elements of drainage core can be seen in the surfaces of the soil specimens, which indicates the considerable penetration of soil into the geotextile and drainage core of GDL.

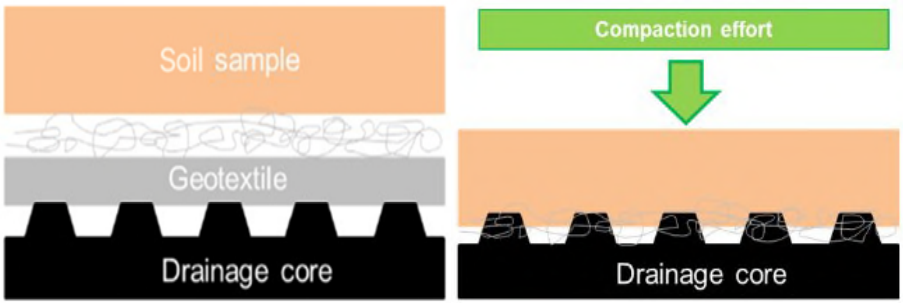

(a) Original state (b) After compaction

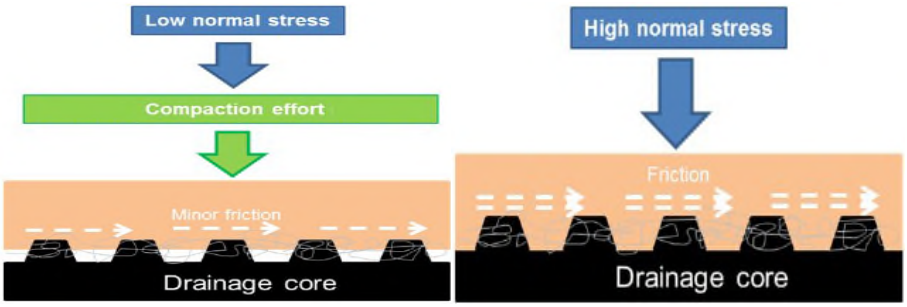

(c)Under low normal stress (d)Under high normal stress

Figure 7.1 The interaction mechanism between soil and GDL (Chao and Fowmes, 2021)

(a)Mercia Mudstone Clay (b)Kaolin Clay

Figure 7.2 The surface of the soil specimens after shearing (Chao and Fowmes, 2021)

Due to the presence of thermo-softening plastic materials, the stiffness (modulus) of HDPE drainage core and fibres of geotextiles bonded on the drainage core decreases in elevated temperature, which results in the softening of the cuspate elements on the drainage core and the fibres of geotextiles (Hanson et al., 2015). In elevated temperature, the softening cuspate elements are easier to be compressed, which reduces the penetrating depth of the cuspate elements into soil. Also, the softening cuspate elements are easier to deform during the shearing process, weakening the interlocking effects between soil and GDL. Meanwhile, the softening fibres are easier to

align during the shearing process to decrease the skin friction between soil and GDL. Additionally, whilst likely a minor effect, the viscosity of water in soil reduces at elevated temperature, which increases the pore water pressure in soil and decreases its effective stress, causing the reduction in the shear strength of soil (Perkins and Sjursen, 2009). For the interfaces subjected to drying-wetting cycles and thermal cycle, respectively, when the temperature of interfaces decreases to the normal level again, although an increase can occur in the stiffness of drainage core, the compressive deformation of the cuspate elements on the drainage core caused by elevated temperature cannot recover (Karademir, 2011). It results in the small penetrating depth of the cuspate elements into soil, weakening the interlocking effects between soil and GDL. Thus, in this research, the peak shear strength of soil-GDL interfaces subjected to drying-wetting cycles/thermal cycle and in elevated temperature is lower than that of the original interfaces, respectively.

To further analyse the interaction mechanism, the consolidated undrained triaxial shear tests on Mercia Mudstone Clay and Kaolin Clay specimens, subjected to the same process of drying-wetting cycles on clayey soil-GDL interfaces, by soil specimens being submerged into water for 24 hours to wet and placed in 40 ℃ temperature for 24 hours to dry, were conducted. Based on the experimental results, the peak shear strength of Mercia Mudstone Clay and Kaolin Clay specimens subjected to drying-wetting cycles is presented in Figure 7.3.

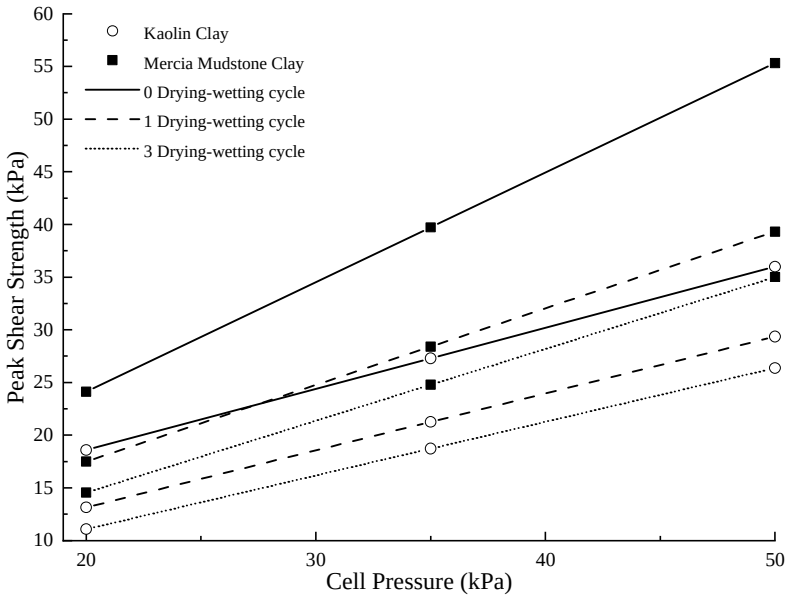

Figure 7.3 Peak shear strength of soil specimens subjected to drying-wetting cycles

Based on Figure 7.3, the peak shear strength of both Mercia Mudstone Clay and Kaolin Clay specimens reduces consistently during the drying-wetting cycles. This may be attributed to the microcracks that develop within the soil during drying-wetting cycles to damage the internal structure of the soil samples (Pasculli et al., 2017), Thus, when the clayey soil-GDL interfaces were subjected to drying-wetting cycles, the reducing shear strength of the soil above GDL further weakens the interlocking effects between the clayey soil and GDL. This results in a greater reducing magnitude in shear resistance of the interfaces subjected to 1 drying-wetting cycle than those subjected to 1 thermal cycle to cause the peak shear strength of the interfaces subjected to 1 drying-wetting cycle being lower than that subjected to 1 thermal cycle.

The reason that the peak shear strength of clayey soil-GDL interfaces subjected to drying-wetting cycle without heating is slightly lower than that of original specimens but significantly higher than the interfaces subjected to drying-wetting cycles and thermal cycle, respectively, can be attributed to the fact that that in the absence of elevated temperatures, the stiffness of the drainage core and geotextile fibres of the interfaces subjected to drying-

wetting cycles without heating is identical to that of original specimens during the tests. The aforementioned softening of the drainage core/fibres and weakening of the interlocking effects between soil and GDL caused by the decrease in the stiffness of the GDL drainage core/geotextiles does not occur in clayey soil-GDL interfaces subjected to drying-wetting cycle without heating. Only the impacts of drying-wetting cycles alone, which are mentioned in above paragraph are imposed on the short-term mechanical properties of clayey soil-GDL interfaces. This also indicates that the impacts of drying-wetting cycles alone on the decrease in peak shear strength of clayey soil-GDL interfaces during drying-wetting cycles with heating are marginal, with the main influence factor being elevated temperature.

Another aspect should be noted is that Mercia Mudstone Clay-GDL interfaces have higher peak shear strength than that of Kaolin Clay-GDL interfaces. It may be attributed to the stronger interlocking effects between Mercia Mudstone Clay and GDL than that between Kaolin Clay and GDL, which is resulted from the higher peak shear strength of Mercia Mudstone Clay than that of Kaolin Clay, as presented in Figure 7.3.

7.3 Mechanism analysis associated with the impacts of environmental loadings on the creep mechanical properties of interfaces

In this section, the mechanism analysis of the impact of thermal cycles, drying-wetting cycle without heating and drying-wetting cycles on the mechanical properties of clayey soil-GDL interfaces during creep tests in Chapter 6 is carried out to research the action mechanism of the environmental factors on the creep mechanical properties of clayey soil-GDL interfaces.

As mentioned in section 7.2, the peak shear strength of clayey soil-GDL interfaces is mobilised from two components: the skin friction and the interlocking effects between soil and GDL (Bacas et al., 2015). The creep

shear resistance between soil and GDL can also be attributed to the skin friction and interlocking effects between soil and GDL, as shown in Figure 7.1. In this research, the adopted normal stress in creep tests is 25 kPa, and as with the rapid loading shear tests, before imposing creep shear stress in the creep tests, the interfaces were conducted 24 hours consolidation with being submerged by water. Although the imposed normal stress was not very high, the long-time consolidation process allowed saturated soil to be sufficiently pressed into the geotextile and drainage core of GDL, leading to the interlocking effects as an important factor to influence the creep shear resistance between soil and GDL. The clear indentations on the surface of soil caused by the cuspate elements of drainage core indicate the considerable penetration of soil into the geotextiles and drainage core of GDL, as shown in Figure 7.2.

As mentioned in Section 7.2, regarding the presence of thermo-softening materials, the stiffness (modulus) of HDPE drainage core and fibres of geotextiles bonded on the drainage core decreases at elevated temperature, which results in the softening of the cuspate elements on the drainage core and the fibres of geotextiles to weaken the interlocking effects and skin friction between soil and GDL. Additionally, at elevated temperature, the viscosity of water in soil reduces, which increases the pore water pressure in the soil to decrease its effective stress, causing the decline in the shear strength of the soil. Thus, in this research, during drying cycles and heating cycles, the creep deformation of clayey soil-GDL interfaces rises because of the decreasing creep shear resistance caused by elevated temperature. When the temperature decreases to the normal level again, an increase can occur in the stiffness of the cuspate elements on drainage core and the fibres of geotextiles, which results in the rise in the interlocking effects and skin friction between soil and GDL. The higher impacts of the first drying cycle and heating cycle on the creep deformation of clay-GDL interfaces than those of the following drying cycles and heating cycles can be ascribed to that, after the first drying cycle and heating cycle, even though the temperature decreases to the normal level, the interlocking effects and skin friction of the

interfaces cannot fully rise to the original level before the first increase in temperature because the compressive deformation of the cuspate elements caused by elevated temperature cannot recover and the aligned fibres caused by elevated temperature cannot return to the original state. Thus, after experiencing the elevated temperature in the first drying cycle and heating cycle, before imposing the following drying cycles and heating cycles, the interlocking effects and skin friction of the interfaces are already lower than the original levels, respectively. During the following drying cycles and heating cycles, at elevated temperature, when the interlocking effects and skin friction of the interfaces decrease to the same level with those in the first drying cycle and heating cycle, the decreasing magnitudes are lower than those during the first drying cycle and heating cycle, respectively, which results in the rise in the horizontal displacement of clayey soil-GDL interfaces during the first drying cycle and heating cycle is higher than those during the following drying cycles and heating cycles, respectively. Moreover, the higher creep deformation during heating cycles than that of drying cycles can be attributed to the existence of water. During the heating cycles, the clayey soil-GDL interfaces were submerged by water. As aforementioned, the added water can soften the overlying soil sample, dissolving the cement between soil particles, which provides more lubrication between soil particles and clayey soil-GDL interface, respectively, decreasing the shear strength of clayey soil-GDL interfaces. In comparison, during the drying cycles, the overlying soil sample is unsaturated, which leads to the generation of suction in soil to enhance the shear strength of clayey soil-GDL interfaces.

Variation in the horizontal displacement of interfaces during the drying cycles and the heating processes of thermal cycles is significantly higher than that of the drying cycle without heating. This can be attributed to the fact that the stiffness (modulus) of the cuspate elements on the HDPE drainage core and the fibres of geotextiles remains stable at the room temperature. Therefore, there is no softening of the cuspate elements and fibres to weaken the interlocking effects and skin friction between soil and GDL. Additionally, the viscosity of water in soil specimens remains stable at room temperature,

which does not increase the pore water pressure of soil to decrease its effective stress. Thus, the variation in creep deformation of clay-GDL interfaces during drying cycles without heating is significantly lower than those of the drying cycles with heating and the heating processes in thermal cycles. This indicates that the impacts of drying alone on the increase of the horizontal displacement of clayey soil-GDL interfaces during drying cycles with heating are marginal, with the main influence factor being elevated temperature. The increase in the horizontal displacement of the clayey soil-GDL interfaces during the wetting process of drying-wetting cycle without heating may be ascribed to the reduction in the peak shear strength of clayey soil during drying-wetting cycles, as mentioned in Section 7.2. When clayey soil-GDL interfaces were subjected to drying-wetting cycles without heating, the peak shear strength of soil above the GDL reduces, causing the weakening of the interlocking effects between soil and GDL, which decreases the creep shear resistance of interfaces. Thus, the ascent in the horizontal displacement of clayey soil-GDL interfaces during the wetting process of drying-wetting cycle without heating occurs.

According to the outcomes of the triaxial shear experiments on Mercia Mudstone Clay and Kaolin Clay specimens subjected to drying-wetting cycles presented in Figure 7.3, under the same cell pressure and the same number of drying-wetting cycles, the shear strength of Mercia Mudstone Clay specimens is larger than that of Kaolin Clay specimens. The larger shear strength of clayey soil overlying the GDL can result in larger interlocking effects between clayey soil and GDL, leading to higher creep shear resistance of the interfaces. Therefore, the Mercia Mudstone Clay-GDL interfaces can bear a higher creep shear stress level and remain stable under a larger creep shear stress level when subjected to drying-wetting cycles, thermal cycles and elevated temperature compared to Kaolin Clay-GDL interfaces.

7.4 Summary

This chapter discusses the research results presented in Chapter 5 and Chapter 6 to provide an in-depth mechanism analysis of the research results. The main outcomes are summarised as follows:

(1) In rapid loading shear tests, the lower peak shear strength is observed for interfaces subjected to drying-wetting cycles, thermal cycle and elevated temperature compared to the original interfaces. This may be ascribed to the weakening of interlocking effects and skin friction between soil and GDL caused by the softening of drainage core and geotextile fibres of GDL as well as the decline in the peak shear strength of the soil.

(2) Due to the larger peak shear strength of Mercia Mudstone Clay than that of Kaolin Clay, the peak shear strength and creep shear resistance of Mercia Mudstone Clay-GDL interfaces is higher than that of Kaolin Clay-GDL interfaces.

(3) Due to the reduction in the peak shear strength of clayey soil above GDL during drying-wetting cycles, the peak shear strength of clayey soil-GDL interfaces subjected to 1 drying-wetting cycle is lower than that subjected to 1 thermal cycle.

(4) The impacts of drying alone on the decrease in the peak shear strength of clayey soil-GDL interfaces during drying cycles with heating is small, and the main influence factor is elevated temperature. The decrease in the peak shear strength of clayey soil-GDL interfaces during drying-wetting cycle without heating can be ascribed to the reduction in the peak shear strength of clayey soil.

(5) In creep tests, increase in the horizontal displacement of clayey soil-GDL interfaces during drying cycles and heating cycles can be

ascribed to the weakening of the interlocking effects and skin friction between soil and GDL. This is caused by the softening of drainage core and geotextile fibres as well as the decline in the peak shear strength of soil.

(6) The greater impacts of the first drying cycle and heating cycle on the creep deformation of clayey soil-GDL interfaces than those of the subsequent cycles, respectively, can be ascribed to the larger decreasing magnitudes of the interlocking effects and skin friction between soil and GDL during the first drying cycle and heating cycle than those of the following drying cycles and heating cycles, respectively.

(7) The higher creep deformation of clayey soil-GDL interfaces during thermal cycles compared to that during drying cycles can be attributed to the presence of water. During thermal cycles, the clayey soil-GDL interfaces were submerged into water which softened the overlying soil sample and dissolved the cement between soil particles. This provided more lubrication between soil particles and clayey soil-GDL interfaces, respectively, reducing the shear strength of clayey soil-GDL interfaces. In comparison, during the drying cycles, the overlying clay sample was unsaturated, leading to the generation of suction in soil to enhance the shear strength of clayey soil-GDL interfaces.

(8) The impacts of drying alone on the increase in the horizontal displacement of clayey soil-GDL interfaces during drying cycles with heating is marginal and the main influence factor is elevated temperature. The increase in the horizontal displacement of clayey soil-GDL interfaces during the wetting process of drying-wetting cycle without heating can be ascribed to the reduction in the peak shear strength of clayey soil during drying-wetting cycles.

Chapter 8

Conclusions

8.1 Principal findings related to the study aim and objectives

8.1.1 The aim

(1) To quantify the mechanical behaviour of cover soil-GDL interfaces subjected to environmental loadings

Based on the physical experiments, the influence of environmental loadings, such as elevated temperature, drying-wetting cycles, drying-wetting cycle without heating and thermal cycles on the mechanical behaviour of cover soil-GDL interfaces has been quantified comprehensively.

8.1.2 Objective 1: To measure the impacts of elevated temperature, drying-wetting cycles and thermal cycles on the short-term mechanical behaviour of cover clayey soil-GDL interfaces

A bespoke large stress and temperature-controlled direct shear apparatus for testing soil-geosynthetics interfaces was developed. By adopting the apparatus, a series of validation tests and repetitive experiments were carried out to evaluate the functionality of the apparatus. Also, the experimental results from the bespoke apparatus were compared to the results from conventional displacement-controlled equipment to further support the reliability of the apparatus. The experimental results indicate that the modified apparatus allows for the shear deformation behaviour of soil-geosynthetics interfaces subjected to environmental loadings such as drying-wetting cycles, thermal cycles and elevated temperature to be investigated with reliable performance.

A series of rapid loading shear tests were conducted on clayey soil-GDL

interfaces subjected to drying-wetting cycles, thermal cycles, drying-wetting cycle without heating and elevated temperature, using the self-designed large temperature and stress-controlled direct shear apparatus. The impacts of environmental loadings on the short-term mechanical characteristics of clayey soil-GDL interfaces were investigated.

The experimental results indicate that the ductility of Mercia Mudstone Clay-GDL interfaces is higher than that of Kaolin Clay-GDL interfaces. Mercia Mudstone Clay-GDL interfaces can remain stable under a large horizontal displacement, whilst for Kaolin Clay-GDL interfaces, a small deformation can lead to sudden failure. This indicates that Kaolin Clay-GDL interfaces are more brittle than Mercia Mudstone Clay-GDL interfaces; The peak shear strength and failure time of specimens subjected to drying-wetting cycles and elevated temperature are more sensitive to the increase in normal stress compared to original specimens; Under low normal stress, the peak shear strength and failure time are more sensitive to drying-wetting cycles and elevated temperature than those under high normal stress, respectively; Compared to original interfaces, the interfaces subjected to drying-wetting cycles, thermal cycles and elevated temperature, have lower peak shear strength and failure time. This is due to the weakening of the interlocking effects and skin friction between soil and GDL caused by the softening of drainage core and geotextile fibres; Variation amplitudes of the strength parameters at elevated temperature are considerably greater than those during drying-wetting and thermal cycles, respectively; The decreasing magnitude of peak shear strength and failure time of clayey soil-GDL interfaces subjected to 1 drying-wetting cycle without heating is lower than those subjected to 1 drying-wetting cycle with heating and 1 thermal cycle, respectively, which indicates that the impacts of drying alone on the decrease in peak shear strength and failure time of clayey soil-GDL interfaces during drying cycles with heating is marginal and the main influence factor is the elevated temperature; The decrease in the peak shear strength and failure time of clayey soil-GDL interfaces subjected to drying-wetting cycle without heating can be ascribed to the reduction in peak shear strength of clayey soil

during drying-wetting cycle; Due to the larger peak shear strength of Mercia Mudstone Clay than that of Kaolin Clay, the peak shear strength of Mercia Mudstone Clay-GDL interfaces is higher than that of Kaolin Clay-GDL interfaces; Due to the reduction in peak shear strength of clayey soil above GDL during drying-wetting cycles, the peak shear strength and failure time of clayey soil-GDL interfaces subjected to 1 drying-wetting cycle is lower than those subjected to 1 thermal cycle, respectively.

8.1.3 Objective 2: To measure the impacts of drying-wetting cycles and thermal cycles on the creep mechanical behaviour of cover clayey soil-GDL interfaces

The impacts of environmental loadings on the creep mechanical characteristics of clayey soil-GDL interfaces were investigated. Using the self-designed large temperature and stress-controlled direct shear apparatus, a series of creep shear tests were carried out on clayey soil-GDL interfaces subjected to drying-wetting cycles, drying-wetting cycle without heating and thermal cycles.

The tests results indicated that both Kaolin Clay-GDL interfaces and Mercia Mudstone Clay-GDL interfaces subjected to drying-wetting cycles and thermal cycles fail under a lower creep shear stress level than that of the interfaces that do not undergo drying-wetting cycles and thermal cycles, respectively. This may be attributed to, at elevated temperature, the weakening of the interlocking effects and skin friction between soil and GDL caused by the softening of the drainage core and geotextile fibres as well as the decrease in the effective stress of soil due to the increase in the pore water pressure of soil; The impacts of drying cycles and heating cycles on the horizontal displacement of clayey soil-GDL interfaces is significantly higher than that of wetting cycles, respectively. This can be attributed to the decrease in the stiffness of HDPE drainage core and geotextile fibres at elevated temperature; The first drying cycle and first heating cycle has the largest

impacts on the horizontal displacement compared to those of the following cycles, respectively. This can be ascribed to the larger decreasing magnitude of interlocking effects and skin friction between soil and GDL during the first drying cycle and first heating cycle than those during the following cycles, respectively; The rise of horizontal displacement during drying cycle without heating is significantly lower than those during drying cycles with heating and the heating processes of thermal cycles, respectively. This can be attributed to the fact that the impacts of drying alone on the rise in horizontal displacement of clayey soil-GDL interfaces during drying cycles with heating are marginal and the main influence factor is elevated temperature; The increase in horizontal displacement of clayey soil-GDL interfaces during the wetting process of drying-wetting cycle without heating can be ascribed to the reduction in the peak shear strength of clayey soil during drying-wetting cycles; Mercia Mudstone Clay-GDL interfaces can bear a higher creep shear stress level and remain stable under a higher creep shear stress level when subjected to drying-wetting cycles and thermal cycles than those of Kaolin Clay-GDL interfaces, respectively. This is due to the higher peak shear strength of Mercia Mudstone Clay than that of Kaolin Clay leading to a higher creep shear resistance of Mercia Mudstone Clay-GDL interfaces than that of Kaolin Clay-GDL interfaces; The impacts of drying-wetting cycles and thermal cycles on clayey soil-GDL interfaces under a higher creep shear stress level are larger than those under a low creep shear stress level, respectively; The rise in the horizontal displacement of clayey soil-GDL interfaces during heating cycles is higher than that during drying cycles. This can be attributed to that, during heating cycles, the clayey soil-GDL interfaces were submerged into water, which softened the overlying soil sample and provided more lubrication between soil particles and clayey soil-GDL interfaces, respectively, decreasing the peak shear strength of clayey soil-GDL interfaces. In comparison, during drying cycles, the overlying soil sample was unsaturated, which led to the generation of suction in soil and enhanced the peak shear strength of clayey soil-GDL interfaces; The highest displacement rate of clayey soil-GDL interfaces occurs at the primary creep stage after creep shear stress is imposed or the failure of the interfaces caused

by the drying-wetting cycle, thermal cycle or creep shear stress; Overall, the highest displacement rate of clayey soil-GDL interfaces increases with the increase in creep shear stress level; Regarding the displacement rate during drying-wetting cycles and thermal cycles, the highest displacement rate occurs during the first drying-wetting cycle and thermal cycle, respectively; Although the peak displacement rate for interfaces during heating cycles is lower than the corresponding drying cycles under the same creep shear stress level, the decreasing speed of the displacement rate during the heating cycles once reaching the peak value is lower than that during the drying cycles. This demonstrates that the variation of displacement during heating cycles is smoother and lasts for a longer period than that during drying cycles; The peak displacement rates of Mercia Mudstone Clay-GDL interfaces are lower than those of Kaolin Clay-GDL interfaces under the same creep shear stress level, respectively. This can be contributed to the greater brittleness of Kaolin Clay-GDL interfaces than that of Mercia Mudstone Clay-GDL interfaces; The displacement rate of clayey soil-GDL interfaces during drying cycle without heating is evidently lower than that during drying cycles with heating and the heating processes in thermal cycles, respectively. This indicates that elevated temperature is the main reason for the increase of creep deformation rate and drying alone has marginal influence.

8.2 Limitations of the research and recommendations for future work

Limitations of the research and recommendations for future work are listed as follows:

(1) Environmental factors, such as leachate, vegetation, etc., have not been included in this research. These factors also have large influence on the stability of GDL cover systems. In the future, efforts in this aspect should be taken.

(2) During drying cycles on soil-GDL interfaces, the overlying soil is in unsaturated states, resulting in the generation of suction in soil, which

affects the shear strength of the interfaces. However, due to the limitation of the experimental device, the suction of the overlying soil sample on the GDL cannot be measured. Thus, in the future, it is worthy to further modify the apparatus to enable the measurements of soil sample suction.

(3) During the shearing process of soil-GDL interfaces, generated pore water pressure causes the decrease in the effective stress of the interfaces and the actual normal stress on the interfaces is lower than the imposed normal stress by the normal stress loading system. This decreases the peak shear strength of the interfaces. Therefore, it is more accurate to use effective stress to describe the mechanical behaviour of interfaces. However, due to the limitation of the experimental device, the pore water pressure of the interfaces cannot be measured. Thus, in the future, it is worthwhile further modifying the apparatus to enable the measurements of the pore water pressure of interfaces.

(4) Due to the limitation in experimental time, the creep deformation time of soil-GDL interfaces is set to be relatively short (within 2 weeks). This may not comprehensively reflect the creep deformation of soil-GDL interfaces during a long duration. Therefore, in the future, a longer duration of creep deformation, TTS or SIM should be adopted to research the creep deformation of soil-GDL interfaces subjected to environmental factors over a long-time span.

(5) In this research, two types of soil: Mercia Mudstone Clay and Kaolin Clay, and one type of GDL were adopted to investigate the stability of GDL cover systems. In the future, it is recommended to use more soil and GDL types to research the stability of GDL cover systems subjected to environmental variations, with different combinations of soil and GDL.

(6) Due to the limitation in experimental time, the number of drying-wetting cycles and thermal cycles is low (up to 3 cycles). This may not

comprehensively reflect the influence of a large number of drying-wetting cycles and thermal cycles on the mechanical characteristics of soil-GDL interfaces. Thus, in the future, investigation into the short-term and creep mechanical characteristics of soil-GDL interfaces subjected to a large number of drying-wetting cycles and thermal cycles should be carried out.

Reference

ABG.Ltd, 2020. Available from:http://www.abg-geosynthetics.com/products/pozidrain.html, [View 19/06/2020].

Abu-Farsakh, M., Coronel, J., Tao, M., 2007. Effect of soil moisture content and dry density on cohesive soil–geosynthetic interactions using large direct shear tests. Journal of Materials in Civil Engineering 19, 540-549.

Abuel-Naga, H.M., Bouazza, A., 2013. Thermomechanical behavior of saturated geosynthetic clay liners. Journal of geotechnical and geoenvironmental engineering 139, 539-547.

Achereiner, F., Engelsing, K., Bastian, M., Heidemeyer, P., 2013. Accelerated creep testing of polymers using the stepped isothermal method. Polymer Testing 32, 447-454.

Alwis, K., Burgoyne, C., 2006. Time-temperature superposition to determine the stress-rupture of aramid fibres. Applied Composite Materials 13, 249-264.

Anubhav, Basudhar, P., 2013. Interface behavior of woven geotextile with rounded and angular particle sand. Journal of materials in civil engineering 25, 1970-1974.

Arulrajah, A., Rahman, M.A., Piratheepan, J., Bo, M., Imteaz, M., 2014. Evaluation of interface shear strength properties of geogrid-reinforced construction and demolition materials using a modified large-scale direct shear testing apparatus. Journal of Materials in Civil Engineering 26, 974-982.

ASTM, 2008. Standard practice for obtaining samples of geosynthetic clay liners.

ASTM, 2014. Standard Test Method for Determining the Shear Strength of Soil–Geosynthetic and Geosynthetic–Geosynthetic Interfaces by Direct Shear. ASTM International West Conshohocken, PA.

Athanasopoulos, G.A., 1996. Results of direct shear tests on geotextile reinforced cohesive soil. Geotextiles and Geomembranes 14, 619-644.

Bacas, B., Cañizal, J., Konietzky, H., 2015. Frictional behaviour of three critical geosynthetic interfaces. Geosynthetics International 22, 355-365.

Bagheri, M., Nezhad, M.M., Rezania, M., 2020. A CRS oedometer cell for unsaturated and non-isothermal tests. Geotechnical Testing Journal 43, 20-37.

Bagheri, M., Rezania, M., Mousavi Nezhad, M., 2019. Rate Dependency and Stress Relaxation of Unsaturated Clays. International Journal of Geomechanics 19, 04019128.

Bahador, M., Evans, T., Gabr, M., 2013. Modeling effect of geocomposite drainage layers on moisture distribution and plastic deformation of road sections. Journal of geotechnical and geoenvironmental engineering 139, 1407-1418.

Barone, F., Costa, J., Ciardullo, L., 2000. Temperatures at the base of a municipal solid waste landfill, Proc. 6th Can Environ. Engng Conf., London, Ontario, pp. 41-48.

Basudhar, P., 2010. Modeling of soil–woven geotextile interface behavior from direct shear test results. Geotextiles and Geomembranes 28, 403-408.

Benjamim, C., Bueno, B., Lodi, P., Zornberg, J., 2008. Installation and ultraviolet exposure damage of geotextiles, Proceedings of the 4th European Geosynthetics Conference, Edinburgh, UK, 8p.

Benson, C.H., Edil, T.B., Wang, X., 2012. Evaluation of a final cover slide at a landfill with recirculating leachate. Geotextiles and Geomembranes 35, 100-106.

Benson, C.H., Kucukkirca, I.E., Scalia, J., 2010. Properties of geosynthetics

exhumed from a final cover at a solid waste landfill. Geotextiles and Geomembranes 28, 536-546.

Bilodeau, J.-P., Dore, G., Savoie, C., 2015. Laboratory evaluation of flexible pavement structures containing geocomposite drainage layers using light weight deflectometer. Geotextiles and Geomembranes 43, 162-170.

Bleiker, D.E., Farquhar, G., McBean, E., 1995. Landfill settlement and the impact on site capacity and refuse hydraulic conductivity. Waste management & research 13, 533-554.

Bouazza, A., Nahlawi, H., Aylward, M., 2011. In situ temperature monitoring in an organic-waste landfill cell. Journal of geotechnical and geoenvironmental engineering 137, 1286-1289.

Briançon, L., Girard, H., Poulain, D., 2002. Slope stability of lining systems—experimental modeling of friction at geosynthetic interfaces. Geotextiles and geomembranes 20, 147-172.

Bueno, B., Costanzi, M., Zornberg, J., 2005. Conventional and accelerated creep tests on nonwoven needle-punched geotextiles. Geosynthetics International 12, 276-287.

Chai, J.-C., Saito, A., 2016. Interface shear strengths between geosynthetics and clayey soils. International Journal of Geosynthetics and Ground Engineering 2, 19.

Chao, Z., Fowmes, G., 2021. Modified stress and temperature-controlled direct shear apparatus on soil-geosynthetics interfaces. Geotextiles and Geomembranes.

Chinkulkijniwat, A., Horpibulsuk, S., Bui Van, D., Udomchai, A., Goodary, R., Arulrajah, A., 2017. Influential factors affecting drainage design considerations for mechanical stabilised earth walls using geocomposites.

Geosynthetics International 24, 224-241.

Choudhary, A.K., Krishna, A.M., 2014. Influence of different types of soils on soil-geosynthetics interaction behavior. IJIRSET 3, 60-68.

Collins, H., 1993. Impact of the temperature inside the landfill on the behaviour of barrier systems, Proceedings Sardinia.

Corser, P., Cranston, M., 1991. Observations on the performance of composite clay liners and covers, Proc. Geosynthetic Design and Performance, pp. 59-63.

Crawford, J.F., Smith, P.G., 2016. Landfill technology. Elsevier.

Cui, X.-z., Li, J., Su, J.-w., Jin, Q., Wang, Y.-l., Cui, S.-q., 2019. Effect of Temperature on Mechanical Performance and Tensoresistivity of a New Sensor-Enabled Geosynthetic Material. Journal of Materials in Civil Engineering 31, 04019060.

Datta, M., 2010. Factors affecting slope stability of landfill covers, Advances in Environmental Geotechnics. Springer, pp. 620-624.

Dixon, N., Jones, D.R.V., Fowmes, G.J., 2006. Interface shear strength variability and its use in reliability-based landfill stability analysis. Geosynthetics International 13, 1-14.

Dove, J.E., Frost, J.D., 1999. Peak friction behavior of smooth geomembrane-particle interfaces. Journal of Geotechnical and Geoenvironmental Engineering 125, 544-555.

Dumbleton, M., 1981. The British soil classification system for engineering purposes: Its development and relation to other comparable systems[Final Report].

Duttine, A., Tatsuoka, F., Salotti, A., Ezaoui, A., 2015. Creep and stress

relaxation envelopes of granular materials in direct shear, Proc. of 15th Pan-American Conference on Soil Mechanics and Geotechnical Engineering and 6th International Conference on Deformation Characteristics of Geomaterials, Buenos Aires.

Edil, T.B., Kim, W.-H., Benson, C.H., Tanyu, B.F., 2007. Contribution of geosynthetic reinforcement to granular layer stiffness, Soil and Material Inputs for Mechanistic-Empirical Pavement Design, pp. 1-10.

Ellithy, G., Gabr, M., 2000. Compaction moisture effect on geomembrane/clay interface shear strength, Advances in Transportation and Geoenvironmental Systems Using Geosynthetics, pp. 39-53.

Feng, S.-J., Cheng, D., 2014. Shear strength between soil/geomembrane and geotextile/geomembrane interfaces, Tunneling and Underground Construction, pp. 558-569.

Ferreira, F., Vieira, C.S., Lopes, M., 2015. Direct shear behaviour of residual soil–geosynthetic interfaces–influence of soil moisture content, soil density and geosynthetic type. Geosynthetics International 22, 257-272.

Fishman, K., Pal, S., 1994. Further study of geomembrane/cohesive soil interface shear behavior. Geotextiles and Geomembranes 13, 571-590.

Fleming, I., Sharma, J., Jogi, M., 2006. Shear strength of geomembrane–soil interface under unsaturated conditions. Geotextiles and Geomembranes 24, 274-284.

Fleureau, J.-M., Verbrugge, J.-C., Huergo, P.J., Correia, A.G., Kheirbek-Saoud, S., 2002. Aspects of the behaviour of compacted clayey soils on drying and wetting paths. Canadian geotechnical journal 39, 1341-1357.

Fowmes, G.J., Dixon, N., Fu, L., Zaharescu, C.A., 2017. Rapid prototyping of geosynthetic interfaces: Investigation of peak strength using direct shear

tests. Geotextiles and Geomembranes 45, 674-687.

Fowmes, G.J., Dixon, N., Jones, D.R.V., 2008. Validation of a numerical modelling technique for multilayered geosynthetic landfill lining systems. Geotextiles and Geomembranes 26, 109-121.

Fox, P.J., Stark, T.D., 2015. State-of-the-art report: GCL shear strength and its measurement–ten-year update. Geosynthetics International 22, 3-47.

França, F., Bueno, B., 2011. Creep behavior of geosynthetics using confined-accelerated tests. Geosynthetics International 18, 242-254.

Fred Lee, G., Jones‐Lee, A., 2005. Municipal Solid Waste Landfills—Water Quality Issues. Water Encyclopedia 2, 163-169.

Frost, J., Karademir, T., 2016. Shear-induced changes in smooth geomembrane surface topography at different ambient temperatures. Geosynthetics International 23, 113-128.

Ghazizadeh, S., Bareither, C.A., 2018a. Stress-controlled direct shear testing of geosynthetic clay liners I: Apparatus development. Geotextiles and Geomembranes 46, 656-666.

Ghazizadeh, S., Bareither, C.A., 2018b. Stress-controlled direct shear testing of geosynthetic clay liners II: Assessment of shear behavior. Geotextiles and Geomembranes 46, 667-677.

Giroud, J., Darrasse, J., Bachus, R., 1993. Hyperbolic expression for soil-geosynthetic or geosynthetic-geosynthetic interface shear strength. Geotextiles and Geomembranes 12, 275-286.

Grebneva, V., Utkina, K., Sabri, M., Stolyarov, O., 2015. Application of stepped isothermal method for prediction the creep behavior of extruded polypropylene geogrid, Applied Mechanics and Materials. Trans Tech Publ,

pp. 611-616.

Guan, G.S., Rahardjo, H., Choon, L.E., 2010. Shear strength equations for unsaturated soil under drying and wetting. Journal of Geotechnical and Geoenvironmental Engineering 136, 594-606.

Gulec, S., Benson, C., Edil, T., 2005. Effect of acidic mine drainage on the mechanical and hydraulic properties of three geosynthetics. Journal of Geotechnical and Geoenvironmental Engineering 131, 937-950.

Guney, Y., Sari, D., Cetin, M., Tuncan, M., 2007. Impact of cyclic wetting–drying on swelling behavior of lime-stabilized soil. Building and environment 42, 681-688.

Guyonnet, D., Touze-Foltz, N., Norotte, V., Pothier, C., Didier, G., Gailhanou, H., Blanc, P., Warmont, F., 2009. Performance-based indicators for controlling geosynthetic clay liners in landfill applications. Geotextiles and Geomembranes 27, 321-331.

Hanson, J., Chrysovergis, T., Yesiller, N., Manheim, D., 2015. Temperature and moisture effects on GCL and textured geomembrane interface shear strength. Geosynthetics International 22, 110-124.

Hosney, M., Rowe, R.K., 2013. Changes in geosynthetic clay liner (GCL) properties after 2 years in a cover over arsenic-rich tailings. Canadian Geotechnical Journal 50, 326-342.

Hsieh, C.-W., Chen, G.-H., Wu, J.-H., 2011. The shear behavior obtained from the direct shear and pullout tests for different poor graded soil-geosynthetic systems. Journal of GeoEngineering 6, 15-26.

Hsiehl, C.W., Lee, K., Yoo, H.K., Jeon, H., 2008. Tensile creep behavior of polyester geogrids by conventional and accelerated test methods. Fibers and Polymers 9, 476-480.

Hsuan, Y., Yeo, S.-S., 2005. Comparing the creep behavior of high density polyethylene geogrid using two accereration methods, Slopes and Retaining Structures Under Seismic and Static Conditions, pp. 1-15.

Hsuan, Y., Yeo, S., Koerner, R., 2005. Compression creep behavior of geofoam using the stepped isothermal method, Geosynthetics Research and Development in Progress, pp. 1-5.

Ishimori, H., Katsumi, T., 2012. Temperature effects on the swelling capacity and barrier performance of geosynthetic clay liners permeated with sodium chloride solutions. Geotextiles and Geomembranes 33, 25-33.

Jafari, N.H., Stark, T.D., Rowe, R.K., 2014. Service life of HDPE geomembranes subjected to elevated temperatures. Journal of Hazardous, Toxic, and Radioactive Waste 18, 16-26.

Jang, Y.-S., Kim, B., Lee, J.-W., 2015. Evaluation of discharge capacity of geosynthetic drains for potential use in tunnels. Geotextiles and Geomembranes 43, 228-239.

Jeon, H.Y., Kim, S.H., Yoo, H.K., 2002. Assessment of long-term performances of polyester geogrids by accelerated creep test. Polymer testing 21, 489-495.

Jones, C., Clarke, D., 2007. The residual strength of geosynthetic reinforcement subjected to accelerated creep testing and simulated seismic events. Geotextiles and Geomembranes 25, 155-169.

Jones, D.R.V., Dixon, N., 1998. Shear strength properties of geomembrane/geotextile interfaces. Geotextiles and Geomembranes 16, 45-71.

Karademir, T., 2011. Elevated temperature effects on interface shear behavior. Georgia Institute of Technology.

Khire, M.V., Benson, C.H., Bosscher, P.J., 1997. Water balance modeling of earthen final covers. Journal of geotechnical and geoenvironmental engineering 123, 744-754.

Khire, M.V., Haydar, M.M., 2005. Leachate recirculation using geocomposite drainage layer in engineered MSW landfills, Waste Containment and Remediation, pp. 1-11.

Khire, M.V., Haydar, M.M., 2007. Leachate recirculation in bioreactor landfills using geocomposite drainage material. Journal of geotechnical and geoenvironmental engineering 133, 166-174.

Koerner, G., Koerner, R., 2006a. Long-term temperature monitoring of geomembranes at dry and wet landfills. Geotextiles and Geomembranes 24, 72-77.

Koerner, G.R., Koerner, R.M., 2006b. Geotextile tube assessment using a hanging bag test. Geotextiles and Geomembranes 24, 129-137.

Koerner, R.M., 2012. Designing with Geosynthetics-; Vol2. Xlibris Corporation.

Kong, L., Sayem, H.M., Tian, H., 2018. Influence of drying–wetting cycles on soil-water characteristic curve of undisturbed granite residual soils and microstructure mechanism by nuclear magnetic resonance (NMR) spin-spin relaxation time (t 2) relaxometry. Canadian Geotechnical Journal 55, 208-216.

Kongkitkul, W., Tatsuoka, F., 2007. A theoretical framework to analyse the behaviour of polymer geosynthetic reinforcement in temperature-accelerated creep tests. Geosynthetics International 14, 23-38.

Koutsourais, M., Sprague, C., Pucetas, R., 1991. Interfacial friction study of cap and liner components for landfill design. Geotextiles and Geomembranes 10, 531-548.

Lackner, C., Bergado, D.T., Semprich, S., 2013. Prestressed reinforced soil by geosynthetics–Concept and experimental investigations. Geotextiles and Geomembranes 37, 109-123.

Lambe, T.W., Whitman, R.V., 1991. Soil mechanics. John Wiley & Sons.

Lechowicz, Z., Goławska, K., Wrzesiński, G., SULEWSKA, M., 2019. Evaluation of creep behaviour of organic soils in a torsional shear hollow cylinder test, Proc. XVII European Conference on Soil Mechanics and Geotechnical Engineering, Reykjavik, Iceland, doi:. Crossref Export Citation.

Lee, K., Manjunath, V., 2000. Soil-geotextile interface friction by direct shear tests. Canadian geotechnical journal 37, 238-252.

Li, D., Yang, X., Chen, J., 2017. A study of triaxial creep test and yield criterion of artificial frozen soil under unloading stress paths. Cold Regions Science and Technology 141, 163-170.

Li, J., Li, L., Chen, R., Li, D., 2016. Cracking and vertical preferential flow through landfill clay liners. Engineering Geology 206, 33-41.

Li, R., 2000. Time-temperature superposition method for glass transition temperature of plastic materials. Materials Science and Engineering: A 278, 36-45.

Ling, H.I., Tatsuoka, F., 1994. Performance of anisotropic geosynthetic-reinforced cohesive soil mass. Journal of geotechnical engineering 120, 1166-1184.

Liu, C.-N., Ho, Y.-H., Huang, J.-W., 2009. Large scale direct shear tests of soil/PET-yarn geogrid interfaces. Geotextiles and Geomembranes 27, 19-30.

Liu, H., Martinez, J., 2014. Creep behaviour of sand–geomembrane interfaces. Geosynthetics International 21, 83-88.

Liu, P., Chen, R.-P., Wu, K., Kang, X., 2020. Effects of Drying-Wetting Cycles on the Mechanical Behavior of Reconstituted Granite-Residual Soils. Journal of Materials in Civil Engineering 32, 04020199.

Lopes, M.-L., Ferreira, F., Carneiro, J.R., Vieira, C.S., 2014. Soil–geosynthetic inclined plane shear behavior: influence of soil moisture content and geosynthetic type. International Journal of Geotechnical Engineering 8, 335-342.

Lv, Y., Li, F., Liu, Y., Fan, P., Wang, M., 2017. Comparative study of coral sand and silica sand in creep under general stress states. Canadian Geotechnical Journal 54, 1601-1611.

Mahmood, A., Zakaria, N., Ahmad, F., 2000. Studies on geotextile/soil interface shear behavior. Electronic Journal of Geotechnical Engineering 5.

Makkar, F.M., Chandrakaran, S., Sankar, N., 2019. Experimental Investigation of Response of Different Granular Soil–3D Geogrid Interfaces Using Large-Scale Direct Shear Tests. Journal of Materials in Civil Engineering 31, 04019012.

McCartney, J.S., Berends, R.E., 2010. Measurement of filtration effects on the transmissivity of geocomposite drains for phosphogypsum. Geotextiles and Geomembranes 28, 226-235.

McCartney, J.S., Kuhn, J.A., Zornberg, J.G., 2005. Geosynthetic drainage layers in contact with unsaturated soils, PROCEEDINGS OF THE INTERNATIONAL CONFERENCE ON SOIL MECHANICS AND GEOTECHNICAL ENGINEERING. AA BALKEMA PUBLISHERS, p. 2301.

McCartney, J.S., Zornberg, J.G., 2010. Effects of infiltration and evaporation on geosynthetic capillary barrier performance. Canadian Geotechnical Journal 47, 1201-1213.

Md, S.H., Ling-wei, K., Song, Y., 2016. Effect of drying-wetting cycles on saturated shear strength of undisturbed residual soils. American Journal of Civil Engineering 4, 143-150.

Mofiz, S.A., Taha, M.R., Sharker, D.C., 2004. Mechanical stress-strain characteristics and model behavior of geosynthetic reinforced soil composites, 17th ASCE Eng. Mechanics Conf, pp. 23-31.

Monteiro, C., Araújo, G., Palmeira, E., Neto, M., 2013. Soil-geosynthetic interface strength on smooth and texturized geomembranes under different test conditions, Proceedings of the 18th international conference on soil mechanics and geotechnical engineering, Paris, pp. 3053-3056.

Montgomery, R., Parsons, L., 1990. The Omega Hills final cover test plot study: Fourth year data summary, Proc. Mid-Atlantic Ind. Waste Conf., 22nd, Philadelphia, PA, p. 27.

Mosallanezhad, M., Alfaro, M., Hataf, N., Taghavi, S.S., 2016. Performance of the new reinforcement system in the increase of shear strength of typical geogrid interface with soil. Geotextiles and Geomembranes 44, 457-462.

Müller, W., Jakob, I., Li, C., Tatzky-Gerth, R., 2009. Durability of polyolefin geosynthetic drains. Geosynthetics International 16, 28-42.

Müller, W., Jakob, I., Seeger, S., Tatzky-Gerth, R., 2008. Long-term shear strength of geosynthetic clay liners. Geotextiles and Geomembranes 26, 130-144.

Naeini, S.A., Khalaj, M., Izadi, E., 2013. Interfacial shear strength of silty sand–geogrid composite. Proceedings of the Institution of Civil Engineers-Geotechnical Engineering 166, 67-75.

Othman, M., 2016. Interface behaviour and stability of geocomposite drain/soil systems. Loughborough University.

Othman, M., Frost, M., Dixon, N., 2014. Soil interface softening from capillary break formation in geocomposite drainage systems, 10th International Conference on Geosynthetics, pp. 1-13.

Othman, M., Frost, M., Dixon, N., 2015. Effect of interface soil softening on stability of geocomposite drainage systems, 2nd International GSI-Asia Geosynthetics Conference, pp. 1-5.

Othman, M., Frost, M., Dixon, N., 2018. Stability performance and interface shear strength of geocomposite drain/soil systems, AIP Conference Proceedings. AIP Publishing LLC, p. 020049.

Oweis, I.S., Smith, D.A., Brian Ellwood, R., Greene, D.S., 1990. Hydraulic characteristics of municipal refuse. Journal of Geotechnical Engineering 116, 539-553.

Palmeira, E., Lima Jr, N., Mello, L., 2002. Interaction between soils and geosynthetic layers in large-scale ramp tests. Geosynthetics international 9, 149-187.

Pasculli, A., Sciarra, N., Esposito, L., Esposito, A.W., 2017. Effects of wetting and drying cycles on mechanical properties of pyroclastic soils. Catena 156, 113-123.

Pilarczyk, K., 2000. Geosynthetics and geosystems in hydraulic and coastal engineering. CRC Press.

Rezania, M., 2008. Evolutionary polynomial regression based constitutive modelling and incorporation in finite element analysis. University of Exeter.

Rezania, M., Bagheri, M., Mousavi Nezhad, M., 2020. Creep and consolidation of a stiff clay under saturated and unsaturated conditions. Canadian Geotechnical Journal 57, 728-741.

Rhodes, E., 2019. Creep Behaviour of Geosynthetic Interfaces in Landfill Applications. Loughborough University.

Roodi, G.H., Morsy, A.M., Zornberg, J.G., 2018. Soil–geosynthetic interface shear in different testing scales. Transportation Research Record 2672, 129-141.

Rowe, R., Rimal, S., Sangam, H., 2009. Ageing of HDPE geomembrane exposed to air, water and leachate at different temperatures. Geotextiles and Geomembranes 27, 137-151.

Sadrekarimi, A., Olson, S.M., 2009. A new ring shear device to measure the large displacement shearing behavior of sands. Geotechnical Testing Journal 32, 1-12.

Sarsby, R.W., 2006. Geosynthetics in civil engineering. Woodhead Publishing.

Sawicki, A., 1999. Creep of geosynthetic reinforced soil retaining walls. Geotextiles and Geomembranes 17, 51-65.

Sawicki, A., Kazimierowicz-Frankowska, K., 1998. Creep behaviour of geosynthetics. Geotextiles and Geomembranes 16, 365-382.

Shukla, S.K., 2017. An introduction to geosynthetic engineering. CRC Press.

Shukla, S.K., Shukla, S.K., 2002. Geosynthetics and their applications. Thomas Telford London.

Shukla, S.K., Yin, J.-H., 2006. Fundamentals of geosynthetic engineering. CRC Press.

Sia, H.-I., 2007. Landfill lining engineering designs: a probabilistic approach. Loughborough University.

Singh, R.M., Bouazza, A., 2013. Thermal conductivity of geosynthetics. Geotextiles and Geomembranes 39, 1-8.

Sposito, G., 1995. The environmental chemistry of aluminum. CRC Press.

Stark, T.D., Poeppel, A.R., 1994. Landfill liner interface strengths from torsional-ring-shear tests. Journal of Geotechnical Engineering 120, 597-615.

Stark, T.D., Santoyo, R.F., 2017. Soil/geosynthetic interface strengths from torsional ring shear tests, Geotechnical Frontiers 2017, pp. 260-268.

Stępień, S., Szymański, A., 2015. Influence of strain rate on tensile strength of woven geotextile in the selected range of temperature. Studia Geotechnica et Mechanica 37, 57-60.

Stormont, J.C., Henry, K., Roberson, R., 2009. Geocomposite capillary barrier drain for limiting moisture changes in pavements: Product application. Final Rep., Contract No. NCHRP 113.

Suits, L.D., Hsuan, Y.G., 2003. Assessing the photo-degradation of geosynthetics by outdoor exposure and laboratory weatherometer. Geotextiles and Geomembranes 21, 111-122.

Sumi, S., Unnikrishnan, N., Mathew, L., 2018. Durability studies of surface-modified coir geotextiles. Geotextiles and Geomembranes 46, 699-706.

Suzuki, M., Koyama, A., Kochi, Y., Urabe, T., 2017. Interface shear strength between geosynthetic clay liner and covering soil on the embankment of an irrigation pond and stability evaluation of its widened sections. Soils and Foundations 57, 301-314.

Tajvidi, M., Falk, R.H., Hermanson, J.C., 2005. Time – temperature superposition principle applied to a kenaf-fiber/high-density polyethylene composite. Journal of applied polymer science 97, 1995-2004.

Tan, S., Chew, S., Wong, W., 1998. Sand–geotextile interface shear strength by torsional ring shear tests. Geotextiles and Geomembranes 16, 161-174.

Tang, H., Duan, Z., Wang, D., Dang, Q., 2020. Experimental investigation of creep behavior of loess under different moisture contents. Bulletin of Engineering Geology and the Environment 79, 411-422.

Tuna, S., Altun, S., 2012. Mechanical behaviour of sand-geotextile interface. Scientia Iranica 19, 1044-1051.

Van Gurp, M., Palmen, J., 1998. Time-temperature superposition for polymeric blends. Rheol. Bull 67, 5-8.

Vieira, C.S., Lopes, M.d.L., Caldeira, L., 2013. Sand-geotextile interface characterisation through monotonic and cyclic direct shear tests. Geosynthetics International 20, 26-38.

Wang, D.-Y., Tang, C.-S., Cui, Y.-J., Shi, B., Li, J., 2016a. Effects of wetting–drying cycles on soil strength profile of a silty clay in micro-penetrometer tests. Engineering Geology 206, 60-70.

Wang, J., Liu, F., Wang, P., Cai, Y., 2016b. Particle size effects on coarse soil-geogrid interface response in cyclic and post-cyclic direct shear tests. Geotextiles and Geomembranes 44, 854-861.

Yang, W., Wang, Y., Wang, L., Guo, J., 2020. Time-dependent behaviour of clay-concrete interfaces with different contact surface roughnesses under shear loading. Mechanics of Time-Dependent Materials, 1-26.

Yeo, S.-S., 2007. Evaluation of creep behavior of geosynthetics using accelerated and conventional methods.

Yeo, S.-S., Hsuan, Y., 2010. Evaluation of creep behavior of high density polyethylene and polyethylene-terephthalate geogrids. Geotextiles and

Geomembranes 28, 409-421.

Yeşiller, N., Hanson, J.L., Liu, W.-L., 2005. Heat generation in municipal solid waste landfills. Journal of Geotechnical and Geoenvironmental Engineering 131, 1330-1344.

Yoshida, H., Rowe, R., 2003. Consideration of landfill liner temperature, Proceedings Sardinia. Citeseer.

Zaharescu, C.A., 2018. Wear-quantification of textured geomembranes using digital imaging analysis. Loughborough University.

Zanzinger, H., Alexiew, N., 2000. Prediction of long term shear strength of geosynthetic clay liners with shear creep tests, Proceedings 2nd European Conference on Geosynthetics, Bologna, pp. 567-571.

Zanzinger, H., Saathoff, F., 2012. Long-term internal shear strength of a reinforced GCL based on shear creep rupture tests. Geotextiles and Geomembranes 33, 43-50.

Zhang, B., Zhang, J., Sun, G., 2015. Deformation and shear strength of rockfill materials composed of soft siltstones subjected to stress, cyclical drying/wetting and temperature variations. Engineering Geology 190, 87-97.

Zornberg, J.G., Byler, B.R., Knudsen, J.W., 2004. Creep of geotextiles using time–temperature superposition methods. Journal of geotechnical and geoenvironmental engineering 130, 1158-1168.